HYPER-TEMPORAL REMOTE SENSING

FOR LAND COVER MAPPING AND MONITORING

Amjad Ali

Examining committee:

Prof.dr. M. Molenaar	University of Twente, ITC
Prof.dr. V.G. Jetten	University of Twente, ITC
Prof.dr. S.M. de Jong	Utrecht University
Prof. G. Menz	University of Bonn, Germany

ITC dissertation number 240
ITC, P.O. Box 217, 7500 AA Enschede, The Netherlands

ISBN 978-90-6164-369-2
Cover designed by O. Zia, Asad Ali and Benno Masselink
Printed by ITC Printing Department

UNIVERSITY OF TWENTE.

FACULTY OF GEO-INFORMATION SCIENCE AND EARTH OBSERVATION

HYPER-TEMPORAL REMOTE SENSING

FOR LAND COVER MAPPING AND MONITORING

DISSERTATION

to obtain
the degree of doctor at the University of Twente,
on the authority of the rector magnificus,
prof.dr. H. Brinksma,
on account of the decision of the graduation committee,
to be publicly defended
on Wednesday 8 January2014 at 14.45 hrs

by

Amjad Ali

born on 15 March 1978.

in Kurrum Agency, Pakistan

This thesis is approved by
Prof. dr. Andrew Skidmore, promoter
Dr. C.A.J.M de Bie, assistant promoter

I dedicate this humble effort, the fruit of

my thoughts and research to my parents,

brothers, sisters and to my family.

Amjad Ali

Acknowledgements

All acclamation and appreciation are for almighty Allah who created the universe and bestowed the mankind with knowledge and wisdom to search for its secrets.

This study is result of support of a number of organizations. I thank Higher Education Commission (HEC) Pakistan, Pakistan Space and Upper atmosphere Research Commission (SUPARCO), Nuffic and UT-ITC for financial and logistic help during the study. I express my gratitude to all involved for their support and encouragement.

I feel great pleasure and honour to express my sincere and heart full thanks to the honourable promoter Prof. Andrew Skidmore for his concerted technical guidance, keen interest and encouragement during research. Graceful acknowledgment is made for wise counselling received from Prof Dr. Ir. E.M.A. Smaling at initial stages of PhD.

I am indebted to assistant promoter Dr. Ir. C.A.J.M. de Bie for constant supervision, invaluable guidance and encouragement that enabled me to investigate and accomplish this task.

Special thanks are extended to all staff and faculty members of NRS department for their support throughout my study in ITC-UT. I am particularly indebted to Willem Nieuwenhuis for his very kind attitude and sincere help in programming.

I acknowledge the services and support of all SUPARCO Officials in this achievement. Special thanks are extended to Member SAR Mr. Imran Iqbal, DG Mr Muhammad Shafique and GM Mr. Muhammad Farooq for their support during the study.

I am indebted to honourable research Head professor Paul van Dijk, student affairs staff Loes Colenbrander, Theresa van den Boogaard and Marie Chantal Metz and Bettine Geerdink, Secretary NRS department Esther Hondebrink for the counselling and support that enabled me to live nicely and accomplish this task. I extend true thanks to Job Duim and Benno Masselink for their technical assistance during my studies. Library services can also be not ignored in research so special thanks extended to all the staff of library.

I must thank office-mates Dr. Ha Thi Nguyen, Dr. Mobasher Riaz Khan, Dr Abel Ramoelo, John Wasige, Maria Buitrago, Parinaz Rashidi for their outstanding help during my study.

Very warm and special thanks are paid to my sincere friends Muhammad Jahanzeb Malik, Saleem Ullah, Dr Shafique, Haris Akram Bhatti, Aamir Khan Momand, Irfan Akhtar Iqbal, Muhammad Yaseen for their unending kindness and active support throughout my research work and made this study a success.

Thanks are extended to all the colleagues for their help in obtaining the data for this research particularly Mina Naeimi, Amit Kumar Srivastava, Shirin Taheri, Johanna Ngula Niipele and Amina Hamad, Eric, John, Alexy McIntire.

In the end I would like to cordially owe my tribute to my affectionate parents, brothers (Dr. Qaiser Ali, Irshad Ali, and Asad Ali), sisters, wife and kids (Ali Abbas and Hussain Abbas) for their support with an extra sense of gratitude.

"Thank you all"
Amjad Ali.

Table of Contents

List of figures

List of tables

1 General Introduction

1.1 *Introduction*

1.1.1 *Why land cover mapping and monitoring?*

Land cover information is important to support policy formulation regarding food security (Millennium Development Goal 1) and environmental sustainability (Millennium Development Goal 7) (Dai and Khorram, 1998; Cihlar, 2000; Defries and Belward, 2000). Up-to-date and accurate land cover information is required from regional to global levels to effectively monitor set MDG targets. MDG 1 concerns global elimination of hunger and poverty, MDG 7 aims at sustainable use of natural resources.

For proper land resources management, Cihlar (2000) considered that land cover data represents key information for biodiversity conservation, and Jones et al (2009) states that land cover data are even of vital importance. Land cover data are also relevant to study the impacts of precipitation on soil erosion, run-off, flooding and crop production (Helmer et al., 2000). Accurate land cover information extraction is the main focus of global research which established its importance for society for example; the International Geosphere-Biosphere Program (IGBP), the Framework Convention for Climate Change, the Kyoto Protocol, the Biodiversity Convention, NASA's Land Cover-Land Use Change (LCLUC) program, FAO land use and land cover information program and Intergovernmental Panel on Climate Change (IPCC) (IPCC, 2001).

Land cover (LC) change is a key component in adaptation to global climate change at regional to global scales (Cihlar, 2000; Ray et al., 2009). Land cover change is one of the important sources of CO_2 emissions globally (20%) (Rodriguez-Yi et al., 2000; IPCC, 2001). Climate change is important to mitigate because it is intensifying disasters, including extreme weather events, storm surges, floods and droughts. This is adversely affecting the progress on the targets set for the MDG 1 and MDG 7; hence it highlights the importance of land cover change information to mitigate the issues.

1.1.2 *Remote sensing derived land cover information: a historical perspective*

Remote sensing, due to its synoptic coverage, is one of the important sources of obtaining the valuable land cover information accurately and regularly (Cihlar, 2000; Lillesand et al., 2004). Through remote sensing, Earth can be observed easily and regularly, which can help to understand the earth's surface features and processes (Xie et al., 2008) and monitor targets for MDG 1 and MDG 7. It is possible to obtain land cover information at different spatial and temporal scale.

The necessity to obtain accurate, quick and regular earth surface information over a large area has started the development of remote sensing over time. In 1840s for the first time, still pictures of earth surface were obtained using balloons (Lillesand et al., 2004). In the American Civil War, still cameras mounted on balloons were used to obtain the information about enemy positions. In the meantime, rockets, kites, and birds were used to obtain land surface information. During the First World War, cameras installed on airplanes were used to get information about enemy territory. Cameras mounted on airplanes are more stable than balloons and other sources used so far. In World War II, visible-spectrum photography, infrared detection and radar, systems were used to acquire earth surface information (Lillesand et al., 2004).

The term 'remote sensing' was used for the first time in the United States in the 1950s by Ms Evelyn Pruitt of the U.S. Office of Naval Research (http://earthobservatory.nasa.gov/Features/RemoteSensing Access date: 11/10/2012). It refers to the obtaining of information about an object without being in direct physical contact with the object (Lillesand et al., 2004). In 1957, the first man-made satellite (Sputnik 1) was developed by Russia in 1957, and this started the era of space borne satellites (Williams et al., 2006). However, the first photo was obtained from space in 1959 by the United States Explorer 6. Landsat 1 (1972) was the first satellite to collect data, specifically about the Earth's surface and natural resources. Landsat 1 was a key milestone in the history of remote sensing (Franklin, 2001). This started the era of utility of satellite imagery for monitoring of natural resources (Lillesand et al., 2004; Williams et al., 2006). The first problem detected by using satellite imagery was the Amazonian deforestation (Peres and Terborgh, 1995). Since the first Landsat satellite (1972), a series of sensors named Thematic Mapper (TM) were developed, for example Landsat 4 (1982), Landsat 5 (1984) and Landsat 7 (Enhanced Thematic Mapper Plus (ETM+) (1999) (Williams et al., 2006; Xie et al., 2008). The Landsat Thematic Mapper provides data having higher spectral, spatial, and radiometric resolution. The spectral channels of Thematic Mapper is specifically designed to map vegetation type, soil moisture, and other key landscape features (Jensen, 2000). Indian Remote Sensing (IRS) also launched a series of satellites in 1988, 1991, 1994 and 1997 for observing earth surfaces.

The Advanced Very High Resolution Radiometer (AVHRR) sensor on-board the National Oceanic and Atmospheric Administration (NOAA) satellite data (1.1 km resolution) is in use for studying land resources since 1980. Besides that Syste`me Pour l'Observation de la Terre-1 (SPOT-1) satellite launched in 1986 (20 m and a panchromatic channel of 10 m) has provided a multispectral information for improved land-cover and land-use monitoring

(Pellemans et al., 1993). In 1998, SPOT launched a mid-infrared channel (SPOT-4 sensor), suitable for land-cover and land-use monitoring (Stroppiana et al., 2002). SPOT-5 sensor, was launched in 2002, which collects panchromatic, visible and near-infrared, and mid-infrared data at 5, 10 and 20m spatial resolution respectively. The Advanced Space borne Thermal Emission and Reflection Radiometer (ASTER), an instrument on the Terra platform, acquires visible and near-infrared information at 15 m spatial resolution and mid-infrared information at 30m spatial resolution. IKONOS (1999) having 4m resolution and QuickBird (2000) multispectral imagery at 2.6 m resolutions provide high resolution imagery for local scale studies.

1.1.3 *Common image classification methods*

To date, a number of image classification methods have been developed and used to extract meaningful information from remote sensing imagery (Lu and Weng, 2007). Selection of suitable classification methods is very important to successfully extract information from imagery (Lu and Weng, 2007). Maximum likelihood classification is the most frequently used image classification method used for land-cover and land-use mapping. However, if the histogram of the image does not follow the normal distribution curve, insufficient ground verification data and high correlation between two bands result in poor classification because the covariance matrix becomes unstable (Richards and Jia, 2006). Minimum distance classification is supervised technique used when sufficient training data is not available. This method is faster in operations but less accurate and less reliable because it does not take into account covariance matrix. Parallelepiped supervised classification suffers from class overlaps and gaps between the parallelepiped, so pixels in that regions will not be classified (Lillesand et al., 2004; Richards and Jia, 2006). Non parametric classifiers such as artificial neural network (Foody, 1995, 2002; Kavzoglu and Mather, 2003), decision tree classifier (Hansen et al., 2000), support vector machine and expert system require no assumption about the data. They do not use statistical parameters to identify classes. They are better suited for analysing multi-modal, noisy, and/or missing data (Rogan and Chen, 2004; Lu and Weng, 2007). However, prior and detailed knowledge of the area is needed to train the dataset (Černá and Chytrý, 2005). In case of neural network the selection of network architecture, initial values of learning rate and momentum, the number of iterations and initial weights make it less suitable for land cover mapping and monitoring.

The Iterative Self-Organizing Data Analysis Technique (ISODATA) and the K-means clustering algorithm are the most commonly used unsupervised classification methods. ISODATA (Ball and Hall, 1965) is iterative and self-organizing, which repeats itself and locate clusters with minimum user input (Tou and Gonzalez, 1974; Swain and Davis, 1978). No prior knowledge of the

area is needed; however, classified land cover maps need to be labelled with field data later (Jensen, 1996). This technique has more consistent results (Cihlar, 2000). Different form of statistics such as divergence statistics; Jeffries-Matsushita can be used to select the optimum number of classes (de Bie et al., 2012). The K mean has subjected nature of selection of clusters.

To deal with more complex spectral features in vegetation, new classification techniques have also been developed and used (Xie et al., 2008). The continuous classification technique has been used to distinguish savanna (Stuart et al., 2006) and complex wetland vegetation. Similarly spectral angle classifier (SAC) has been used to classify same type of vegetation based on distance between pair of signatures (Sohn and Rebello, 2002).

Fuzzy logic approaches are used in mixed classes vegetation (Zhang and Foody, 1998), which calculates probability of pixels. Decision tree (DT) approaches matches the spectral features from objects of remote sensing images with that of vegetation types (Hansen et al., 2000). Similarly hybrid methods are used to improve the accuracy of complex land cover classifications (Lo and Choi, 2004).

1.1.4 *Use of vegetation indices for mapping*

The use of vegetation indices such as Normalized Difference Vegetation Index (NDVI) and Enhanced Vegetation Index (EVI) has also improved the vegetation mapping (Xie et al., 2008) from optical sensors remote sensing imagery. The use of VIs have improved the vegetation mapping because it tracks change in specific vegetation types and provide information to distinguish vegetation groups (Geerken et al., 2005). Currently, NDVI is widely used for improved mapping and monitoring of vegetation. These indices are is also available in different spatial and temporal resolution from different sources such as SPOT, MERIS and MODIS.

The imagery captured by different satellites are widely available via the internet in a near real-time therefore, the remotely sensed data is widely used for earth resources related research and management work for example wetland mapping and monitoring (Nielsen et al., 2008; Zhao et al., 2009); crop mapping and monitoring (Zhan et al., 2002; Sakamoto et al., 2006; Zhao et al., 2009); modelling for ecosystem sustainability (Moulin et al., 1998; Rogan and Chen, 2004; Bénié et al., 2005; Lasaponara, 2006; Hayes and Cohen, 2007; He et al., 2009) etc. Advancement in geographical information systems in the last two decades has made available a wide variety of data handling tools to handle the data and is used effectively to get land cover information.

1.2 *Challenges in land cover mapping and monitoring*

Research efforts are underway to effectively derive land cover information accurately and visualize it appropriately using the newly available imagery and improved techniques. The two main challenges in accurate mapping and monitoring of land cover are the lack of gradient representation and the use of the limited time imagery (2-3 times imagery) of irregular time period. These two aspects are considered in this thesis.

Representing gradients

Environmental gradient is important characteristic of variability in environmental conditions e.g. soil moisture, precipitation, temperature etc. (Whittaker, 1978a; Begon et al., 1990; Foody and Boyd, 1999). These environmental conditions (Begon et al., 1990) influence biodiversity in space and time. Consequently, species abundance and composition change along environmental gradients (Whittaker and Levin, 1977; Whittaker, 1978a; Townsend, 2000; Tapia et al., 2005; Tang et al., 2010). Spatially, it appears as a gradient that represents gradual changes in space. Recognizing such a gradient and visualize it in maps is more important for accurate and realistic representation of land cover (Whittaker, 1978a; Austin, 1990; Begon et al., 1990; Gosz, 1992; Kent et al., 1997; Foody and Boyd, 1999; Cihlar, 2000; Townsend, 2000; Coppin et al., 2004; Southworth et al., 2004) (Figure 1.1).

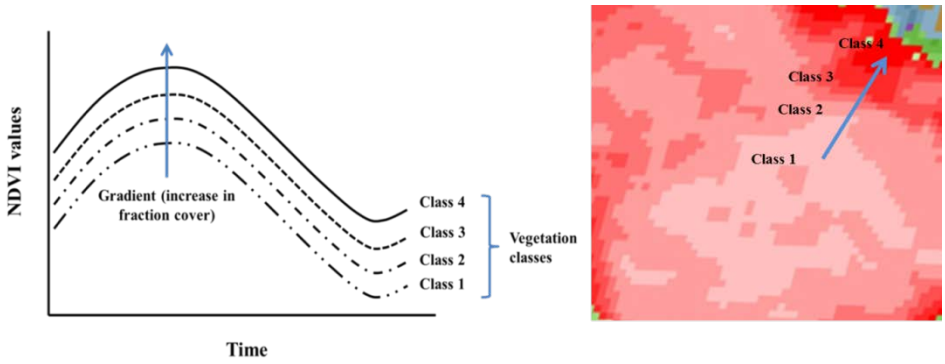

Figure 1.1. The concept of gradient as visualized in this thesis.

Land cover gradients are the result of variable spatio-temporal phenomenon as mentioned earlier (Müller, 1998; Löffler and Finch, 2005; Sklenár et al., 2008). Underlying factors (e.g. geology, climate, topography) responsible for such gradients vary continuously over space and time (Foody and Boyd, 1999). Consequently, the land cover composition changes continuously both in space and time (Delcourt and Delcourt, 1991; Lambin and Geist, 2006) depending upon the factors causing it (Lambin and Geist, 2006).

To date, a variety of analytical methods available to map land cover and changes in its composition use temporally-limited set of imagery (Haralick et al., 1973; Wood and Foody, 1989; Bradshaw and Spies, 1992; Foody, 1992; Skidmore and Turner, 1992; Trodd, 1992; Foody and Trodd, 1993; Gulinck et al., 1993; Trodd, 1993; Foody, 1996a, b; Bastin, 1997; Zhang and Foody, 1998; Foody and Boyd, 1999; Gopal et al., 1999; Csillag and Kabos, 2002; Mendel and John, 2002; Deer and Eklund, 2003; Kavzoglu and Mather, 2003; Fonte and Lodwick, 2004; Camarero et al., 2006; Fisher et al., 2006; Arnot and Fisher, 2007b; Berberoglu et al., 2007; Fisher et al., 2007; Verstraete et al., 2007; Dixon and Candade, 2008; Krishnaswamy et al., 2009; Fisher, 2010; Mitrakis et al., 2011). The limited time imagery of irregular time period potentially imposed limitation to adequately capture seasonal profiles of land cover that can be used to accurately map land cover gradients and monitor land cover composition changes. This has clearly articulated the need to use long term spatio-temporal datasets to identify land cover gradients (Austin, 1990; Begon et al., 1990; Gosz, 1992; Kent et al., 1997).

Temporal resolution of earth observation data

The temporal dynamics of imagery is important for accurate characterization and mapping of land cover due to its ability to closely track seasonal profiles and changes (Zhan et al., 2002; Lunetta et al., 2004; Sakamoto et al., 2005; Zhang et al., 2009). Hyper-temporal imagery can greatly enhance the information gained from processing due to its high repetitive coverage (Xiao et al., 2006a; Lu and Weng, 2007; Sakamoto et al., 2007; Alexandridis et al., 2008; Khan et al., 2011). It is found effective for mapping complex land use and land cover accurately (Lunetta and Balogh, 1999; Tucker et al., 2001; Sakamoto et al., 2006; de Bie et al., 2008; Khan et al., 2010; de Bie et al., 2011; Nguyen et al., 2011).

The spatial patterns of green cover that represent gradual changes in the form of gradient can be discerned using the local vegetation seasonal trends (Ali et al., 2013). These seasonal variations are specific to different species, its density and composition, which can help in identification of land cover type and state (Justice et al., 1985; Neeti et al., 2011; Ali et al., 2013). These trends project the influence of different biotic and abiotic environmental factors such as soil, temperature, solar illumination, photoperiod and moisture over time which is responsible for gradients in land cover.

Most of the research studies used multi-temporal imagery (2-3 dates) for mapping and monitoring of land cover for example's (Byrne et al., 1980; Howarth and Wickware, 1981; Nelson, 1983; Wood and Foody, 1989; Lambin and Strahlers, 1994; Elvidge et al., 1998; Vogelmann et al., 1998; Helmer et al., 2000; Young and Wang, 2001; Homer et al., 2004; Fraser et al., 2005;

Ingram et al., 2005; Cakir et al., 2006; Desclée et al., 2006; Knight et al., 2006). Due to the limited time imagery used it is not possible to remove the seasonal aspects of mapping process and make accurate identification and estimation. The maps produced are less accurate because the seasonal aspects are not removed. The thematic information possible to extract is also limited as only spatial extent is considered. Due to inaccuracy and less detailed information, the output maps are less useful for management purposes (Nguyen et al., 2011).

In the last decade, due to the free availability of remote sensing imagery in different spectral, spatial and temporal resolutions, research related to land cover mapping and monitoring benefitted from it (Sakamoto et al., 2006; Xiao et al., 2006a; Khan et al., 2010; de Bie et al., 2011; Nguyen et al., 2011; de Bie et al., 2012). To follow up the rapid vegetation seasonal changes in the ecosystem, high temporal resolution imagery (hyper-temporal imagery) is needed (Tucker et al., 2001; Lunetta et al., 2004; Islam and Bala, 2008; Zhang et al., 2009).

Still limited numbers of studies are available, that use long term hyper-temporal datasets. Thus there is a need to exploit this data rich hyper-temporal imagery for improved land cover mapping and monitoring. In this regard both spatial and hyper-temporal resolution perspectives offer an opportunity to enable new approaches of mapping and monitoring of land cover.

1.3 *Research objective and organization of the thesis*

The objective of the research is to develop and test methods to improve land cover mapping and monitoring in terms of gradient representation and the use of hyper-temporal remote sensing. The specific objectives are; (i) to devise a simple technique for characterizing long-duration cloud contamination in hyper-temporal NDVI imagery analysis (ii) identifying and mapping land cover gradient through analysis of hyper-temporal NDVI imagery (iii) to test a spatiotemporally explicit and gradient based landscape heterogeneity mapping approach (LaHMa; de Bie et al., 2012) in natural and semi-natural landscapes and (iv) to develop a land cover composition change assessment method (CoverCAM) that extracts from hyper-temporal NDVI imagery over time and by location the probabilities that the original land cover composition changed. To achieve the objective, this research is organized into six chapters.

Chapter 1. General Introduction
This chapter provides an introduction to the problem, rationale of the study, objective and organization of this research.

Chapter 2. Detecting long duration cloud contamination in hyper-temporal NDVI imagery
This chapter deals with long duration cloud contamination impacts on the quality of time series NDVI imagery. Normally, short-duration cloud impacts are removed by using upper envelope filters, but long-duration cloud contamination of NDVI imagery remains. This study attempts to devise a simple technique for characterizing long-duration cloud contamination in hyper-temporal NDVI imagery analysis. This is important due to the increasing use of NDVI time series imagery for land cover mapping and monitoring.

Chapter 3. Mapping land cover gradients through analysis of hyper-temporal NDVI imagery
Gradient representation is more accurate and a realistic way to signify land cover in maps. The existing land cover maps shows at best, mapping units with different cover densities and/or species compositions, but typically fail to express such differences as gradients. They did not use hyper-temporal imagery and hence fail to properly identify and/or visualize land cover gradients. This chapter aims at identifying and mapping land cover gradients through the analysis of hyper-temporal NDVI imagery.

Chapter 4. Mapping the heterogeneity of natural and semi natural landscapes
Natural and semi-natural landscape cover is heterogeneous and show progressive transitions spatially. Land cover heterogeneity being a non-static phenomenon depends upon temporal developments. This study tested spatiotemporally explicit and gradient based approach called Landscape Heterogeneity Mapping (LaHMa) method to map the heterogeneity of natural and semi-natural landscapes on the island of Crete, Greece. This method involves calculating the relative heterogeneity of each pixel area, using the long-term spatiotemporal variability in land cover. It exhibits spatial heterogeneity at various strengths of ecotones and ecoclines at any selected scale therefore, it can be useful for understanding landscape structures and functions.

Chapter 5. CoverCAM: a land cover composition change assessment method
Land cover composition continuously undergoes changes over time due to natural and anthropogenic factors. Accurate detection of the land cover composition changes require a method which removes seasonality aspects

such weather, phenology and crop calendars differences from change detection process. The available techniques do not use hyper-temporal records. They did not concern land cover composition changes because they represent changes in discrete manner. Some current methods use hyper-temporal imagery and fail to project composition changes in continuous values. Accordingly, this study aims to develop a new land cover composition change detection method (CoverCAM) that extracts probabilities that the original land cover composition changed; from hyper-temporal NDVI imagery over time and by location in the form of maps.

Chapter 6. Synthesis

This chapter synthesizes the main findings of the research and discusses its practical relevance.

2 Detecting long-duration cloud contamination in hyper-temporal NDVI imagery[1]

[1] Chapter is based on: A. Ali., C. A. J. M. de Bie., A. K. Skidmore., 2013. Detecting long-duration cloud contamination in hyper-temporal NDVI imagery. International Journal of Applied Earth Observation and Geoinformation 24, 22-31.

Abstract

Cloud contamination impacts on the quality of hyper-temporal NDVI imagery and its subsequent interpretation. Short-duration cloud impacts are easily removed by using quality flags and an upper envelope filter, but long-duration cloud contamination of NDVI imagery remains. In this paper, an approach that goes beyond the use of quality flags and upper envelope filtering is tested to detect when and where long-duration clouds are responsible for unreliable NDVI readings, so that a user can flag those data as missing. The study is based on MODIS Terra and the combined Terra-Aqua 16-day NDVI product for the south of Ghana, where persistent cloud cover occurs throughout the year. The combined product could be assumed to have less cloud contamination, since it is based on two images per day. Short-duration cloud effects were removed from the two products through using the adaptive Savitzky-Golay filter. Then for each 'cleaned' product an unsupervised classified map was prepared using the ISODATA algorithm, and, by class, plots were prepared to depict changes over time of the means and the standard deviations in NDVI values. By comparing plots of similar classes, long-duration cloud contamination appeared to display a decline in mean NDVI below the lower limit 95% confidence interval with a coinciding increase in standard deviation above the upper limit 95% confidence interval. Regression analysis was carried out per NDVI class in two randomly selected groups in order to statistically test standard deviation values related to long-duration cloud contamination. A decline in seasonal NDVI values (growing season) were below the lower limit of 95% confidence interval as well as a concurrent increase in standard deviation values above the upper limit of the 95% confidence interval were noted in 34 NDVI classes. The regression analysis results showed that differences in NDVI class values between the Terra and the Terra-Aqua imagery were significantly correlated ($p<0.05$) with the corresponding standard deviation values of the Terra imagery in case of all NDVI classes of two selected NDVI groups. The method successfully detects long-duration cloud contamination that results in unreliable NDVI values. The approach offers scientists interested in time series analysis a method of masking by area (class) the periods when pre-cleaned NDVI values remain affected by clouds. The approach requires no additional data for execution purposes but involves unsupervised classification of the imagery to carry out the evaluation of class-specific mean NDVI and standard deviation values over time.

Keywords: Cloud, Contamination, MODIS, NDVI, Hyper-temporal, Mapping

2.1 *Introduction*

The availability of accurate land cover information is important for policy formulation and the management of natural resources, including biodiversity, forestry and the issue of food security (Cihlar, 2000; Defries and Belward, 2000). Climate change issues further enhance the general interest in the availability and use of accurate land use/land cover information at regional to global scales (Cihlar, 2000). The common method of generating land cover information is the use of satellite imagery (Cihlar, 2000; Lillesand et al., 2004). During the past decade Normalized Difference Vegetation Index (NDVI) time series imagery has increasingly been used for land use/land cover mapping and monitoring (Zhang et al., 2003; Xiao et al., 2006a; Wardlow et al., 2007; Bontemps et al., 2008; Zhang et al., 2008; de Bie et al., 2011; Nguyen et al., 2011). NDVI provides a measure of photosynthetically active biomass (Sarkar and Kafatos, 2004). The available NDVI time series data suffer from cloud contamination, thus limiting the quality of the maps generated (Jonsson and Eklundh, 2002; Fensholt et al., 2006; Ma and Veroustraete, 2006; Hird and McDermid, 2009; Clark et al., 2010).

The presence of clouds and haze reduces the spectral reflectance in infra-red, causing reduced NDVI readings (Gu et al., 2009). To overcome contamination caused by clouds and atmospheric effects at data supplier level, the pre-processing routines for satellite data include the generation of quality flags, and maximum value composite (MVC) imagery (Holben, 1986; Stowe et al., 1991). The remaining cloud corrections and adjustments are made at user level through the use of provided quality flags and data adjustment algorithms.

The quality flags provide pixel-level information about presence of atmospheric aerosols, cloud cover, presence of snow and ice cover, likelihood of shadow, and bidirectional reflectance (Stowe et al., 1991; Ackerman et al., 1998; Stowe et al., 1999). At user level, they provide important information that serves to reduce the use of spurious NDVI data (Jonsson and Eklundh, 2002).

The maximum value composite technique (Holben, 1986; Stowe et al., 1991) selects the highest recorded value for each pixel during a pre-defined period of time. The technique has improved the overall data quality, reducing the effects of clouds and haze. However, in the tropics and some coastal regions where cloud cover persists for long duration, maximum value composite technique is known to be poor in dealing with cloud contamination (Holben, 1986; Goward et al., 1991; Verhoef et al., 1996; Cihlar et al., 1997; Roerink et al., 2000; Fensholt et al., 2010).

To adjust NDVI values affected by undetected clouds and those marked missing using quality flags, researchers have proposed a number of methods. These include best index slope extraction (BISE) (Viovy et al., 1992), the weighted least squares regression approach (Swets et al., 1999), geostatistical methods (Addink and Stein, 1999; Van der Meer, 2012), modified BISE filtering (Lovell and Graetz, 2001), Fourier analysis (Verhoef et al., 1996; Roerink et al., 2000; Moody and Johnson, 2001; Wagenseil and Samimi, 2006), mean value iteration (Ma and Veroustraete, 2006), function fitting approaches (adaptive Savitzky-Golay and logistics function fitting) (Jönsson and Eklundh, 2004), the whittaker smoother (Atzberger and Eilers, 2011b), wavelets (Lu et al., 2007) and iterative interpolation for data reconstruction (Julien and Sobrino, 2010). However, scientists have reported that, although they are able to adjust data affected by short-duration clouds, they are unable to correct the long-duration cloud contamination problem (Jonsson and Eklundh, 2002; Chen et al., 2004; Jönsson and Eklundh, 2004; Lu et al., 2007; Atzberger and Eilers, 2011a). The characterization of cloud duration as short or long is relative and changes with different correction tools applied; depending upon their robustness to deal with data contamination resulted due to clouds.

The NDVI time series data affected by long-duration clouds reduce the quality of any subsequent interpretation. The authors recognized the need and aims to develop a procedure to detect which data are affected by long-duration cloud contamination particularly in the case of hyper-temporal NDVI time series. After detection, a user can flag those values as missing and avoid their use during subsequent analysis. The method builds on statistically derived unsupervised classification of the time series imagery.

2.2 *Materials and methods*

2.2.1 *Study area*

Ghana was selected as study area because of the high frequency of cloudy days (Figure 2.1). It has a tropical savanna climate (Peel et al., 2007), with annual temperatures above 24^{o}C (Ghana Environmental Protection Agency, 2001). Ghana has two distinct rainfall regimes in two different parts of the country. Southern Ghana has a high frequency of cloudy days and receives more rainfall than the northern parts (Kakane and Sogaard, 1997; Shahin, 2002; Fensholt et al., 2007). Annual average rainfall varies from 600 to 2100 mm in the southern regions and is marked by two wet seasons: March-July, and September-November (Owusu et al., 2008). In northern Ghana, rainfall occurs in one season (May to October), with annual rainfall ranging from 700 to 1100 mm.

2.2.2 *Data pre-processing*

MODIS Terra (MOD13Q1) and MODIS Aqua (MYD13Q1) 16-day maximum value composite NDVI imagery with a 250 m spatial resolution was downloaded from https://wist.echo.nasa.gov/wist-bin (accessed February 2010). The imagery covered the period from 1 January 2003 to 31 December 2009.

Terra and Aqua sensors acquire images at two different times of the day (Terra 10:30 am and Aqua 01:30 pm local standard time). The downloaded Terra and Aqua 16-day maximum value composite imagery has similar spatial, spectral and radiometric characteristics. NDVI values of Terra and Aqua are reported to be strongly correlated (R^2=0.97, RMSE=0.04) (Gallo et al., 2005).

The Vegetation Index Quality (VIQ) layers provide pixel values affected by clouds, haze and other atmospheric effects, which were used to set the value of those pixels to missing. All NDVI values were transformed to DN values (0-255) using Eq. 1, where DN=0 is coded as missing.

$$NDVI\ (DN\text{-}\ value) = integer_{16\text{-}bit\ signed}\ of\ NDVI * 0.02133 + 43.117 \qquad \text{(Eq. 1)}$$

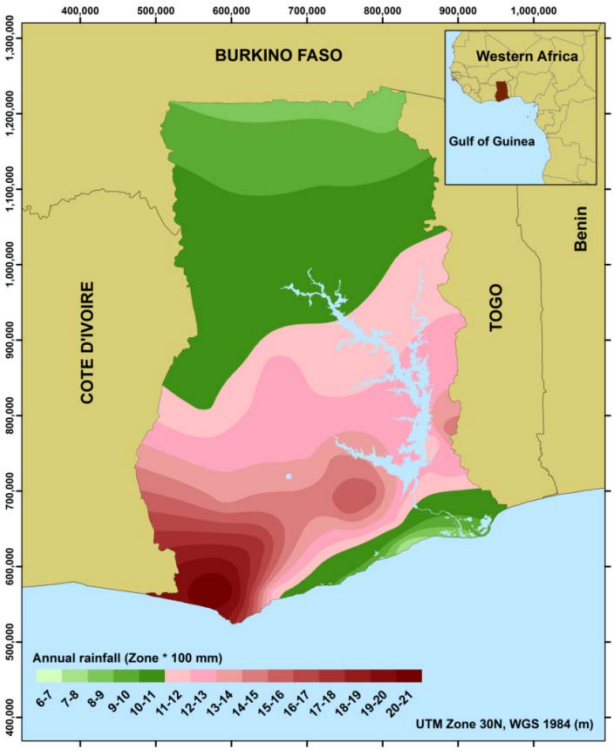

Figure 2.1. Rainfall map of Ghana, showing spatial distribution of mean annual rainfall (1961-1997) (source: Ghana Meteorological Services Department, Leigon, Ghana).

The Terra-Aqua dataset was generated by combining both Terra and Aqua maximum value composite NDVI imagery. The combined dataset was expected to suffer less from cloud contamination because it is based on two images a day instead of one.

Pixel-specific date stamps were used to combine the two images. They have an 8-day difference in the start dates of their 16-day maximum value composite periods, meaning that an 8-day shift between the two imagery series occurred. We retained the Terra 16-day period as default when merging the Aqua data. Using pixel-specific date stamps, the pixel-specific Aqua values were compared with the corresponding maximum value composite values of the Terra imagery; the highest values (maximum composite) were kept to represent the relevant Terra period and pixel.

Finally, the adaptive Savitzky-Golay method built in TIMESAT was used to remove short-duration impacts on cloud-affected pixel values of the Terra and Terra-Aqua NDVI datasets (Jönsson and Eklundh, 2004; Beltran-Abaunza, 2009). This method is widely used and found useful for noisy and

non-uniform NDVI time series datasets (Jönsson and Eklundh, 2004; Feng et al., 2008; Beltran-Abaunza, 2009; Boschetti et al., 2009).

2.2.3 *Long-duration cloud contamination detection*

The pre-processed Terra hyper-temporal NDVI dataset, composed of 161 layers, was classified into 10 to 100 classes using the Iterative Self-Organizing Data Analysis (ISODATA) algorithm (Ball and Hall, 1965; Tou and Gonzalez, 1974). ISODATA is used for an unsupervised classification of patterns in remote–sensing into clusters or classes (Jain et al., 1999). It is iterative and self-organizing, which repeats itself and locates classes with minimum user input (Tou and Gonzalez, 1974; Swain and Davis, 1978). No prior knowledge is needed to train the processing. This has more consistent results and easy to reproduce. Similarly different forms of statistics such as divergence statistics; Jeffries-Matsushita can be calculated for each class to finally select the optimum classification result (de Bie et al., 2012).

The ISODATA algorithm was run with the convergence threshold set to 1 and iterations set to 50. After classification, the average and minimum divergence values between cluster centroids were plotted against the number of classes generated. Coinciding high average and minimum divergence values were used as guidance to select the optimal classified image (Swain and Davis, 1978). The statistics generated by the ISODATA algorithm for selected NDVI classes were used to detect areas affected by long-duration cloud contamination.

NDVI profiles representing the mean NDVI values of all the pixels of the respective class were plotted over time (2003-2009) to visualize their temporal behaviour, and based on shape and intensity the NDVI profiles were assigned to different groups.

The mean NDVI 95% confidence interval lower limit and the standard deviation 95% confidence interval upper limit were calculated to objectively define cloud contamination in NDVI values. To calculate the lower limit of the 95% confidence interval of NDVI, first the mean annual NDVI profiles (23 values) were calculated by averaging each decade from 2003 to 2009. After that a single mean NDVI profile of all the classes in a group was created and used as a reference for calculating the lower limit 95% confidence interval for that group. The mean profile of all the classes portrayed the normal behaviour of all the classes in a group and was used as a reference for defining a suspicious decline. Similarly the standard deviation values of each class in a group were first averaged (pooled standard deviation) on decadal basis across the years (2003-2009) to create a mean profile of each class (23 values) in a group. They were then averaged (pooled standard deviation) per

group to create a single standard deviation profile as a reference to find an upper limit 95% confidence interval of standard deviation values. The 95% confidence interval is used to indicate a statistically safe range within which a value can be considered closer to the actual values (Burns and Burns, 2008). The upper limit 95% confidence interval of standard deviation values was used because cloud contamination negatively affects NDVI values therefore increases the standard deviation values (Figure 2.2).

To identify long-duration cloud contamination within a group of NDVI profiles, the NDVI and standard deviation profile of each class within that group were plotted. The mean NDVI 95% confidence interval lower limit and the standard deviation 95% confidence interval upper limit were added to the NDVI standard deviation plots. A decline in NDVI value below the lower limit of the 95% confidence interval and a concurrent increase in standard deviation above the upper limit of the 95% confidence interval indicate long-duration cloud contamination.

2.2.4 *Validation*

Two groups of Terra-NDVI classes with a suspicious decline in NDVI values were randomly chosen for the validation analysis. Firstly, the level of differences between NDVI values extracted from Terra and Terra-Aqua NDVI imagery was inspected by comparing two NDVI classes from one of the selected group. It was checked to see whether the period showing high differences between the two imagery products coincided with an increase in the standard deviation values of the Terra-based NDVI classes.

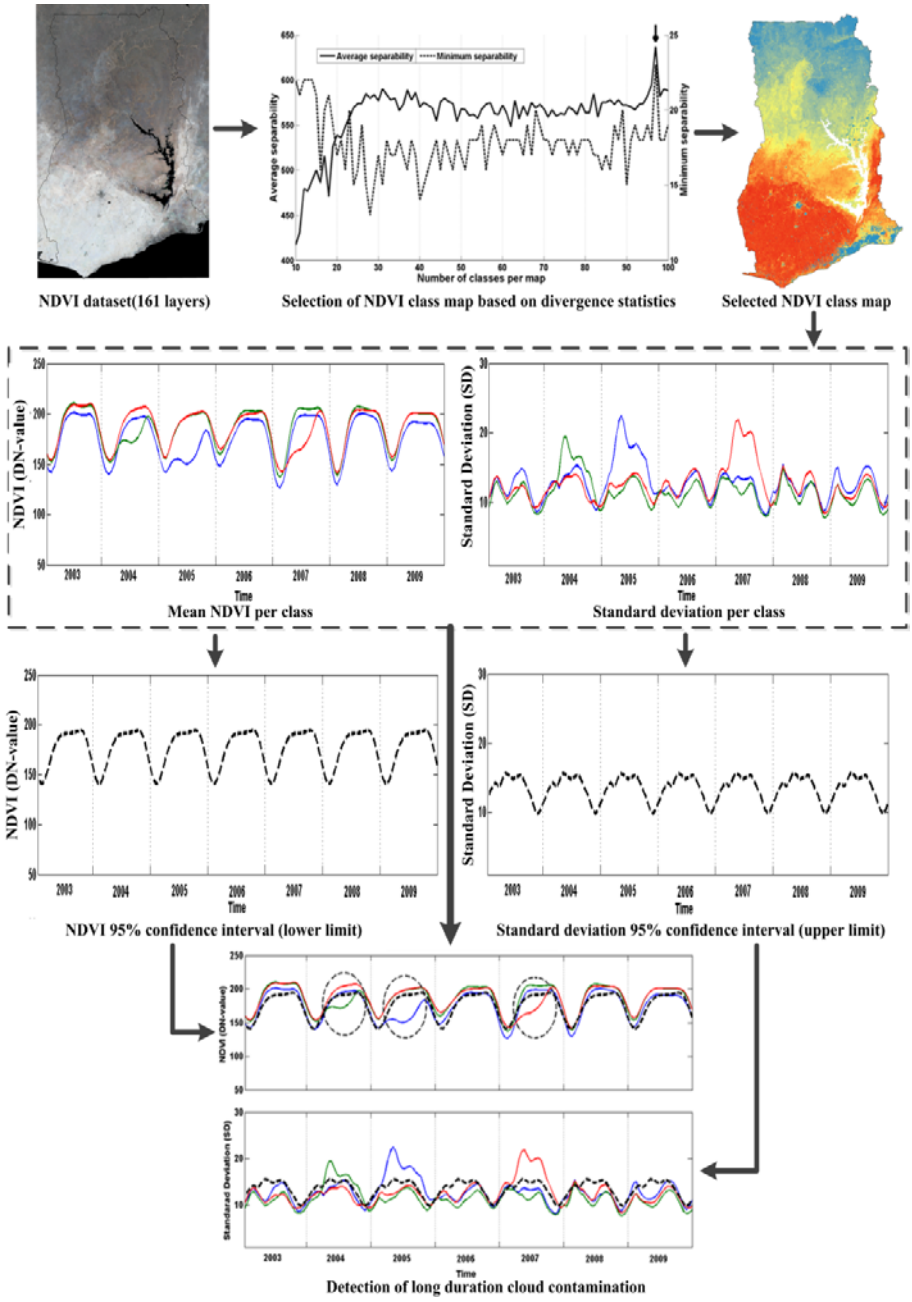

Figure 2.2. Schematic diagram of the method used.

Secondly, regression analyses were carried out per NDVI class to statistically test whether standard deviation values related to long-duration cloud contamination. The analysis was performed using the differences in the NDVI values of the Terra and Terra-Aqua products versus the standard deviation

values of the Terra product for all the NDVI classes in the two selected groups.

2.3 *Results*

2.3.1 *Long-duration cloud contamination detection*

Using the ISODATA algorithm, the pre-processed Terra dataset was classified into maps with 10 to 100 NDVI classes. Divergence statistics revealed a high average separability for the 97-class map, coinciding with a peak in minimum divergence statistics (Figure 2.3). The 97-class map was selected as the optimal classification result. This map and derived statistics were used onwards for detecting long duration cloud contamination.

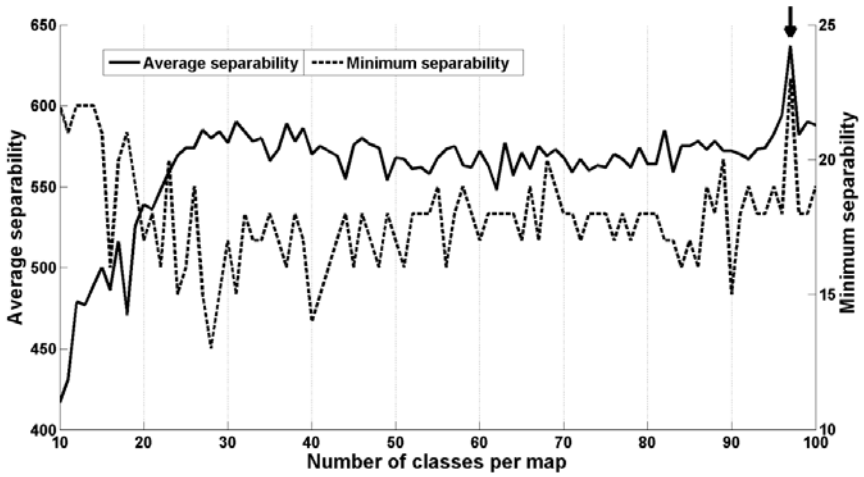

Figure 2.3. Average and minimum divergence statistics of maps with 10 to 100 classes. The arrow points to the coinciding peak in both separability values (97 classes).

The NDVI and standard deviation plots were organized in groups on the basis of comparable temporal behavior, as shown in Figure 2.4. NDVI class profiles of those classes showing a decline in seasonal NDVI values (growing season) below the lower limit of the 95% confidence interval as well as a concurrent increase in standard deviation values above the upper limit of the 95% confidence interval (marked with circles) were found having suspicious NDVI values (Figure 2.4a). These long term drops in NDVI values were considered suspicious because they were not consistent with the historical trends of the classes in same group and it is unlike the annual growth and the decline periods of vegetation of the same group. Similarly high increase in standard values indicates spread of NDVI values, which may be associated with cloud contamination. Similarly high standard deviation values show spread of data values and hence make it suspicious. Figure 2.4a shows 34 NDVI classes

found with suspicious NDVI values. These NDVI classes were located mainly in the annual average rainfall zone of 1200 to 2100 mm (Figure 2.1 and Figure 2.8).

(a)

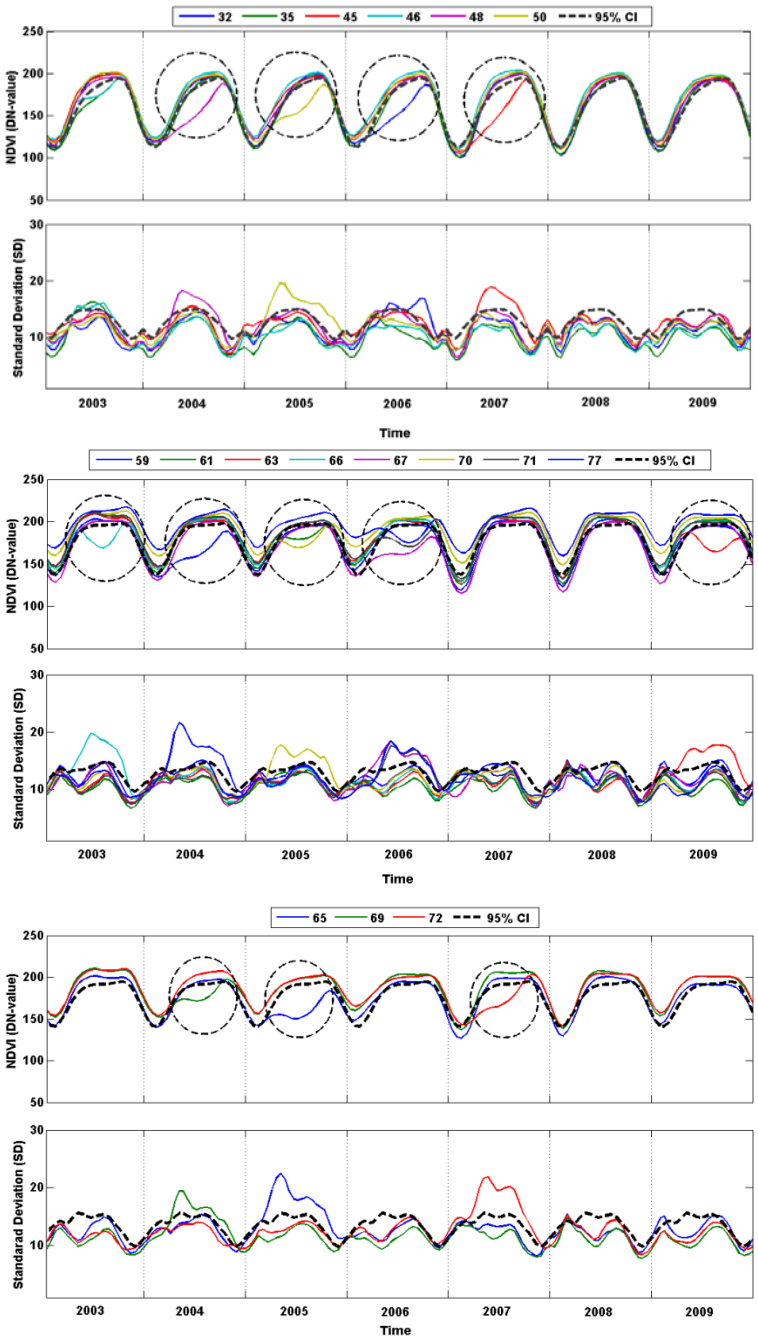

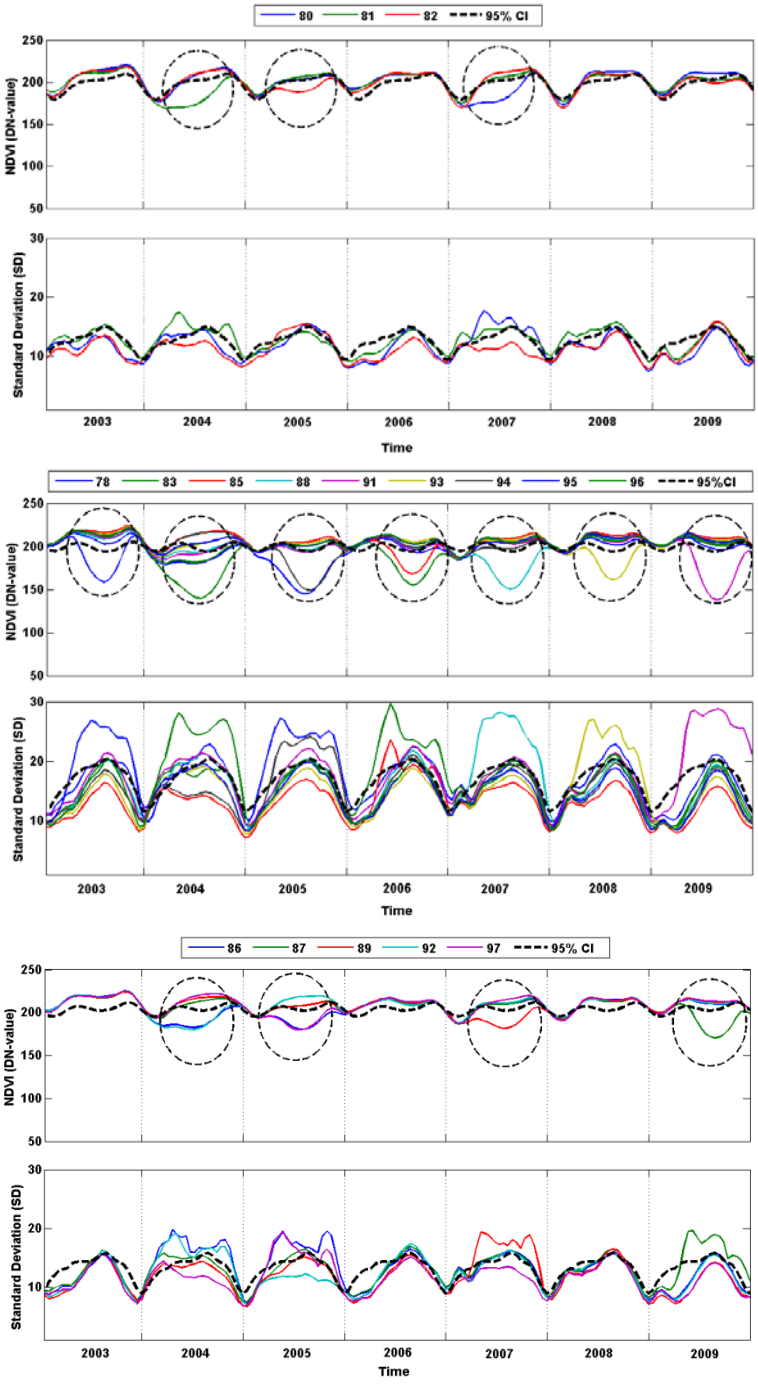
80 81 82 95% CI
NDVI (DN-value)
Standard Deviation (SD)
2003 2004 2005 2006 2007 2008 2009
Time
78 83 85 88 91 93 94 95 96 95%CI
NDVI (DN-value)
Standard Deviation (SD)
2003 2004 2005 2006 2007 2008 2009
Time
86 87 89 92 97 95% CI
NDVI (DN-value)
Standard Deviation (SD)
2003 2004 2005 2006 2007 2008 2009
Time

(b)

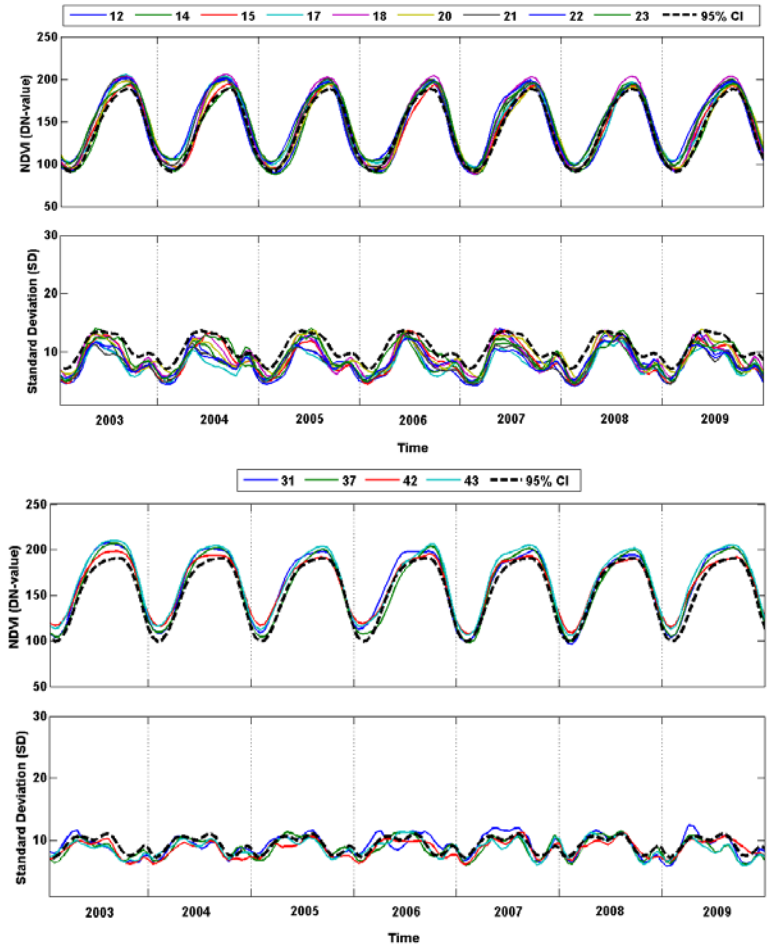

Figure 2.4. Terra-derived NDVI class profiles arranged in groups: (a) characterized by suspicious decline in NDVI values during the growing season (marked with circles) and (b) two groups of NDVI class profiles showing no suspicious decline in NDVI values. 1-sided 95% confidence interval (95% CI) is shown in dashed line.

Compared with Figure 2.4a, groups of the NDVI classes that have a consistent behaviour over time as well as a mean NDVI value that does not decline below the NDVI 95% confidence interval experienced no sharp increase in standard deviation values above the upper limit of the 95% confidence interval (Figure 2.4b). These NDVI classes have smooth and consistent historical trends as compared to profiles of NDVI classes shown in Figure 2.4a. Figure 2.4b shows only two randomly selected NDVI groups which have no suspicious NDVI values. They occur mainly in drier northern zones with less than 1200 mm rainfall (Figure 2.1). The spatial distribution of the NDVI classes is shown in Figure 2.7.

2.3.2 *Validation*

The differences between the NDVI values of the Terra and Terra-Aqua products became large with the decline in seasonal Terra NDVI. The Terra-Aqua profiles do not display such seasonal decline and synchronous sharp increase in standard deviation values (Figure 2.5). It also showed that declines were not related to actual changes in greenness of present land cover but rather to long duration cloud cover.

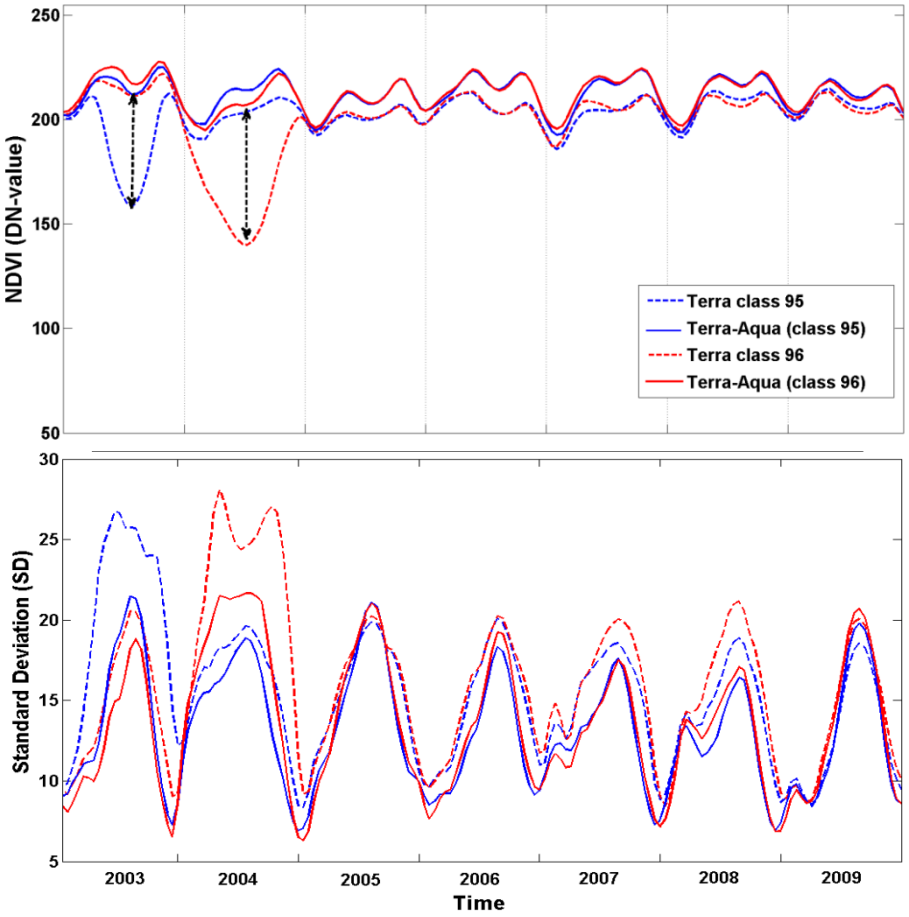

Figure 2.5. Comparison of NDVI and standard deviation profiles of the selected two classes derived from the Terra and Terra-Aqua products. The classes of each product cover similar areas in southern Ghana.

Regression analysis results given in Figure 2.6 showed that the NDVI difference in the Terra product, compared with the Terra-Aqua product, was significantly ($p<0.05$) correlated with the standard deviation values of the Terra product.

(a)

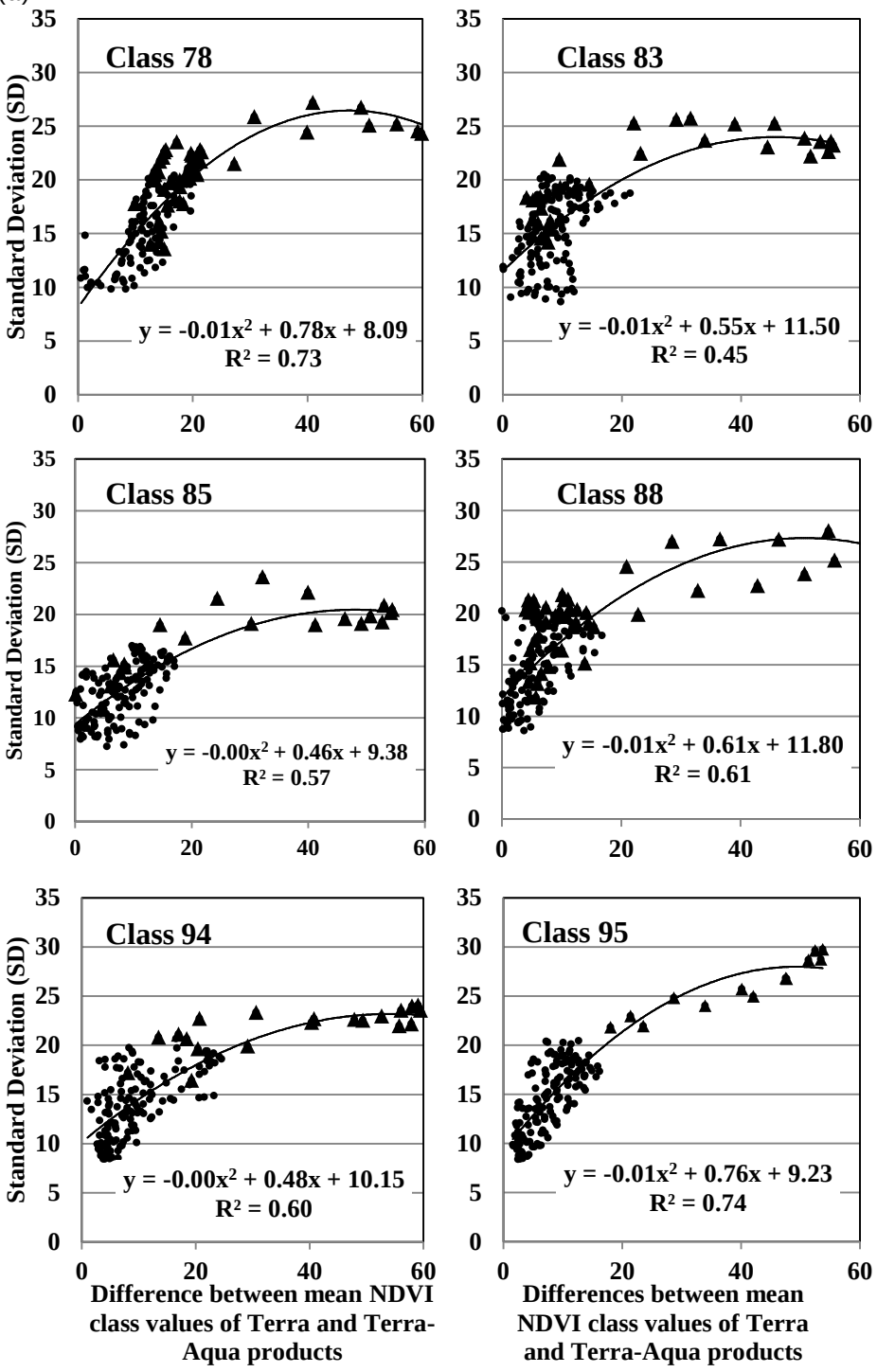
Class 78
y = -0.01x² + 0.78x + 8.09
R² = 0.73
Class 83
y = -0.01x² + 0.55x + 11.50
R² = 0.45
Class 85
y = -0.00x² + 0.46x + 9.38
R² = 0.57
Class 88
y = -0.01x² + 0.61x + 11.80
R² = 0.61
Class 94
y = -0.00x² + 0.48x + 10.15
R² = 0.60
Class 95
y = -0.01x² + 0.76x + 9.23
R² = 0.74
Standard Deviation (SD)
Difference between mean NDVI class values of Terra and Terra-Aqua products
Differences between mean NDVI class values of Terra and Terra-Aqua products

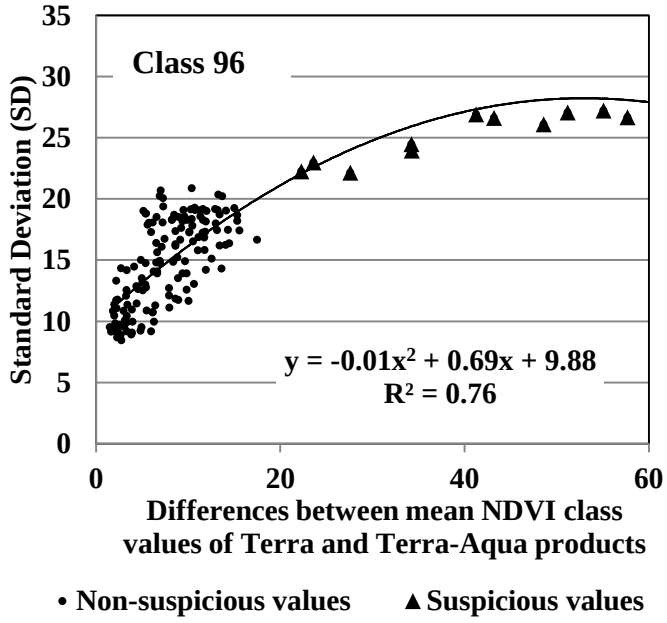
Class 96
Standard Deviation (SD)
y = -0.01x² + 0.69x + 9.88
R² = 0.76
Differences between mean NDVI class values of Terra and Terra-Aqua products
• Non-suspicious values
▲ Suspicious values

(b)

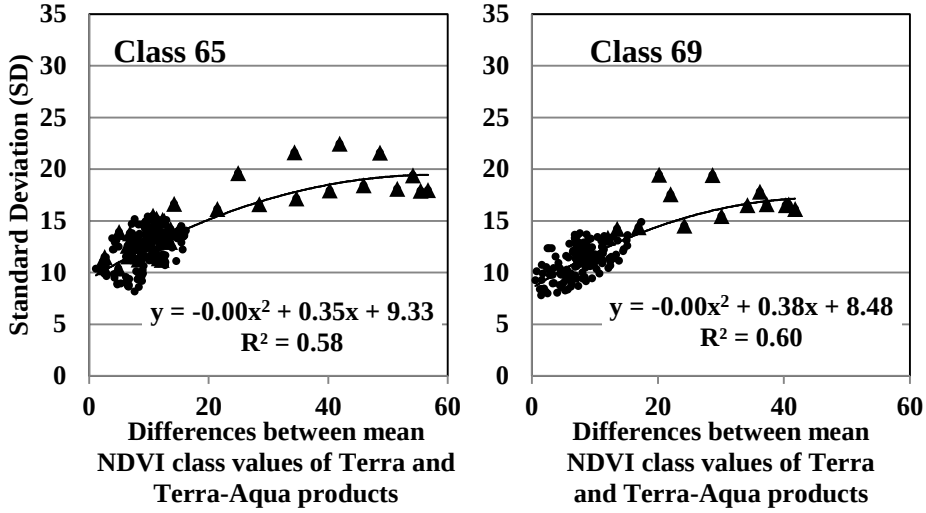
Class 65
Standard Deviation (SD)
y = -0.00x² + 0.35x + 9.33
R² = 0.58
Differences between mean NDVI class values of Terra and Terra-Aqua products
Class 69
y = -0.00x² + 0.38x + 8.48
R² = 0.60
Differences between mean NDVI class values of Terra and Terra-Aqua products

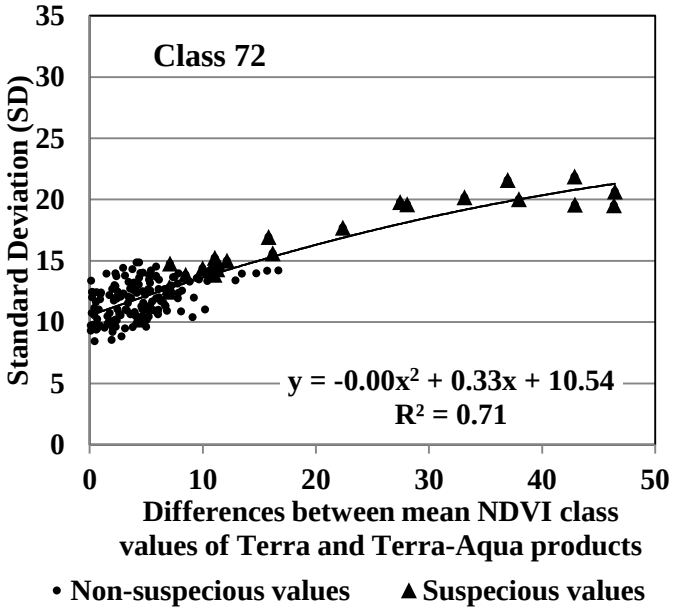

Figure 2.6. Scatterplots showing relationship between differences in NDVI of Terra and Terra-Aqua products and the standard deviation derived from the Terra product of two randomly selected groups of NDVI classes.

The R^2 values of 0.73, 0.45, 0.57, 0.61, 0.60, 0.74 and 0.76 was found in case of NDVI classes 78, 83, 85, 88, 94, 95 and 96 respectively (Figure 2.6a). Similarly the second group of NDVI classes (65, 69 and 72) recorded R^2 of 0.58, 0.60 and 0.71 respectively (Figure 2.6b). From Figure 2.7 it can also be deduced that standard deviation values above a 95% confidence interval upper limit relate to cloud contamination, as discriminated by NDVI classes showing decline in seasonal NDVI values below a 95% confidence interval lower limit.

2.4 *Discussion*

This study has introduced an exploratory method that detects long-duration cloud contamination that in turn results in unreliable NDVI values. The method presented in this article requires no additional source of information or external data for execution purposes but requires the unsupervised classification of the imagery to carry out the evaluation of class-specific mean NDVI and standard deviation values over the time. Including this method in the pre-processing routines of NDVI time series data can help to avoid the use of anomalous NDVI data in time series studies. The method can be applied to any type of time series data, irrespective of spatial and temporal variations. The method is simple to implement and reproduce. This technique

can be beneficial for NDVI spectro-temporal analysis based land use/land cover mapping and monitoring, particularly in the tropics.

A synchronous decline in seasonal NDVI values below a lower limit 95% confidence interval and an increase in the standard deviation above an upper limit 95% confidence interval indicate possible long-term cloud contamination that was not removed by preprocessing routines. From Figure 2.4 it is obvious that the decline in NDVI, which is linked to an increase in standard deviation values above the threshold (95% confidence interval), marks the periods when the NDVI values are affected by long-duration cloud cover. This is also proved in the regression analysis, which shows a positive and linear relation between differences in the Terra and Terra-Aqua imagery products versus standard deviation values of the Terra imagery (Figure 2.6). The use of the 1-sided 95% confidence interval helps to objectively define the contamination. This also eliminates the short time effects in NDVI values unrelated to long-term missing data.

The validation using regression analysis to compare standard deviation and differences between the Terra and Terra-Aqua products was undertaken because standard deviation is considered the most common indicator to explain spread of data values (Myers, 1997). The Terra-Aqua product suffers less from cloud contamination, since it is a combination of two images per day. Fensholt et al., (2006) also used differences between Terra and Aqua as proxy for cloud cover. However, it is also notable that standard deviation alone can mislead interpretations because standard deviation normally increases in summer and decreases in winter owing to contrast in the reflectance of vegetation and soil (Gonza´ Lez Loyarte and Menenti, 2000; Loyarte and Menenti, 2008). It is also clear from the results that the coinciding of seasonal decline in observed NDVI with increased standard deviation readings is suspicious.

This is the first study if its kind that successfully attempts to detect long duration cloud contamination affects in hyper-temporal NDVI imagery. In contrast, the available cloud contaminated data correction techniques are unable to correct long data gaps due to the inherent limitations associated with the models used (Holben, 1986; Swets et al., 1999; Jonsson and Eklundh, 2002; Fensholt et al., 2007; Lu et al., 2007; Gu et al., 2009; Hird and McDermid, 2009; Julien and Sobrino, 2010). By including this method in the preprocessing routines of NDVI time series analysis can help to mark the period and location of long duration cloud contaminated NDVI values, which can be avoided in subsequent data analysis.

The spatial distribution of cloud-contaminated NDVI classes over an areas receiving more rainfall (>1200 mm) signify that areas receiving more rainfall

and cloud cover experienced cloud contamination. More prevalent rainfall in southern Ghana is also reported by and Kakane and Sogaard (1997), Fensholt et al., (2006) and Fensholt et al.,(2007). While in contrast those NDVI classes having no obvious contamination problem are distributed through northern Ghana, which is drier region with less chances of persistent cloud cover (Figure 2.1 and Figure 2.7).

2.5 *Conclusion*

In this paper a simple exploratory method is introduced to detect long duration cloud contamination effects in hyper temporal NDVI imagery analysis. This is an approach, that goes beyond the use of quality flags and upper envelope filtering is tested to detect when and where long-duration clouds are responsible for unreliable NDVI readings. The approach offers the scientists interested in time series analysis, a method of masking by area (class) the periods when pre-cleaned NDVI values remain affected by clouds. It requires no additional data for execution purpose but involves unsupervised classification of the imagery to carry out the evaluation of class-specific mean NDVI and standard deviation values over the time. The method was validated with secondary dataset; however, it needs to be validated with real cloud cover data in future. The method will be useful for time series imagery based land cover mapping and monitoring specifically in areas where cloud cover is prevalent such as tropics.

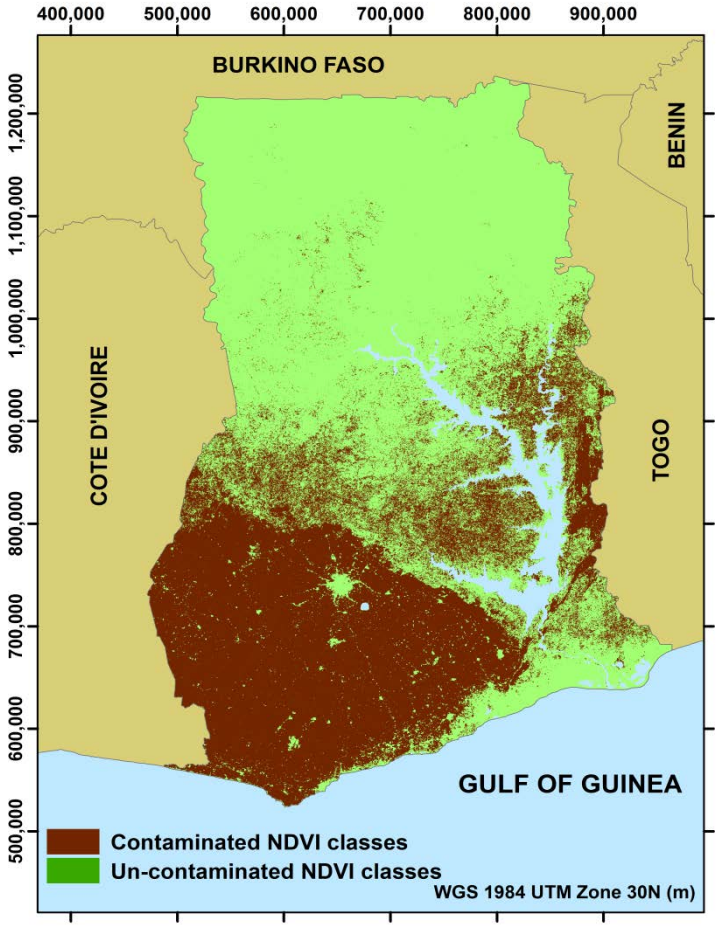

Figure 2.7. The spatial distribution of contaminated and uncontaminated NDVI classes.

Acknowledgements

The authors acknowledge the financial support of the Higher Education Commission of Pakistan, the Pakistan Space and Upper Atmosphere Research Commission (SUPARCO) and Faculty of Geo-Information Science and Earth Observation (ITC), University of Twente. Special thanks are extended to Janice Collins for help with English editing. We would like to thank two anonymous reviewers for their constructive comments to improve this manuscript.

3 Mapping land cover gradients through analysis of hyper-temporal NDVI imagery[2]

[2] Chapter is based on: A. Ali., C. A. J. M. de Bie., A. K. Skidmore, R. G. Scarrott., A. Hamad., V. Venus and P. Lymberakis., 2013. Mapping land cover gradients through analysis of hyper-temporal NDVI imagery," International Journal of Applied Earth Observation and Geoinformation 23, 301–312.

Abstract

The green cover of the earth exhibits various spatial gradients that represent gradual changes in space of vegetation density and/or in species composition. To date, land cover mapping methods differentiate at best, mapping units with different cover densities and/or species compositions, but typically fail to express such differences as gradients. Present interpretation techniques still make insufficient use of freely available spatial-temporal Earth Observation (EO) data that allow detection of existing land cover gradients. This study explores the use of hyper-temporal NDVI imagery to detect and delineate land cover gradients analyzing the temporal behavior of NDVI values. MODIS-Terra MVC-images (250 m, 16-day) of Crete, Greece, from February 2000 to July 2009 are used. The analysis approach uses an ISODATA unsupervised classification in combination with a Hierarchical Clustering Analysis (HCA). Clustering of class-specific temporal NDVI profiles through HCA resulted in the identification of gradients in landcover vegetation growth patterns. The detected gradients were arranged in a relational diagram, and mapped. Three groups of NDVI-classes were evaluated by correlating their class-specific annual average NDVI values with the field data (tree, shrub, grass, bare soil, stone, litter fraction covers). Multiple regression analysis showed that within each NDVI group, the fraction cover data were linearly related with the NDVI data, while NDVI groups were significantly different with respect to tree cover (adj. R^2=0.96), shrub cover (adj. R^2=0.83), grass cover (adj. R^2=0.71), bare soil (adj. R^2=0.88), stone cover (adj. R^2=0.83) and litter cover (adj. R^2=0.69) fractions. Similarly, the mean Sorenson dissimilarity values were found high and significant at confidence interval of 95% in all pairs of three NDVI groups. The study demonstrates that hyper-temporal NDVI imagery can successfully detect and map land cover gradients. The results may improve land cover assessment and aid in agricultural and ecological studies.

Keywords: land cover; gradient; hyper-temporal; NDVI; MODIS; mapping

3.1 *Introduction*

A gradient is an inherent property of all environmental conditions (e.g. soil moisture, precipitation, temperature) (Whittaker, 1978a; Begon et al., 1990; Foody and Boyd, 1999). Each location on the earth's surface is subject to both abiotic and biotic environmental gradients (Begon et al., 1990), which influence species distributions in space and time. Therefore species abundance, and overall community composition can change continuously along environmental gradients (Whittaker and Levin, 1977; Townsend, 2000; Tapia et al., 2005; Tang et al., 2010). Mapping the abundance of individual species can consequently reflect land cover gradients (Müller, 1998). Within the context of this research, a land cover gradient can be considered to be "the gradual spatial changes in green cover of the earth's surface caused by differences in plant species composition and/or their densities". Recognizing land cover gradients is reported as important for many environmental and ecological studies (Whittaker, 1973; Whittaker, 1978b; Gosz, 1992).

The spatial patterns exhibits by green cover that represent gradual changes in space of vegetation density and/or in species composition can be discerned using the growth responses in local vegetation, which are produced as a result of different biotic and abiotic environmental factors. Within the context of this research, a land cover gradient is considered to be a spatial relationship between gradually differencing land cover units having similar vegetative growth patterns (Figure 3.1). Looijen and Andel, (1999) also noted the relationship between spatial patterns as they occur higher or lower in a gradient due to its response to environmental factors. This concept of gradient analysis considering relationship between spatial patterns characterized by gradual changes in structure and variation of vegetation is also noted by Whittaker (1967).

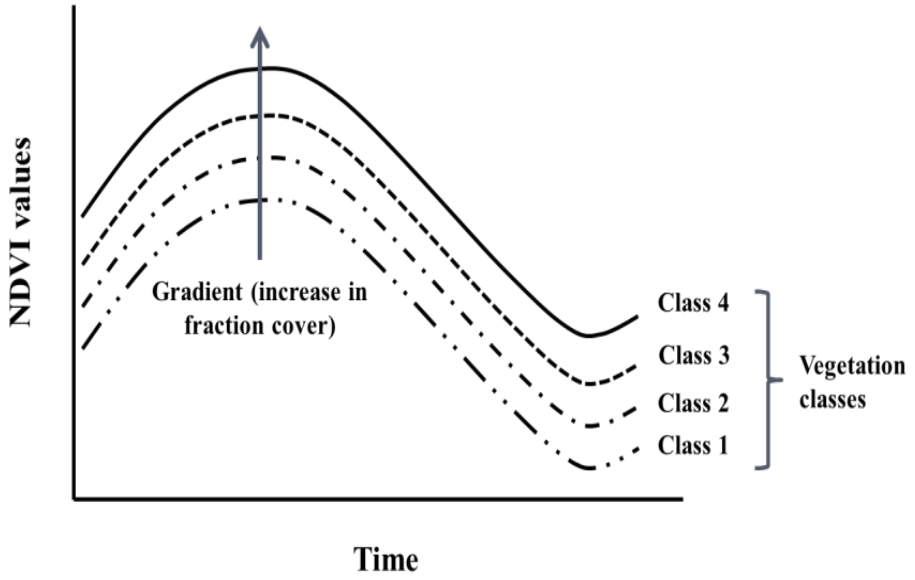

Figure 3.1. A conceptualization of the land cover gradients based on vegetative growth patterns.

The presence of gradients in land cover (LC) is the result of spatio-temporal phenomenon (Müller, 1998; Löffler and Finch, 2005; Sklenár et al., 2008) as underlying factors (e.g. geology, climate, topography) responsible for such gradients vary continuously over space and time (Foody and Boyd, 1999). This emphasizes the importance of exploiting spatio-temporal datasets to identify existing gradients as displayed by land cover (Austin, 1990; Begon et al., 1990; Gosz, 1992; Kent et al., 1997; Foody and Boyd, 1999; Couteron et al., 2006). Thus, the need is clearly articulated to improve land cover maps with specifications of present land cover gradients, using both spatial and temporal aspects of land cover.

Many studies to map land cover gradients have been carried out using imagery from a single date, or at most using imagery acquired on 2 to 3 dates for example (Haralick et al., 1973; Wood and Foody, 1989; Bradshaw and Spies, 1992; Foody, 1992; Skidmore and Turner, 1992; Trodd, 1992; Foody and Trodd, 1993; Gulinck et al., 1993; Trodd, 1993; Foody, 1996a, b; Bastin, 1997; Zhang and Foody, 1998; Foody and Boyd, 1999; Gopal et al., 1999; Csillag and Kabos, 2002; Mendel and John, 2002; Deer and Eklund, 2003; Kavzoglu and Mather, 2003; Fonte and Lodwick, 2004; Camarero et al., 2006; Fisher et al., 2006; Arnot and Fisher, 2007b; Berberoglu et al., 2007; Fisher et al., 2007; Verstraete et al., 2007; Dixon and Candade, 2008; Krishnaswamy et al., 2009; Fisher, 2010; Mitrakis et al., 2011). Because all these studies were based on the use of at most, a few images, mapping

existing land cover gradients has remained elusive. This in spite of the fact that a wide variety of potentially applicable methods have been explored: probability mapping, neural network, wavelet analysis, line intersect method, ordination techniques, Normalised Difference Vegetation Index (NDVI) based Mahalanobis distance measures, textural analysis, adjacent patch analysis, and split windows. No author sought to replace their temporally-limited set of used imagery with hyper-temporal imagery for mapping land cover gradients. This potentially imposed limitations on their studies to adequately capture temporal aspects of land cover growth patterns, caused by differences in species composition and/or in their densities, and their responses to local environmental conditions.

Hyper-temporal imagery can provide the temporal resolution required to capture such patterns in annual growth cycles. The term “hyper-temporal” is used to describe long-term, extensively repeated (daily) time series datasets of an area (Piwowar and LeDrew, 1995; Piwowar et al., 1998; McCloy, 2006; de Bie et al., 2008). Due to their highly repetitive coverage, hyper-temporal image dataset can capture the subtle fluctuations in growth characteristics exhibited by vegetation over time. It has been found useful in studies of vegetation growth cycles in support of agricultural and ecological studies (Reed, 2006; Xiao et al., 2006a; Wardlow et al., 2007; Beck et al., 2008; de Bie et al., 2008; Zhang et al., 2008; Khan et al., 2010), However it has not yet been explored whether such datasets can be used to capture and visualize gradients in land cover. Accordingly, this study aims to explore whether such land cover gradients can be identified and mapped through the use of hyper-temporal NDVI imagery.

3.2 *Method*

3.2.1 *Study area*

Crete (Greece) is a Mediterranean island with an area of 8729 km^2 featuring high plant diversity (Turland et al., 1993; Montmollin and Iatrou, 1995; Vogiatzakis and Griffiths, 2001). The island has varied terrain (high mountains to coastal areas) and regional to local climatic differences which are reflected in distinct vegetation patterning across the island (Turland et al., 1993; Montmollin and Iatrou, 1995; Chartzoulakis et al., 2001; Chartzoulakis and Psarras, 2005).The predominant vegetation types include; Olea and Ceratonia forest (20.69%), Sarcopoterium spinosum phrygana (27.32%), Cupressus (1.12%), Acero-Cupression(4.02%), Oro-mediterranean phrygana (3.52%), Dehesas (5.38%), Mediterranean pine forest (4.84%), Euphorbio-Verbascion phrygana (3.20%) (Sarris et al., 2005b). The geology varies from calcareous rocks (limestone and dolomites) dominate the mountain terrain to limestone, sandstone and marls, cover

large areas of the lowlands (Sarris et al., 2005a). These variations in terrain, climate, geology, combined with high plant diversity, results in a high spatial variability of land cover (Körner, 2000; Löffler and Finch, 2005). This spatial heterogeneity makes the area suitable for exploring the potential of mapping land cover gradients using hyper-temporal NDVI imagery (Figure 3.2).

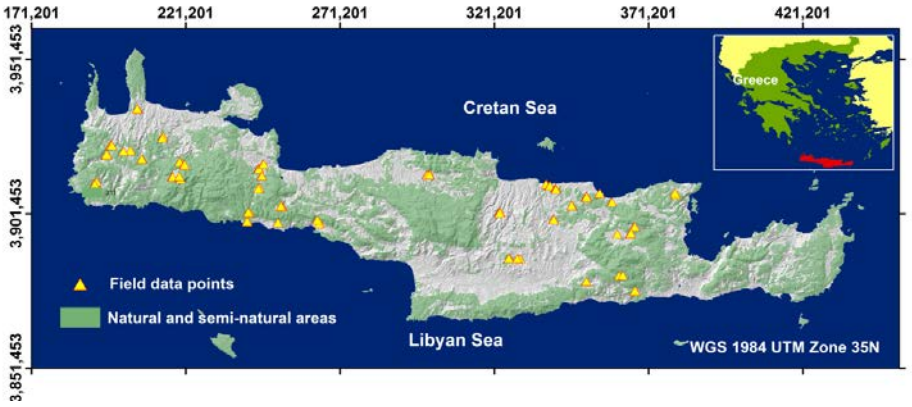

Figure 3.2. The island of Crete, Greece, showing field data points and natural and semi-natural areas.

3.2.2 *Data used*

MODIS NDVI data

A time-series (February 2000 to July 2009) dataset of 293 16-day composite MODIS Terra NDVI data, at 250 m spatial resolution, was downloaded from EOS NASA Land Processes Distributed Active Archive Center (WIST). Those pixels possibly affected by haze, clouds or other atmospheric disturbances were removed using the Vegetation Index Quality (VIQ) information supplied with the NDVI dataset. The NDVI was rescaled to DN values of 0 to 255 for ease of handling and better representation. Note that such a rescaling does not result in a loss of information (Roderick et al., 1996). Pixels with a negative NDVI (representing water) were also removed from the dataset.

The resultant 293 images were compiled into a single NDVI time-series image stack of sequentially ordered NDVI images. To account for data gaps, and to retain the upper envelope of NDVI time-series within the dataset, an Adaptive Savitzky-Golay filter (ASAVGOL) was applied (Jönsson and Eklundh, 2004; Beltran-Abaunza, 2009).

ALOS images

Ten meter spatial resolution ALOS (Advanced Land Observing Satellite) AVNIR-2 multispectral images were acquired for 9 July 2009, 14 July 2009, 26 July 2009, 9 May 2008, and 4 November 2008, from the Remote Sensing

Technology Center (RESTEC) (http://www.alos-restec.jp/products_e.html). They were used during fieldwork to select image objects (disjoint regions characterized by similar properties) for data collection. Only image objects that were different and homogenous in nature were selected for field data collection. The homogeneity of image objects was visually determined based on texture, shape and colour.

CORINE Land cover map

The 2000 Coordination of Information on the Environment (CORINE) Programme datasets contains land cover information for European Member States with a pan-European legend. To gain an initial insight into the area, and guide sample site selection, the CORINE 2000 land cover map of Crete, Greece, was obtained from the European Environmental Agency (EEA). The dataset was used to preselect natural and semi-natural areas (Figure 3.2) for preparation of a sampling scheme to collect field data in order to validate the gradient map.

Field data

Field data were collected using a stratified random clustered sampling scheme. Selected NDVI class map obtained as result of ISODATA clustering of the hyper-temporal NDVI dataset was used as strata. The CORINE land cover map of 2000 was used to mask out agricultural and urban areas related NDVI classes from the sampling scheme. Based on the time available for field work (22 September – 11 October 2009) twenty nine (29) locations were randomly selected on the selected NDVI class map. Figure 3.2 shows the locations and field points sampled during field work. The selected locations were sampled in the field in clusters. The data were collected from the image objects identified on an ALOS image. At each sampled location, data were collected on ground cover composition as well as vegetation traits. Ground cover observations included factors such as percentage cover of stone, litter and bare soil cover, while vegetation observations involved estimation of the percentage cover of tree, shrub and grass layers. Percentage cover was estimated as vertical cover, thus the total percentage for all cover in one sample area was 100. Information was also collected about the dominant plant species within each sample site. Dominant species samples were gathered and stored to be later verified by an expert botanical taxonomist.

To upscale the field data to the NDVI classes, initially an image legend was created, derived from snapshots of homogenous image objects of ALOS image surveyed in the field along with the percentage cover of different land cover components. Based on the image legend, the ALOS image was manually digitized and defined into classes with attributes using fraction cover of land cover components. The digitizing considered feature tone, pattern, shape, texture and association as suggested by Feranec (1999).

Intersecting the digitized ALOS map with the selected NDVI class map, the fractional area of the ALOS classes within each NDVI class was calculated. After obtaining the fractional area, the weighted fraction cover of the trees, shrubs, grass, bare soil, litter and stone cover in each NDVI class were calculated and a single value for each NDVI class was produced. The NDVI classes defined using the fraction cover of trees, shrubs, grass, stone, litter and bare soil were further used in the accuracy assessment of land cover gradients.

3.2.3 *Mapping land cover gradients*

Hyper-temporal image dataset analysis

The pre-processed time-series NDVI image dataset (containing 293 sequential images) was clustered using an Iterative Self-Organizing Data Analysis Technique (ISODATA) (Ball and Hall, 1965; Tou and Gonzalez, 1974) from 10 to 100 clusters. For each ISODATA run, the maximum number of iterations was set to 50 and the convergence threshold was 1 (de Bie et al., 2008; Khan et al., 2010). To identify the best clustering result, statistical separability values denoting average and minimum cluster divergence were used, calculated using Eq. 1 (Swain and Davis, 1978; Singh, 1984).

The output cluster image containing the high average and minimum separability values was selected. The selection is based on compromise, between keeping the number of clusters as low as possible, whilst selecting a cluster number with a local high, or a peak in, separability values. The selected image, and its clusters (classes) associated temporal mean NDVI profiles, was then used to analyse and map land cover gradients.

Gradient identification and mapping

Mean NDVI values were extracted for each 16 day composite period from the signature file of the selected ISODATA classified image. The 16-day mean NDVI values were averaged annually from February 2000 to July 2009. Land cover gradients were identified by comparing NDVI classes and their mean annual NDVI profiles as generated through of the selected ISODATA classification. To establish a gradient, NDVI profiles were grouped using the Hierarchical Cluster Analysis (HCA), an exploratory method designed to reveal natural groupings within a data set (Gauch and Whittaker, 1981). In hierarchical clustering, the nearest neighbour method was used with cosine distance as similarity measure. Final clustering were based on smallest ecological distance (relative similarity in term of fraction cover and species composition), which is important for gradient identification (Gauch and Whittaker, 1981). Using HCA, NDVI class profiles exhibiting similar temporal behaviour are thus grouped, keeping in view the shape and intensity of NDVI values.

After grouping with HCA, the NDVI classes of the selected ISODATA classification were listed and arranged in a relational diagram of increasing average NDVI values. Different NDVI groups were given different colours, whilst classes within a group were assigned a hue within the same colour scale for gradient visualization. Closely related NDVI groups were indicated by means of connecting bars. The relational diagram was used as the NDVI map legend for the land cover "gradient map". NDVI classes with similar vegetative growth patterns were considered spatially related to conceptualize land cover gradients used in this paper.

3.2.4 *Accuracy assessment*

Multiple regression analyses (Greene, 1997; Wooldridge, 2009) were carried out to evaluate the land cover gradient both within and between NDVI groups. The analysis determined whether correlations existed between vegetative growth patterns summarized as an annual average NDVI value, and field collected fraction cover data per NDVI class. Presence of a linear relation was used as positive indicator of gradient presence as per the concept used in this study (Figure 3.2). The analysis allowed as to discern whether NDVI classes, though fundamentally different, are connected along gradients, and whether they can be used to represent gradients in land cover and the NDVI groups could represent different dominant gradients (significant differences between the groups) in the land cover of the area.

The analysis was performed on individual land cover components by NDVI classes. Only those NDVI groups consist of NDVI classes, which were covered in the field work, were used for evaluation analysis. Cover fractions (%) of tree, shrub, grass, bare soil, litter and stone cover were used as the dependent variables, and the annual average NDVI (with defined dummy variables) as the independent variable, using the functional model given in Eq. 1:

$$\textit{Fraction cover} = a + b\,(\textit{if } Q) + c\,(\textit{if } R) + d\,(\textit{NDVI. if } P, Q, \textit{or } R) + e\,(\textit{NDVI. if } Q) + f\,(\textit{NDVI. if } R) + \varepsilon \quad \text{(Eq. 1)}$$

The NDVI groups evaluated were represented by P, Q, and R in model given at Eq. 1. The intercept and slope were calculated for each NDVI group, i.e. *P*, *Q*, and *R*. One of the groups (*P*) was arbitrary chosen to act as a reference group, with the inputs '*a*' and '*d*' being the intercept and slope of the chosen reference group. The intercepts '*b*' and '*c*' were the result of tests on whether the intercepts of groups *Q* and *R* significantly differ from the reference group (*P*) while '*e*' and '*f*' test whether the slopes of *Q* and *R* were significantly different from the reference group (*P*).

The similarity between the three NDVI groups in term of species composition (presence/absence) were investigated by calculating the Sorensen dissimilarity index (*SDI*) (Sørensen, 1948; Jongman et al., 1995). The CI of 95% for the mean dissimilarity was calculated using a bootstrap technique (Efron and Tibshirani, 1986), repeated 1000 times for each pair of analysis. The 1000 simulation was run to test the hypothesis about the dissimilarity between different pairs of NDVI groups. This index measures dissimilarity of species composition between any two NDVI groups.

$$SDI = 1 - 2C/A + B \qquad \text{(Eq. 2)}$$

In the Eq. 2, *C* stands for number of species shared by the two NDVI groups while *A* and *B* are the total number of species in the two NDVI groups respectively. Values ranged between 0 and 1, with 0 indicating that the two groups have common species and 1 meaning that the two groups have a dissimilar species composition.

3.3 *Results*

3.3.1 *Mapping Land cover gradients*

Hyper-temporal image dataset analysis

Analysis of the divergence statistics indicated that 65 clusters generalized the hyper-temporal dataset. Both the average and the minimum separability values were found to be relatively high at the 65 clusters mark, with coincident local peaks (Figure 3.3). The selected cluster and its signature NDVI profiles were subsequently used to study the land cover gradients.

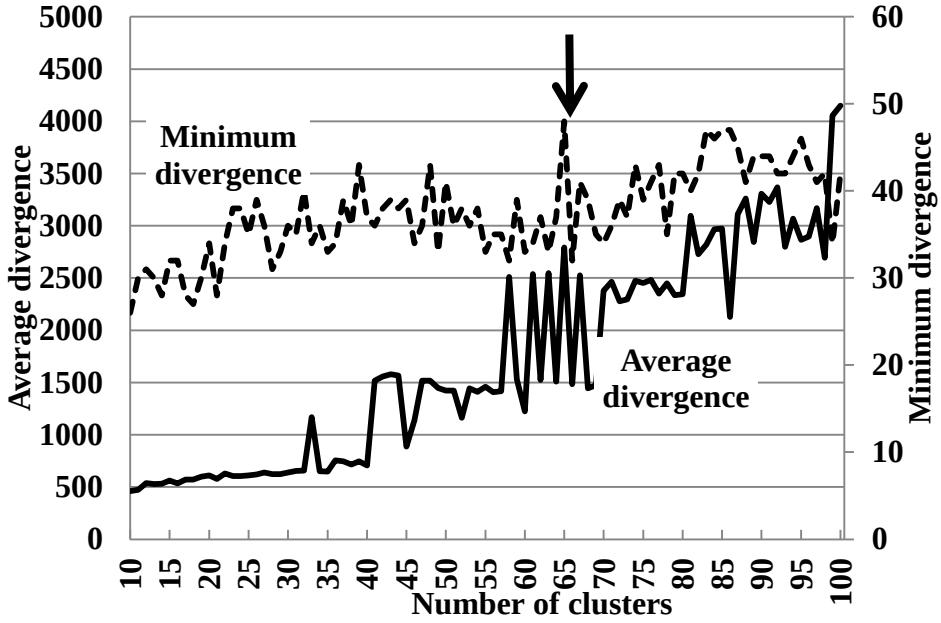

Figure 3.3. Divergence statistics showing high average and minimum separability values for the 65 clusters image (indicated with an arrow).

Gradients identification and mapping

Figure 3.4 is a hierarchical cluster analysis in the form of dendrogram, showing relationships among the classes at different level of similarity. The 65 NDVI class profiles were categorized into 14 groups based on the lowest cosine distance between the NDVI class profiles.

Grouped NDVI class profiles are illustrated in Figure 3.5. Examination of the temporal behavior of annual average NDVI profiles revealed that NDVI classes within groups (A to N) have similar temporal behavior (shape of temporal curve), but different between groups. The only differences between NDVI classes within groups are notably their gradually differentiating NDVI values from low to high.

The relationship between NDVI groups is evident from the clustering results in Figure 3.4 and NDVI profiles in Figure 3.5. For example NDVI groups A, B and C have low NDVI values and little seasonal variation, NDVI groups D, E, F, G, H, I, J, K show prominent seasonal fluctuations while L, M and N show less seasonal fluctuation and high NDVI values throughout the year (Figure 3.5).

To ascertain whether the 14 NDVI groups are also spatially linked, they were arranged in the form of a relational diagram (Figure 3.6) of mean NDVI values of the classes as well as the association between groups. This acts as

guideline to map land cover gradients. Grouped NDVI classes are shown across the rows, and are represented by different shades of the same base color. Different base colors are used for different NDVI groups. Varying bar-lengths serve to visualize the variability in mean annual NDVI values. NDVI group are also cross-linked based on their similarities in temporal behavior, as shown in Figure 3.5.

The class color codes depict (i) each class associated annual average NDVI profile (presented in Figure 3.5), and (ii) the class spatial distribution in the land cover map shown in Figure 3.7. The land cover gradients map (Figure 3.7) portrays the spatial arrangements of NDVI classes and their groups, highlighting the NDVI classes/groups that are spatially linked in the form of gradients.

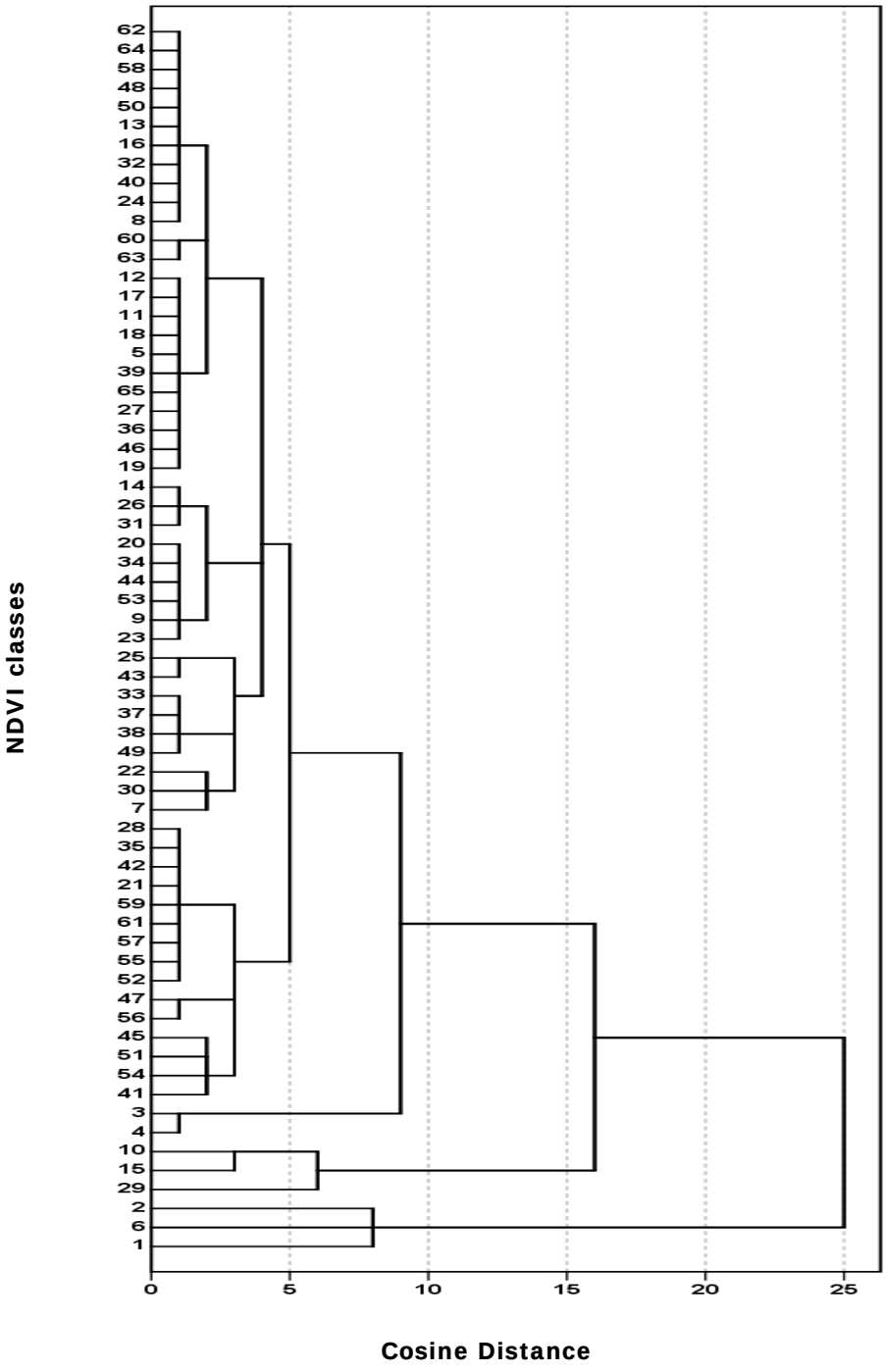

Figure 3.4. A dendrogram resulting from the grouping of the 65 NDVI class profiles.

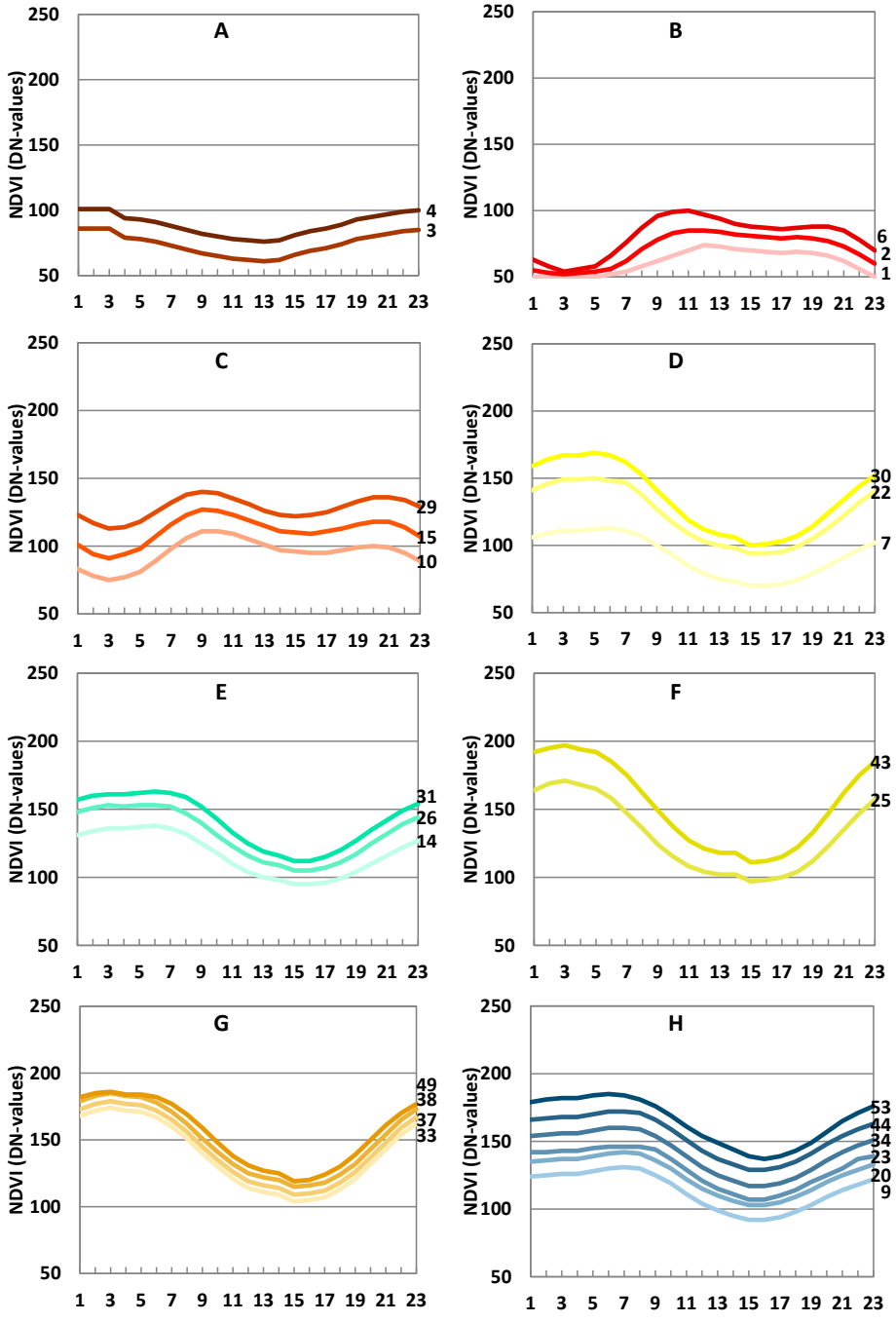
A
B
C
D
E
F
G
H
NDVI (DN-values)
250
200
150
100
50
1 3 5 7 9 11 13 15 17 19 21 23
4
3
6
2
1
29
15
10
30
22
7
31
26
14
43
25
49
38
37
33
53
44
34
23
20
9

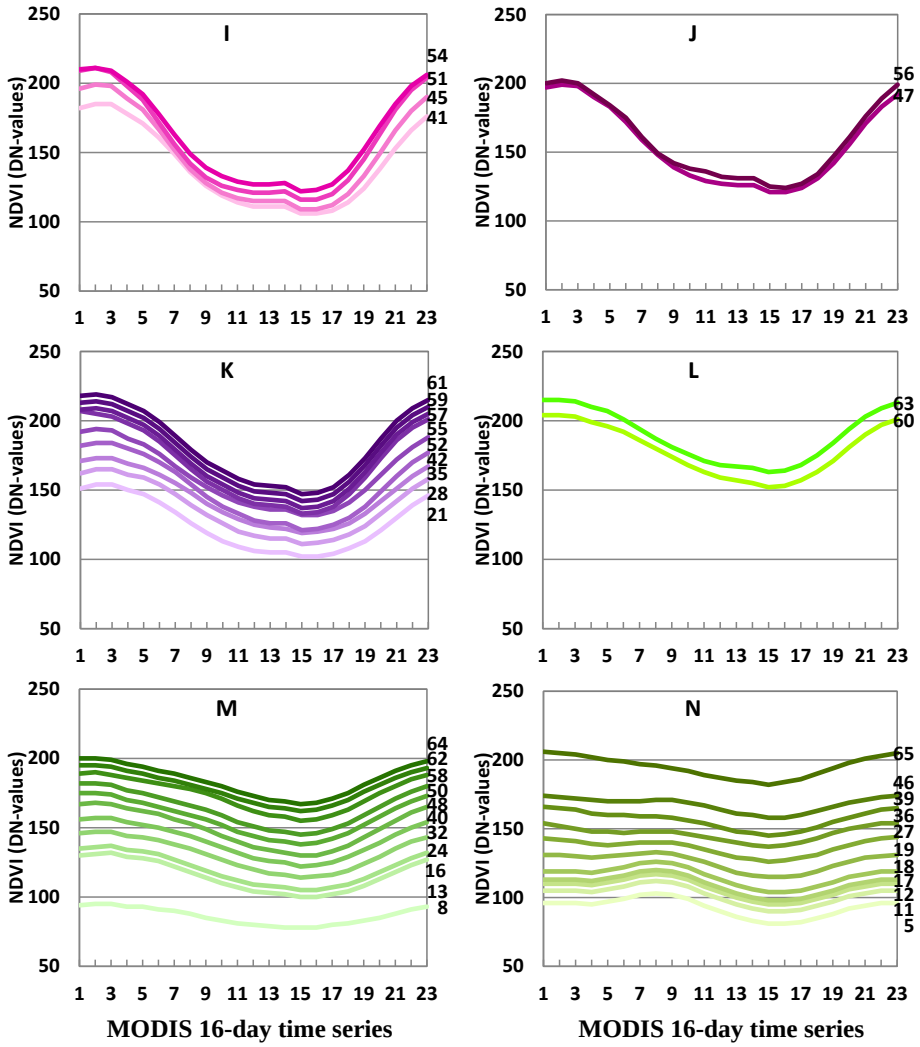

Figure 3.5. Annual average NDVI class profiles, grouped based on results of hierarchical clustering analysis.

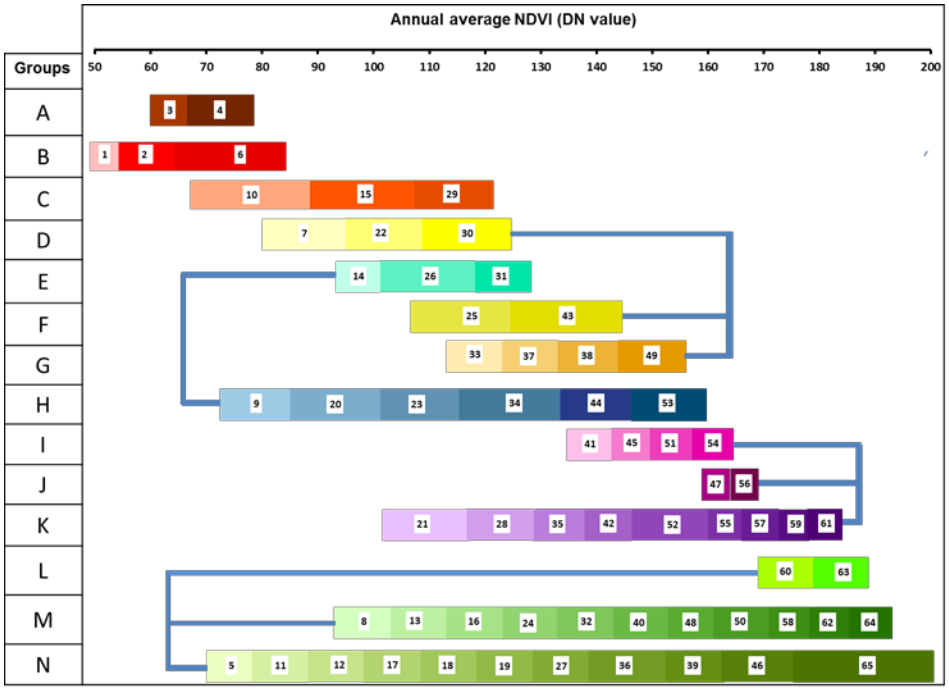

Figure 3.6. NDVI classes arranged in a relational diagram on the basis of their temporal behaviour and value intensity. Class position within a group is determined by its mean NDVI value (top axis). Groups having similarities are linked by bars.

3.3.2 *Accuracy assessment*

The multiple linear regression compared NDVI groups K, M and N using cover fractions of trees, shrubs, grass, bare soil, stone and litter cover (Figure 3.8). Group K was arbitrarily chosen as the reference group. It can be seen that changes in the average annual NDVI of classes within groups, relate to changes in land cover characteristics in term of fraction cover of different land cover components. The results (Figure 3.8) indicate that within each NDVI-group, the collected cover fraction data were linearly related with the given NDVI data, while these linear relationships between NDVI-groups significantly differ. The gradual differences in NDVI class profiles within group as shown in Figure 3.5 can also be compared with the arrangement of NDVI classes along the regression slope. For tree cover, shrubs cover and grass cover, both groups M and N had significantly different slopes from reference group K (Figure 3.8).

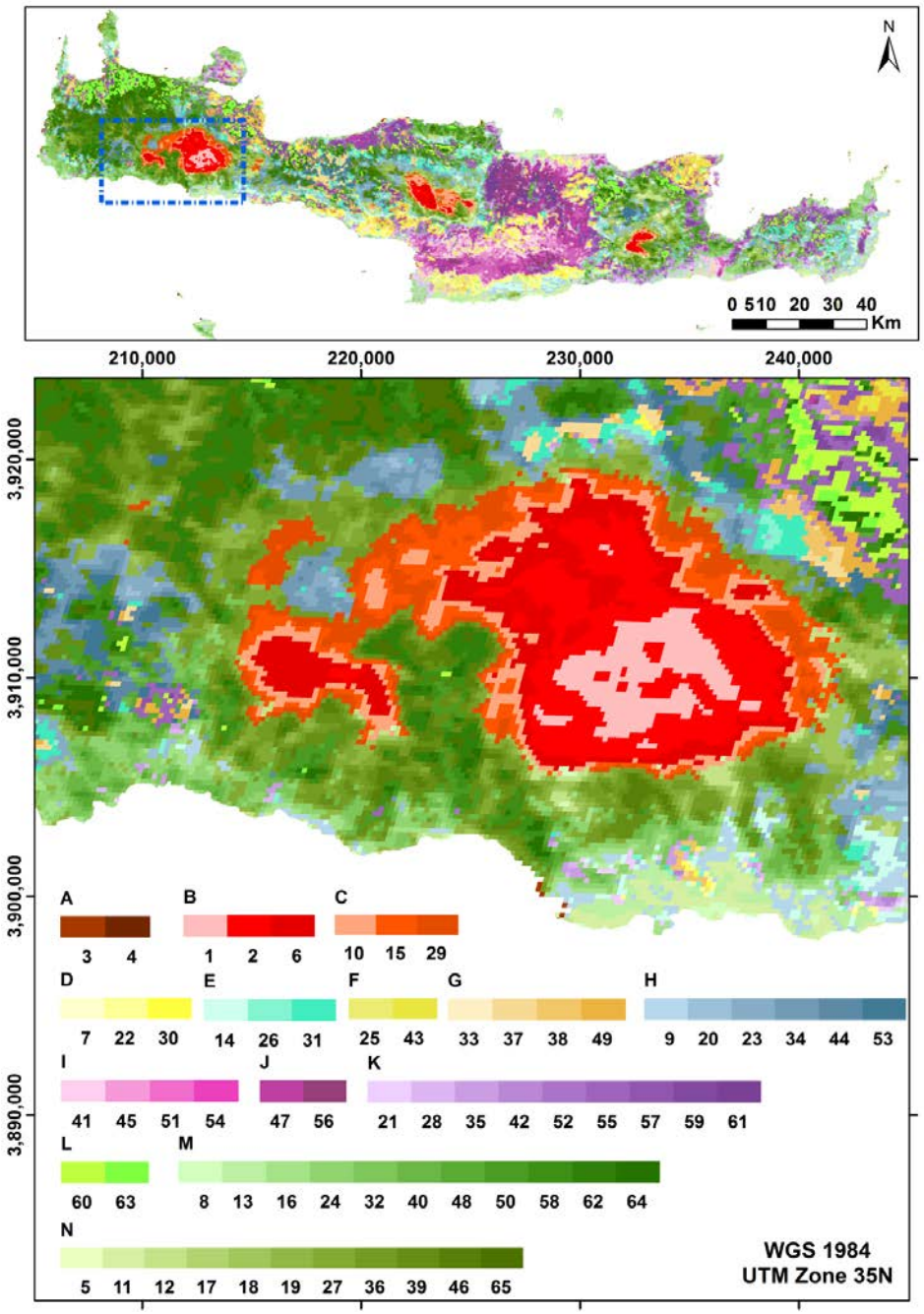

Figure 3.7. The spatial distribution of NDVI classes and groups in the form of gradients in Crete derived using profile analysis of NDVI time-series. Classes depicted here are spatial representations of those shown in Fig. 3, 4 and 5.

The basic differences between the three groups behavior originate from relatively higher proportions of trees, shrubs and grass cover. Within groups, cover differences between NDVI classes are caused by a high variability in tree cover in group M and N while Group K has relatively more shrubs and grass with fewer trees. Regarding the non-green land cover components, bare soil showed no significant differences in slopes between the tested groups. However in stone cover and litter cover both slopes of M and N were found to be different from the slope of reference group K (Figure 3.8). Different slopes represent gradients in NDVI classes within the above defined groups in term of land cover characteristics.

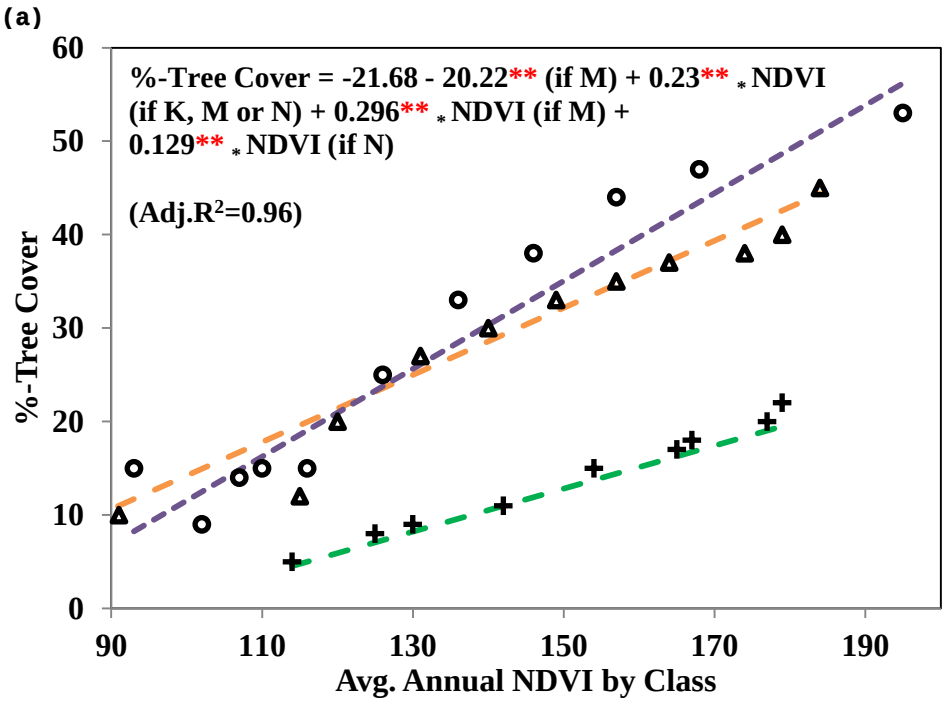

(b)

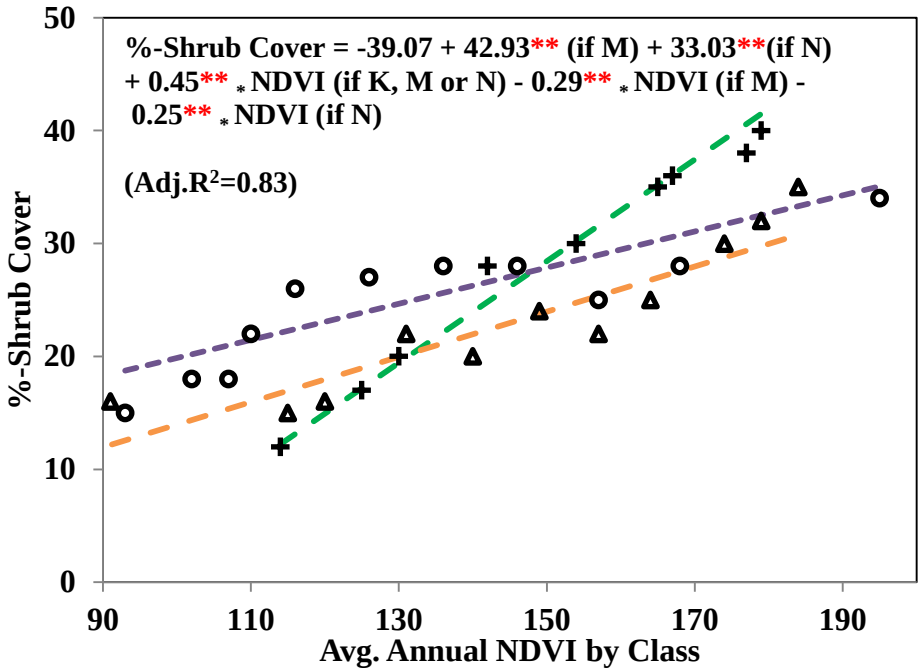
%-Shrub Cover = -39.07 + 42.93** (if M) + 33.03**(if N)
+ 0.45** * NDVI (if K, M or N) - 0.29** * NDVI (if M) -
0.25** * NDVI (if N)
(Adj.R²=0.83)
%-Shrub Cover
0
10
20
30
40
50
90
110
130
150
170
190
Avg. Annual NDVI by Class

(c)

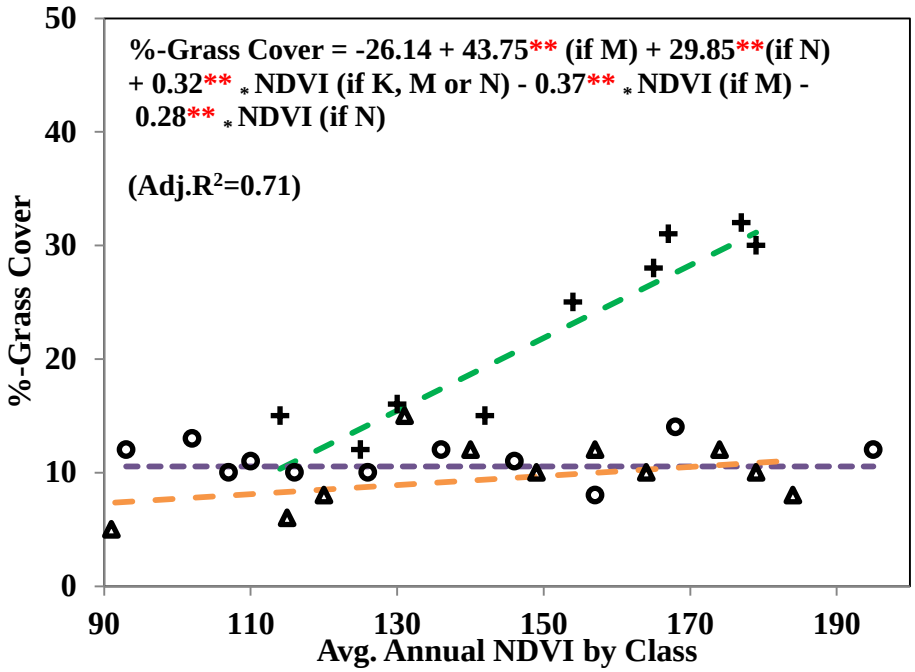
%-Grass Cover = -26.14 + 43.75** (if M) + 29.85**(if N)
+ 0.32** * NDVI (if K, M or N) - 0.37** * NDVI (if M) -
0.28** * NDVI (if N)
(Adj.R²=0.71)
%-Grass Cover
0
10
20
30
40
50
90
110
130
150
170
190
Avg. Annual NDVI by Class

(d)

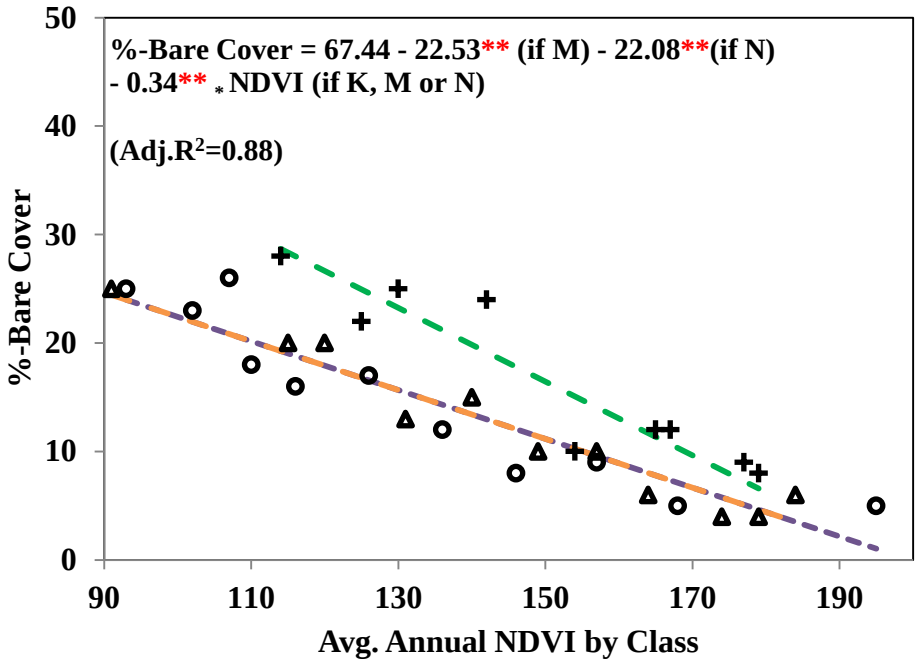
%-Bare Cover = 67.44 - 22.53** (if M) - 22.08**(if N)
- 0.34** * NDVI (if K, M or N)
(Adj.R2=0.88)
%-Bare Cover
Avg. Annual NDVI by Class
0
10
20
30
40
50
90
110
130
150
170
190

(e)

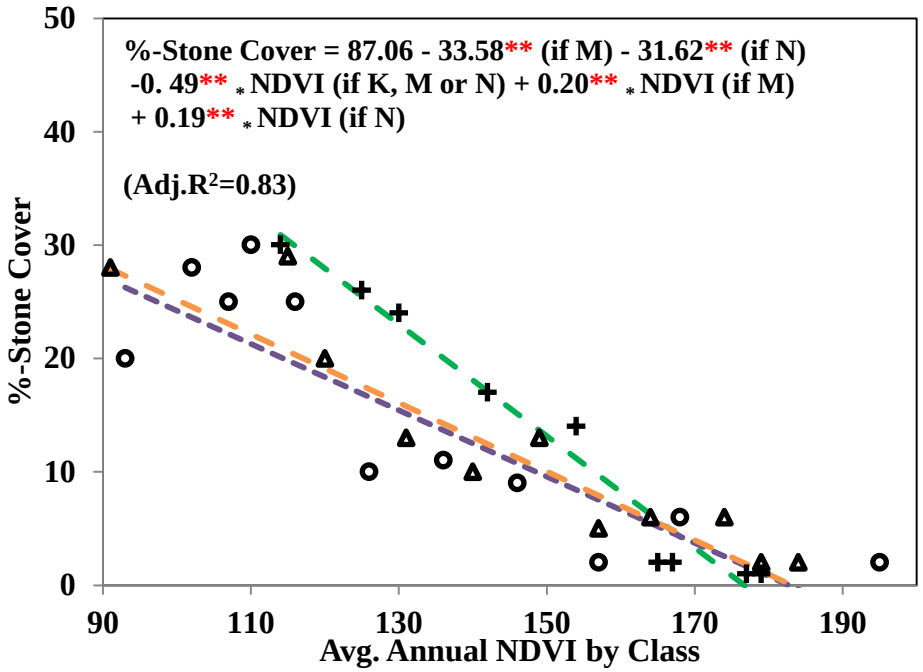
%-Stone Cover = 87.06 - 33.58** (if M) - 31.62** (if N)
-0. 49** * NDVI (if K, M or N) + 0.20** * NDVI (if M)
+ 0.19** * NDVI (if N)
(Adj.R2=0.83)
%-Stone Cover
Avg. Annual NDVI by Class
0
10
20
30
40
50
90
110
130
150
170
190

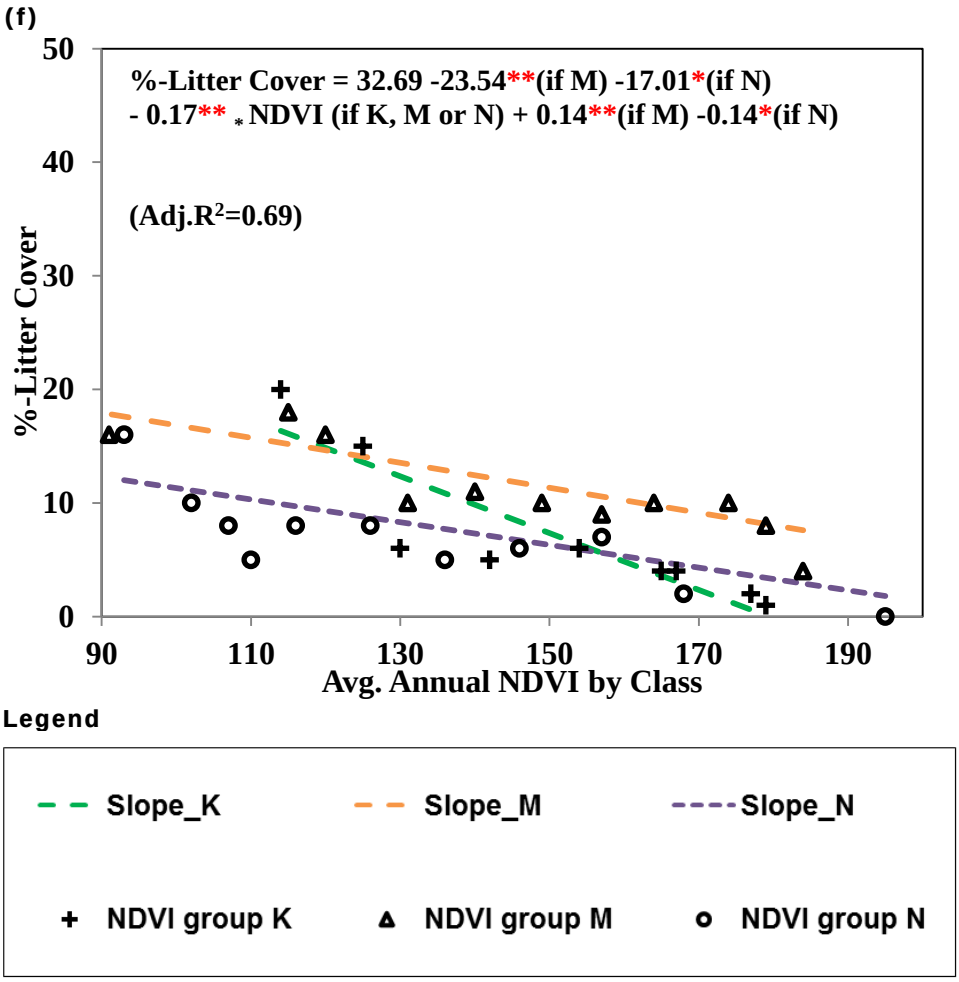

Figure 3.8. Regression results comparing the slopes of NDVI groups M and N to the reference group K with respect to (a) tree cover, (b) shrub cover, (c) grass cover, (d) bare soil, (e) stone cover and (f) litter cover. The labels show NDVI classes in each NDVI group. The regression equation is also shown where "*" depicts a significant difference of 10% from the reference group, and "" depicts a 5% significant difference from the reference group.**

Similarly, high dissimilarity in species composition was found between all pairs of NDVI groups (Table 3.1). Differences between groups K and M and K and N are comparatively high than group M and N, which is confirmed by differences in the temporal profiles of the three groups represented in Figure 3.4. The results suggest that at the level of 95% confidence interval, the mean dissimilarity value ranged between 0.46-0.92, 0.44-0.87 and 0.42-0.79, for the NDVI groups K and M, K and N, and M and N, respectively.

Table 3.1. Mean Sorenson dissimilarity values for pair wise analysis between three NDVI groups (K, M, and N)

NDVI Groups	K	M
M	0.76	**-**
N	0.68	0.61

Overall, the evaluation results support the concept that NDVI classes, though fundamentally different, are connected along gradients, and can be used to represent gradients in land cover. Meanwhile NDVI groups could represent different dominant gradients in the land cover of the area.

3.4 *Discussion*

A map depicting gradients in land cover was successfully extracted using hyper-temporal NDVI imagery. The land cover gradient map is composed of NDVI classes, which are successfully grouped on the basis of the NDVI values and similarities in their shapes (temporal patterns). The map result (Figure 3.7) shows the spatially linked and interconnected NDVI classes which have similar vegetation growth patterns. The NDVI classes within groups display relatively similar seasonal patterns though they are dissimilar in the magnitude of their temporally fluctuating mean NDVI value. The validation results shown in Figure 3.8 indicate that within each NDVI group, the collected cover fraction data are significantly linearly related with the given NDVI data. These gradual differences in NDVI classes within groups support the move to arrange NDVI classes within groups demonstrated in Figure 3.5. Overall this indicates that NDVI classes, though fundamentally different, are related along detectable gradients in vegetative growth patterns which can be visualized in the form of land cover gradients.

Each NDVI group reflects a separate dominant gradient in land cover of the area by showing different vegetation growth patterns. The linear relationships between NDVI-groups are found to be significantly different with respect to tree cover (adj. R^2=0.96), shrub cover (adj. R^2=0.83), grass cover (adj. R^2=0.71), bare soil (adj. R^2=0.88), stone cover (adj. R^2=0.83) and litter cover (adj. R^2=0.69) fractions. For tree cover, shrubs cover and grass cover, NDVI groups M and N had significantly different slopes from reference group K which is also evident from the differences in the shape of NDVI profiles of these groups shown in Figure 3.5. Similarly SDI analysis also supports the significant differences between pairs of NDVI groups in term of species composition. Therefore the NDVI groups could represent different dominant gradients in the land cover of the area.

The results support exploiting hyper-temporal NDVI image datasets to extract and map land cover gradients. The successful representation of land cover gradient using hyper-temporal NDVI imagery may be due to the sensitivity of NDVI values to the vegetation green biomass (Purevdorj et al., 1998; Shunlin, 2004) and accurately tracking of vegetation growth patterns due to the high repetitive coverage of the imagery used (Xiao et al., 2006b; Zhang et al., 2008; He et al., 2009).

The results (Figure 3.7) are unlike current gradient maps which represent gradients as “transition zones” (Trodd, 1992, 1993; Anand and Li, 2001; Arnot and Fisher, 2007a; Dutoit et al., 2007), though this raises the question “where does a transition zone begin and end?”. In this study, not only natural land cover groupings were identifiable, but also the directions of gradients in land cover. Such a representation of gradient could contribute to identifying areas that are fundamentally different, and subsequently indicating how they are grouped across spatial scales and over time.

The land cover gradient map and their profiles indicate a number of potential applications. The land cover gradient map could aid researchers in stratifying sampling regimes, to better focus on areas of interest as features in both the temporal and spatial dimension are taken into account. This may be of particular use to environmental researchers such as ecologists, through providing insight into the land covers and habitats within which a species of interest exists and could be applicable to area frame sampling for agricultural land use research and monitoring. Furthermore, directionally ordered map units also indicate the direction of gradient/change from low to high, which those involved in climate change studies and ecological modeling may find useful.

3.5 *Conclusion*

In conclusion, this study demonstrated the potential utility of hyper-temporal NDVI image datasets in identifying and mapping land cover gradients. Due to the high repetitive coverage of the imagery used, it was possible to accurately track the vegetation growth patterns and from this land cover gradients could be devised. The required datasets are readily available in a variety of spatial and temporal resolutions, from a number of different sources such as SPOT, MODIS etc. The study served to emphasize that work in the near-future should focus on quantitative analysis of phenological indicators (such as Start of Season dates, End of Season dates, Season-peak dates) extracted from NDVI profiles and the underlying factors responsible for such land cover gradients.

Acknowledgements

The authors gratefully acknowledge the financial support of the Higher Education Commission of Pakistan, the Pakistan Space and Upper Atmosphere Research Commission (SUPARCO) and of the ITC research fund. Special thanks extended to Eva Skidmore for help with English editing's. We would also like to thank ITC MSc students Johanna Ngula Niipele and Shirin Taheri for their help in collecting field data for this study.

4 Mapping the heterogeneity of natural and semi-natural landscapes[3]

[3] Chapter is based on: A. Ali., C. A. J. M. de Bie., A. K. Skidmore., R. G. Scarrott., and P. Lymberakis., 2014. Mapping the heterogeneity of natural and semi-natural landscapes, International Journal of Applied Earth Observation and Geoinformation 26, 176-183.

Abstract

Natural and semi-natural landscape cover is heterogeneous. Ideally, mapping land cover requires an approach that represents both gradients and land cover spatiotemporal variability. These aspects can be visualized and depicted by applying a new spatio-temporal analysis based Landscape Heterogeneity Mapping (LaHMa) method to natural and semi-natural landscapes. Using MODIS NDVI 16-day imagery (Feb 2000-July 2009) for Crete, a 65-cluster image was selected from ISODATA classification results using the separability values of the divergence statistics. The 65 clusters appropriately generalize the spatial and temporal variability in land cover. Using classified outputs from 10 to 65 clusters, the frequency of pixels identified as boundaries of homogeneous land cover classes was translated into the form of a landscape heterogeneity map, which was then validated using field data. The results show that the heterogeneity map had moderate correlation (R^2 = 0.60 and 0.63 in two transects) with the sum of differences between neighbouring transect pixels in all land cover components. In general, the study found this new approach (LaHMa) suitable for mapping landscape heterogeneity in the natural and semi-natural landscape of Crete, Greece. The new method appears particularly useful for gradient analysis in ecology.

Keywords: Mapping; landscape; heterogeneity; hyper-temporal; NDVI; MODIS

4.1 *Introduction*

The degree of heterogeneity in a landscape is dictated primarily by interactions amongst natural and anthropogenic processes, and disturbance in landscape (Turner and Gardner, 1991). Quantification of landscape heterogeneity is necessary to understand and study interactions and relationships between ecological processes and spatial patterns (Turner et al., 2003; Peters et al., 2006). Furthermore, management of dynamic landscapes requires maps and monitoring tools that portray the nature of the landscapes spatiotemporal heterogeneity (Gustafson, 1998) at selected spatial and temporal scale (Kent et al., 1997; Gustafson, 1998).

Quantifying the natural and semi natural landscape heterogeneity using continuous values is appropriate because natural and semi natural landscape shows spatially continuous variations in vegetation communities (Austin, 1990; Begon et al., 1990; Couteron et al., 2006). Spatially, different species (flora) in a natural and semi-natural landscape show considerable overlap, which creates gradients that represents gradual changes in space of vegetation density and/or in species composition (Kent et al., 1997; Müller, 1998). Presenting such a landscape in gradient form is important for ecological studies to understand the basic structure of landscape (Gosz, 1992).

Landscape heterogeneity is considered to be a dynamic phenomenon, as it fluctuates over time (Dunn et al., 1991; Fahrig, 1992; Gustafson, 1998). Underlying factors that determine land cover heterogeneity are spatiotemporally varied at different scale, and include soil, geology, climate and topography (Foody and Boyd, 1999). The spatial pattern and the intra-annual (temporal) changes should be considered to quantify landscape heterogeneity (de Bie et al., 2012). Therefore at a landscape level, the continuously changing environment and the dynamic nature of land cover necessitate an understanding of both the spatial and temporal processes of land cover (Fortin et al., 2000; Fagan et al., 2003).

Efforts to quantify the landscape heterogeneity began in the early 1980s (Romme, 1982; Baker and Cai, 1992);However; till date the approaches depicting land cover heterogeneity in a map format has poorly ignored spatiotemporal variability and gradient representation. One approach to quantifying landscape heterogeneity is the Patch Mosaic approach (Goodchild and Quattrochi, 1997; Gustafson, 1998), which builds on information contained in categorical or thematic maps. Information is presented on spatial aspects such as the area, shape, patch density and fractal dimensions of the landscape, while the non-spatial aspects are represented in the form of a matrix containing information on a category's proportions, evenness,

richness and diversity (Li and Reynolds, 1995; Gustafson, 1998). The discrete representation of landscape is an incorrect form of representation and prone to errors in land cover class definitions (Gosz, 1992; Southworth et al., 2004; Boyd and Foody, 2011). They are not based on spatiotemporal explicit data which are important for accurate characterization of land cover (Sakamoto et al., 2006; Nguyen et al., 2011). A second approach involves the application of statistical analyses to point data collected through surveys through the use of semi-variograms, correlograms, amongst other statistical tools (Li and Reynolds, 1995; Gustafson, 1998) and attempts to place a relative value on a landscape's heterogeneity. The point data are always limited, both in space and time, and so cannot accurately represent the spatiotemporal explicit landscape heterogeneity. Thus, all the approaches that claim to capture landscape heterogeneity ignore the likely presence of gradients. Besides that research concerning the accurate mapping of landscape heterogeneity has not specifically focused on the high-frequency temporal dimension of land cover, even though this has already been found very helpful in land cover mapping and monitoring (Xiao et al., 2006a; Sakamoto et al., 2007; Nguyen et al., 2011).

Although techniques such as auto-correlation, semi-variogram analysis, fourier spectral analysis and fractals analysis (Perry et al., 2002; Couteron et al., 2006) do consider gradients in representation, these assume land cover to be aperiodic and always repeats itself within a certain time period (Bradshaw and Spies, 1992). In reality land cover is highly dynamic, and isolating a genuine periodicity is difficult to achieve (Couteron et al., 2006). Therefore, the ability of these techniques to quantify the spatiotemporal aspects of landscape heterogeneity is also limited.

Natural and semi-natural landscapes show continuous changes than landscapes which are more dominated by the boundary features common to human landscape administration (Puech, 1994; Couteron et al., 2006). To be accurately characterized, any method must ensure the presence of gradients in land cover as well as spatiotemporal variability is adequately incorporated into the mapping process. Therefore, an approach used for agricultural landscapes by de Bie et al.,(2012) called Landscape Heterogeneity Mapping (LaHMa) approach which was originally applied in agricultural and man-made landscape is selected to map landscape heterogeneity in the natural and semi-natural landscapes of island of Crete, Greece. This method was not validated with field data therefore a through validation was undertaken using field data composed of the fractional complexity of the area's land cover components.

LaHMa involves calculating the relative heterogeneity of each pixel area, using the long-term spatiotemporal variability in land cover. Differences in

spectro-temporal characteristics of land cover present in a particular pixel is considered here as landscape heterogeneity. The technique exhibits spatial heterogeneity at various strengths of boundaries (ecotones and ecoclines) at any selected scale therefore it can be useful for understanding landscape structures and functions (Wu and Archer, 2005; Peters et al., 2006). It is also robust for locating plants assemblages which is important characteristics of the natural and semi-natural landscape. The heterogeneity determined may be arising by soil, vegetation discontinuities, changes in species composition and its distribution.

4.2 *Study area*

Crete (Figure 4.1) is characterized by high mountains and plateaus (Chartzoulakis and Psarras, 2005). The geology also varies from mountainous areas to lowlands having calcareous rocks to limestone, sandstone and marls respectively(Sarris et al., 2005a). The island has a sub-humid climate, with dry summers and mild wet winters (Sluiter, 1998; Chartzoulakis et al., 2001). An average of about 900 mm of precipitation falls on the island annually. This varies locally, with approximately 300 mm falling at lower altitudes, and up to 2000 mm falling in the mountain areas (Chartzoulakis et al., 2001; Chartzoulakis and Psarras, 2005). The landscape is dominated by both natural and semi-natural land cover, intermixed across the island with herbaceous and woody plant species that form varying proportions of local plant communities (Turland et al., 1993; Montmollin and Iatrou, 1995; Chartzoulakis et al., 2001; Chartzoulakis and Psarras, 2005). The high variability in topography, weather, geology results in high variability in vegetation compositions and structure in Crete, hence creates a heterogeneous landscape. The complex landscape and intermixed vegetation with variable climatic conditions could be only detected if both spatial and temporal aspects of land cover are considered.

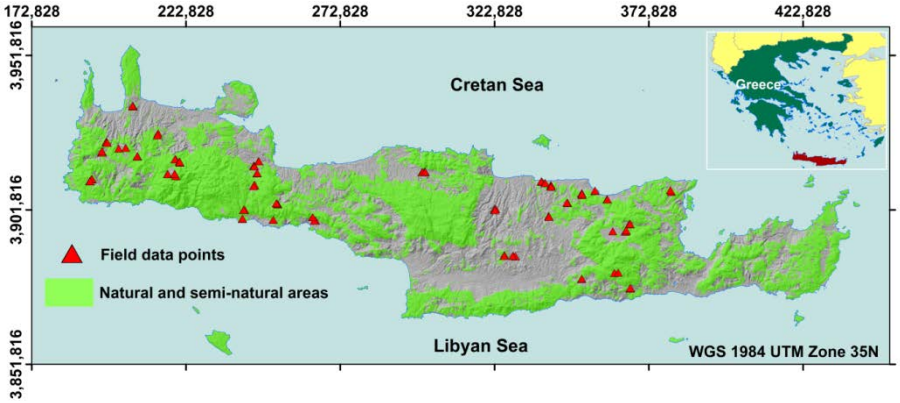

Figure 4.1. The Greek island of Crete. Natural and semi-natural areas (extracted from CORINE map) are displayed with general relief. Field data points are also shown.

4.3 *Method*

4.3.1 *Remote sensing data and maps used*

1. Hyper-temporal time-series Normalized Difference Vegetation Index (NDVI) imagery is freely available at different spatial and temporal resolutions from sensors such as SPOT (1 km), MODIS (1000 m, 500 m, 250 m), MERIS (300 m, 1200 m) and MSG (1 km). NDVI is a well-recognized indicator of green vegetation biomass (Tucker and Sellers, 1986; Henebry, 1993). Sixteen-day maximum value composite (MVC) NDVI image data at a spatial resolution of 250 m, collected by the MODIS Terra sensor between February 2000 and July 2009, was obtained using NASA's Warehouse Inventory Search Tool (WIST) facility. The associated vegetation index quality (VIQ) layers of the data product package were used to identify and remove all pixels affected by haze, cloud and other atmospheric conditions. The per-image pixel NDVI values were rescaled to a Digital Number format (0-255) (de Bie et al., 2012) to facilitate data processing without degrading essential information (Roderick et al., 1996). The dataset was then processed using an Adaptive Savitzky Golay filter (ASAVGOL) to accommodate poor quality data that had been removed by the initial screening, and account for outlying spurious data values (Jönsson and Eklundh, 2004; Beltran-Abaunza, 2009). This method is based on Savitzky-Golay and logistics fitting function (Jönsson and Eklundh, 2004). This is found useful for noisy and non-uniform NDVI time series datasets (Jönsson and Eklundh, 2004; Feng et al., 2008; Beltran-Abaunza, 2009; Boschetti et al., 2009).

2. Fine-resolution 10 m ALOS AVNIR-2 multispectral images acquired on 9 July 2009, 14 July 2009, 26 July 2009, 9 May 2008 and 4 November

2008 were used to support field data collection. These images were acquired from the Remote Sensing Technology Centre (RESTEC) (http://www.alos-restec.jp/products_e.html).

3. The Coordination of Information on the Environment (CORINE) land cover map for the year 2000 was obtained from the European Environmental Agency (EEA), and used to facilitate the gathering of field data.

4.3.2 *Landscape heterogeneity mapping*

The time-series image dataset, composed of 293 sequential image layers, was classified using the Iterative Self-Organizing Data Analysis (ISODATA) algorithm (Ball and Hall, 1965; Tou and Gonzalez, 1974). ISODATA unsupervised classifications were run to generate maps with outputs containing 10 to 100 clusters (Khan et al., 2010; de Bie et al., 2011; Nguyen et al., 2011; de Bie et al., 2012). For each run, the maximum number of iterations was set to 50 and the convergence threshold was set to 1, which were proved useful for optimal classification results in studies for example's (Khan et al., 2010; de Bie et al., 2011; Nguyen et al., 2011; de Bie et al., 2012). The maximum iterations control the ISODATA so that it stops at a certain threshold. The convergence threshold prevents the ISODATA utility from running indefinitely. After classification, both average and minimum separability values, expressed in the form of divergence statistics, were derived for each run output (Swain and Davis, 1978). Average divergence denotes the mean similarity between temporal signatures amongst all possible pairwise combinations of output clusters, while the minimum divergence value expresses the similarity between the temporal signatures of the two most similar clusters. The divergence statistics were used to aid the selection of the number of clusters to generalize the variability in the time-series NDVI dataset (Singh, 1984; Khan et al., 2010). The number of clusters present in the data is based on highest value of divergence statistics used as a validation index (Davies and Bouldin, 1979; Bezdek and Pal, 1998; Halkidi et al., 2001).

All output cluster maps (10 clusters up to selected generalized cluster map) were used to derive the landscape heterogeneity map using the process presented by de Bie et al., (2012). Each cluster output map was converted from raster to vector polygon format, merely maintaining the pixel outlines and therefore the locations of boundaries. The vector polygon file was then converted into a vector polyline format, following which the polylines were subsequently converted into a raster format, with a pixel resolution of 125 m (compared to the original 250 m pixel resolution). Each output cluster file was processed in this manner. Following this, the sum product of the

boundary processed raster files was obtained. This sum product was processed further, initially being converted from a raster to a vector polyline format, and subsequently being converted back into a raster format. Finally, a majority filter of eight cells was run over the modified sum product image to ensure that no non-value raster cells remained. This produced the output landscape heterogeneity map, in which the heterogeneity value at a particular location was essentially determined by the number of times the pixel boundaries represented the boundary line between homogenous units of vegetation. A landscape heterogeneity map shows the strength (within a maximum range of y minus x) with which two adjacent pixels are classified differently.

4.3.3 *Validation*

The landscape heterogeneity map was evaluated using a transect sampling scheme (Skidmore and Turner, 1992; Fortin et al., 2000; Hennenberg et al., 2005) with two linear transects composed of 65 pixels of 250x250 m in two different locations randomly selected. The high resolution ALOS AVNIR-2 image datasets (10 m) were used to analyse pixels within the transects, assisted by data gathered from ground observations. The length of the two transects were based on availability of field data collected to define image objects based on ALOS AVNIR-2 imagery.

Ground observation data were collected between 22 September and 11 October 2009, using a stratified clustered random sampling scheme. NDVI clusters based on a selected NDVI cluster map were considered as strata, which were randomly selected based on areas that did not coincide with the urban and agricultural land cover as designated by the CORINE 2000 land cover dataset. 29 NDVI clusters were visited in the field. Within each selected NDVI cluster, samples were collected based on image objects identified on the ALOS AVNIR-2 images. Different image objects were identified using features such as tone, pattern, shape, texture and association (Feranec, 1999). In total, 230 locations (image objects) were sampled and appraised concerning their land cover characteristics. At each sample location, estimates of the proportions of trees, shrubs, grass, bare soil, stone and litter cover were made. In all the layers of land cover estimates, only vertical projection to the ground was considered, and the sum of all the cover estimates equal to 100%.

To upscale the field data to transect pixel resolution (250 m), an image legend was derived using snapshots of ALOS image objects, along with a field description in terms of percentage cover of land cover components. On the basis of this image legend, the ALOS image transect area was digitized and described. The digitized image objects, known as “ALOS map units”, were

then combined with transect pixels to calculate percent contribution of ALOS map unit within each pixel (Eq. 1).

Area fraction=Area of map unit x *100 / Area of MODIS pixel* *(Eq. 1)*

Where, "*Area fraction"* represents fraction of the area covered by each map unit within a MODIS pixel, *"Area of unit"* shows sum of map unit area in MODIS pixel and *"Area of MODIS pixel"* presents total area of the MODIS pixel.

After calculation of area fraction, through weighted up-scaling the cover fraction of tree, shrub, grass, bare soil, stone and litter cover were derived using the formula given in equation 2.

Weighted land cover = Area fraction x Mean land cover / 100 *(Eq. 2)*

Where weighted land cover is the sum of fraction of ALOS units within each pixel and mean land cover (%) is the mean value for each ALOS classes based on field calculated percent cover.

Finally fraction cover of each component was added up to calculate the total fraction cover of land cover components individually in each pixel.

Regression analysis was then used to appraise the relationship between landscape heterogeneity (in terms of boundary strength) and the proportional difference in land cover components (from the adjacent transect pixels). The absolute difference in percentage cover between two neighbouring pixels of the transect was calculated for each land cover component, and was also summarized as green cover (trees, shrubs and grass cover), non-green cover (litter, bare and stone cover), and the sum of all components.

4.4 *Results*

4.4.1 *The landscape heterogeneity map*

Ninety-one cluster maps were initially produced as outputs from ISODATA unsupervised classifications, and the cluster map containing 65 clusters was deemed to represent the optimal generalization of the hyper-temporal NDVI dataset. As shown in Figure 4.2, a coincident peak occurred in both sets of divergence values at 65 clusters. Sixty and 99 cluster outputs show peaks in average divergence; however, these are not coincident with peaks in minimum divergence value. The selection of the optimal cluster map served to outline the number of clusters output maps (output of 10 to 65 clusters) used for generating the landscape heterogeneity map.

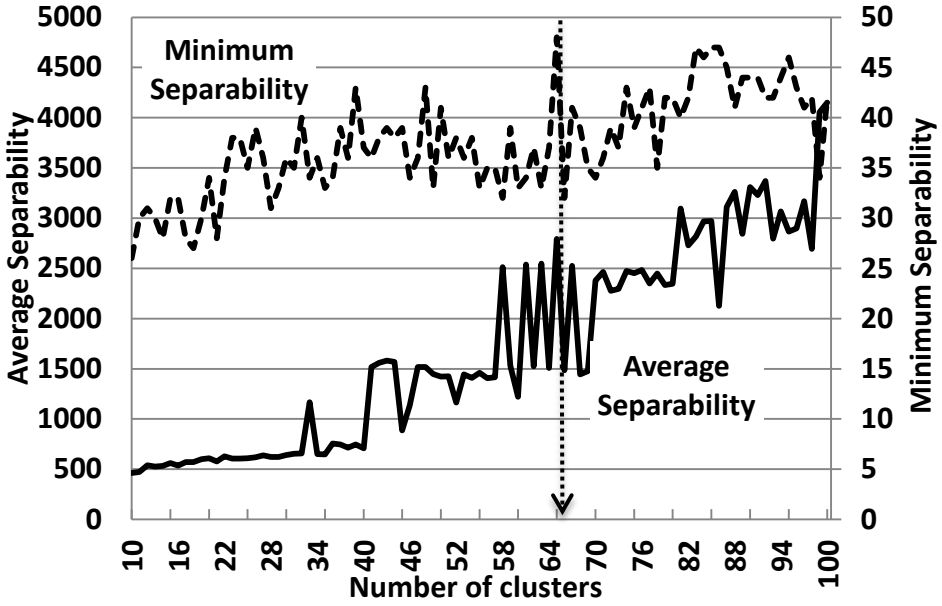

Figure 4.2. Selection of the optimal number of clusters (65-cluster map) with which to generalize the hyper-temporal dataset.

The landscape heterogeneity map was prepared using the 56 output cluster maps (i.e. the maps produced from 10 to 65 clusters, respectively), and is presented in Figure 4.3. The map details landscape heterogeneity in the form of spatial gradients. Visually complex patterns are located in areas where high variability in local topography and complex vegetation cover is present. Some parts in the map look less heterogeneous with plain yellow colour, they represent high mountains with hardly any vegetation and also valley's having less diversity in land cover and land use.

The two transects used for validation are also displayed in Figure 4.3. They were located in two different areas exhibiting high local variations in land cover along a topographical gradient.

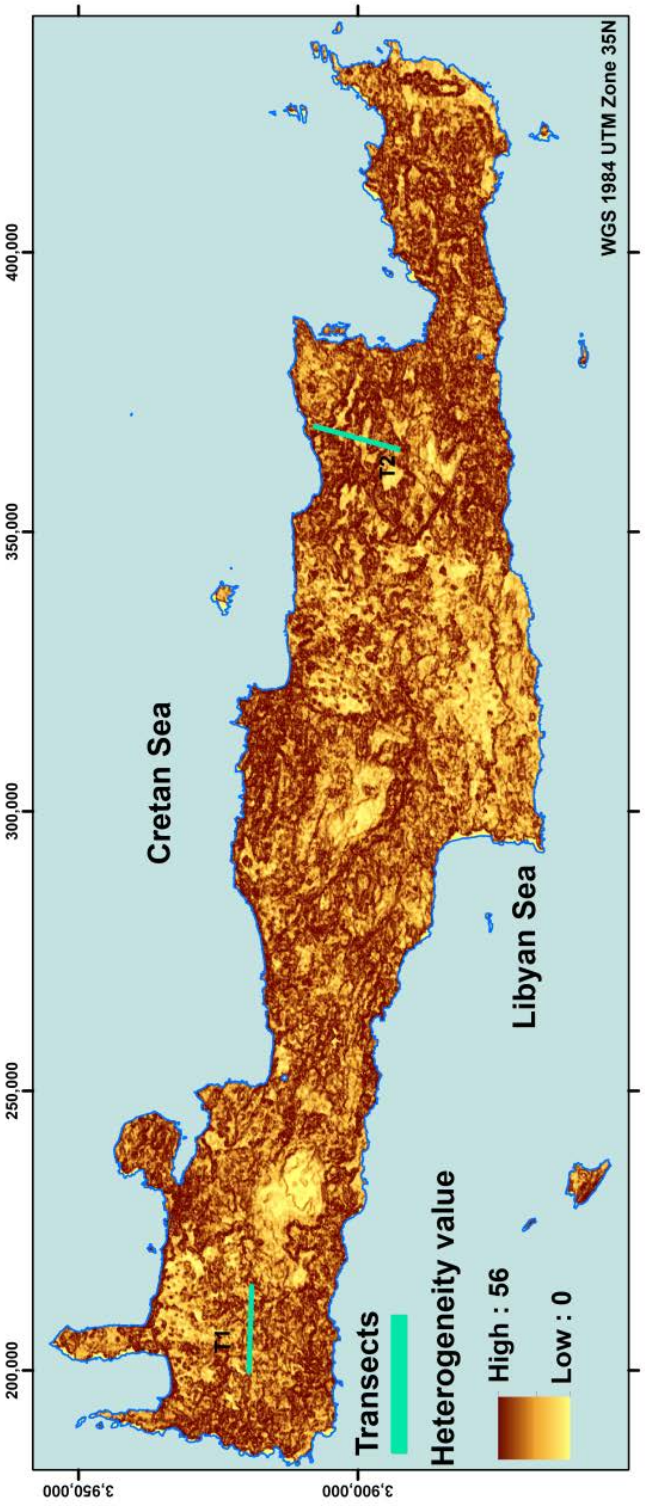

Figure 4.3. The output landscape heterogeneity map of Crete, Greece, depicting spatial heterogeneity patterns resulting from analysis of spatiotemporal vegetation fluctuations over the area. The locations of the two sampling transects, Transect 1 (T1) and Transect 2 (T2), are also outlined.

4.4.2 *Validation*

Figure 4.4 (i) details transect 1 overlaid on the ALOS AVNIR-2 image and image legend (homogenized snap shots of ALOS image objects surveyed); Figure 4.4 (ii) displays the digitized polygons used for up-scaling; and Figure 4.4(iii) shows part of the landscape heterogeneity map represented in the form of graduated boundary strengths.

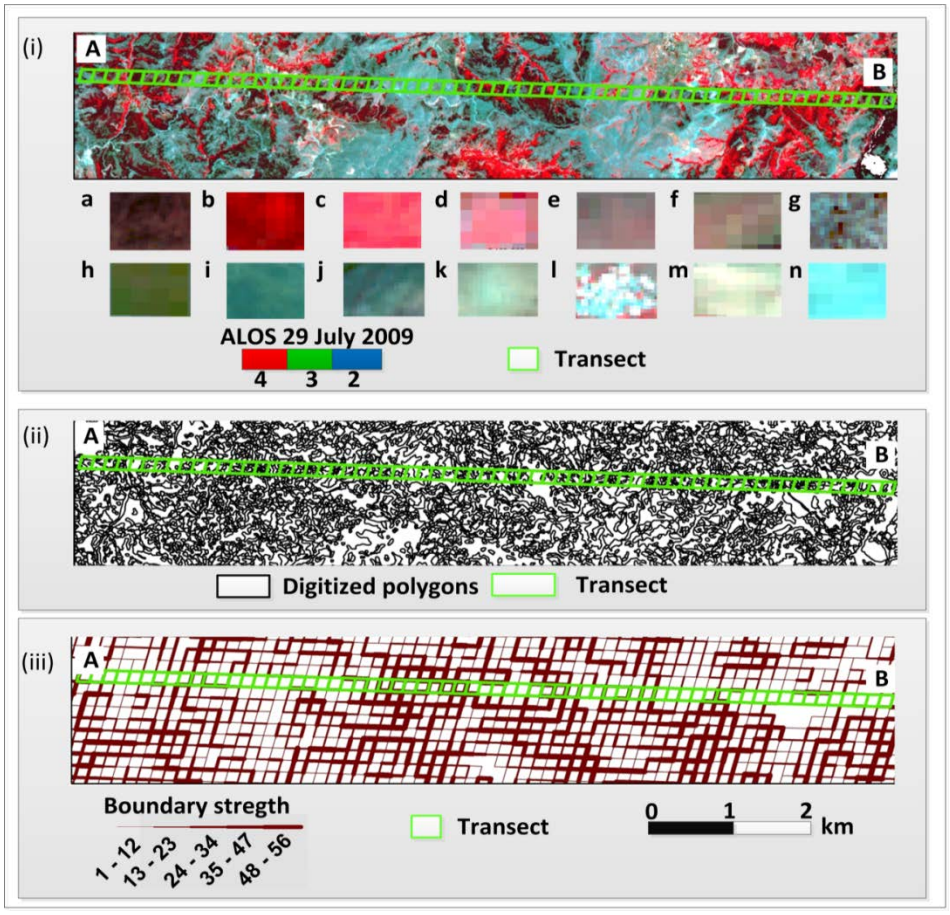

Figure 4.4. Sample Transect 1, composed of 250x250 m areas, overlaid on (i) the ALOS AVNIR-2 10 m resolution RGB (4, 3, 2) image, with the legend used for interpretation (snap shots of ALOS image objects); (ii) digitized polygons; (iii) the boundary strength map.

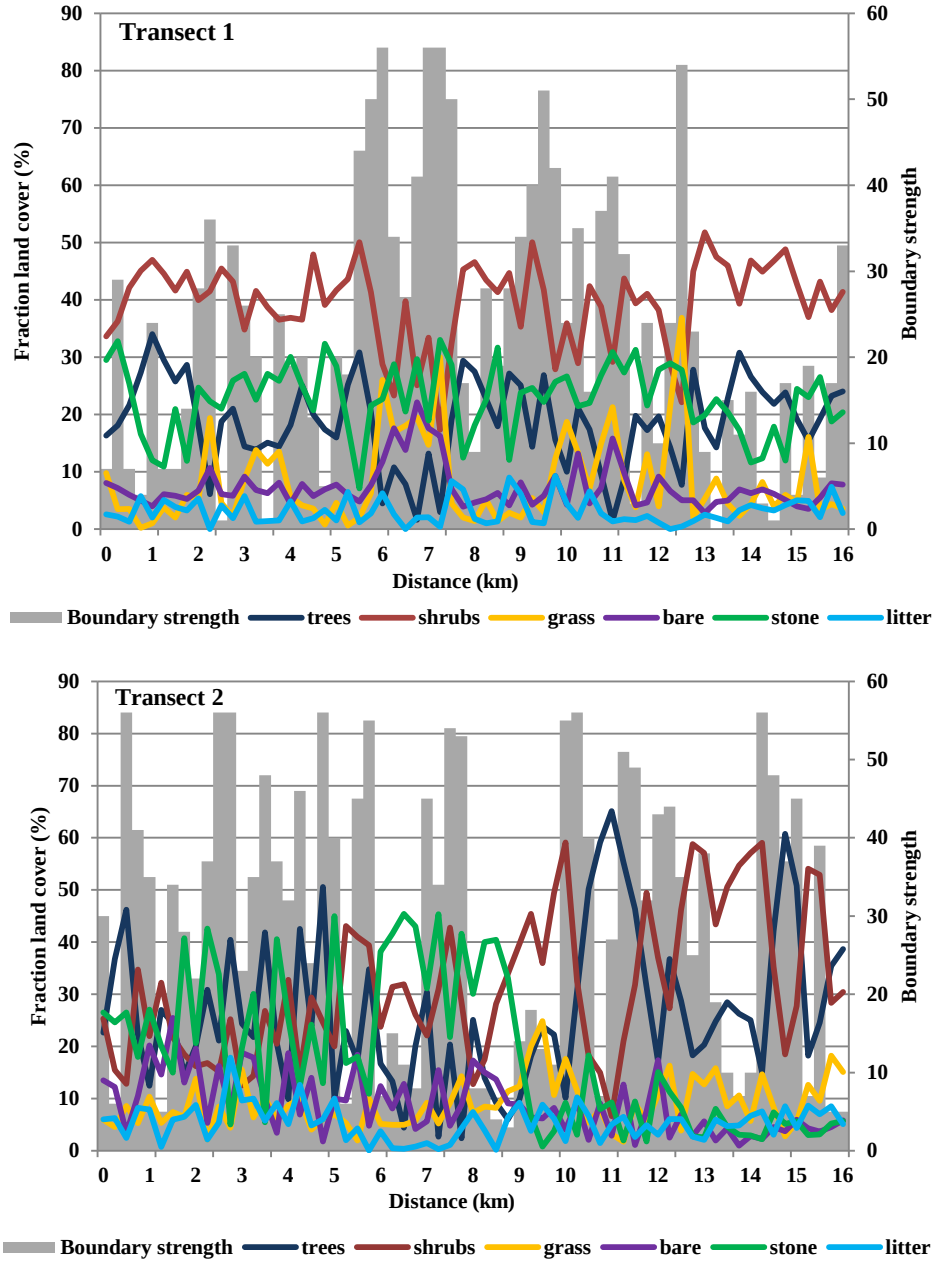

Figure 4.5. Associations between variations in boundary strength and variations in the fractional cover of different land cover (trees, shrubs, grass, bare soil, stone and litter) from A to B in Transects 1 and 2.

The result obtained from the transect analysis with regard to the fractions of land cover components in each transect area is illustrated in Figure 4.5, which indicates the variations in the cover fractions of trees, shrubs, grass, bare soil, stone and litter cover in relation to variations in boundary strength. In both transects, variations in spatial aggregations of green land cover components such as tree, shrub and grass cover closely correspond to the variations in boundary strength.

In the case of transect 1, from the results showing the correlation between boundary strength and the differences in fractional land cover components between neighbouring pixels, the sum of differences with respect to all land cover components (trees, shrubs, grass, bare soil, stone and litter) was found to be higher than those for green and non-green components, having an R^2 value of 0.60 and being associated with the lowest standard error (SE=10.06). The R^2 values indicate that 49% of the variation in boundary strength is correlated with differences in the fraction of green land cover components, with a standard error of 11.26. The sum of differences with respect to non-green (bare soil, stone, litter) land cover has a lower coefficient of determination (R^2=0.20), and a higher standard error (SE=14.20).

The results for individual components (i.e. trees, shrubs, grass, bare soil, stone and litter cover) show significant correlation ($p<0.05$) while stone cover has R^2 of 0.4 and is non-significant ($p>0.05$). However, the coefficient of determination is low in all cases, with the exception of trees (R^2=0.40) and shrubs (R^2=0.46) (Table 4.1).

Table 4.1.Results showing correlation between boundary strength and differences in all individual land cover components as well as the sum of these differences between neighbouring pixels of transect 1(n=65).

Fraction land cover components (%)	R^2	Standard Error (SE)	p-value
Sum of land cover difference between pixels	0.60	10.06	0.00
Green cover (trees, shrubs, grass)	0.50	11.26	0.00
Non-green cover (bare soil, stone, litter)	0.20	14.20	0.00
Trees	0.40	12.33	0.00
Shrubs	0.46	11.70	0.00
Grass	0.20	14.07	0.00
Bare soil	0.29	13.34	0.00
Stone	0.04	15.26	0.15
Litter	0.07	15.23	0.04

Furthermore, transect 2 gives R^2 of 0.63 for the sum of differences with respect to all land cover components (trees, shrubs, grass, bare soil, stone and litter), also have low SE (11.03). Similarly as in transect 1, green cover (R^2=0.59, SE=11.61) was found to be more closely correlated than non-green components (R^2=0.26, SE=15.56). The results with individual components are low which is summarized in Table 4.2. All the results were found significant at $p<0.05$ except grass cover ($p>0.05$).

Table 4.2. Results showing correlation between boundary strength and differences in all individual land cover components as well as the sum of these differences between neighbouring pixels of transect 2 (n=65).

Fraction land cover components (%)	R^2	Standard Error (SE)	p-value
Sum of land cover difference between pixels	0.63	11.03	0.00
Green cover (trees, shrubs, grass)	0.59	11.61	0.00
Non-green cover (bare soil, stone, litter)	0.26	15.56	0.00
Trees	0.46	13.33	0.00
Shrubs	0.34	14.72	0.00
Grass	0.05	17.63	0.07
Bare soil	0.10	17.07	0.00
Stone	0.19	16.25	0.00
Litter	0.11	17.05	0.00

4.5 *Discussion*

The heterogeneity of natural and semi-natural landscapes can be characterized and presented in continuous units with the help of this technique. Such a continuous spatial representation of landscape heterogeneity is consistent with the concept of landscapes being characterized by land cover gradients, and incorporates a realistic approach to summarizing and presenting ground conditions (Whittaker, 1967; Cushman et al., 2010). Legendre and Legendre (1998) and Legendre et al., (2002) noted that in nature spatial patterns are found as gradients that are due to the continuous changes in the physical environment. Continuous spatial fluctuations in natural and semi-natural land cover result in spatially continuous variations in vegetation communities (Puech, 1994).

As advocated by de Bie et al., (de Bie et al., 2012); the rapid follow up of imagery is found effective in case of mapping landscape heterogeneity in natural and semi natural landscapes as well. The high frequency imagery is important for accurate characterization and mapping of land cover due to its ability to closely track seasonal profiles and changes (Lunetta et al., 2004; Xiao et al., 2006a; Lu and Weng, 2007; Sakamoto et al., 2007; Alexandridis et al., 2008; Zhang et al., 2009; Khan et al., 2011). Hyper-temporal imagery is also found effective for mapping the spatial patterns of green cover that represent gradual changes in the form of gradient originated due to the local vegetation seasonal trends (Ali et al., 2013). These seasonal variations are

specific to different species, its density and composition, which can help in identification of land cover type and state (Justice et al., 1985; Neeti et al., 2011; Ali et al., 2013). The spatiotemporal imagery projects the influence of different biotic and abiotic environmental factors such as soil, temperature, solar illumination, photoperiod and moisture over time which is responsible for landscape heterogeneity.

The heterogeneity output maps were shown to be relatable to spatial variation in land cover heterogeneity. Results from the evaluation element of the study revealed that differences in land cover could be related (R^2 of 0.60 and 0.63 in two transects used for validation, $p<0.05$) to the variation in heterogeneity values expressed in the output map. This moderate level of explained variability could be attributed to the duration of field data collection and single date ALOS imagery used for validation, whereas the output heterogeneity map incorporates seasonal variations spanning a long period of time (February 2000 to July 2009). Hyper-temporal datasets are essentially an automated record that captures the effects of landscape dynamics (seasonality), while the field data, being limited in space and time, do not account for these dynamics.

The output landscape heterogeneity map of Crete represents landscape as advocated by many scientists (Gosz, 1992; Kent et al., 1997; Martín et al., 2006). The inherent mosaic structure originates from small spatial and temporal scale changes (climate change/fire disturbances, growing season length, moisture availability, species compositions, local patterns in soils or micro-topography), as well as the effects of grazing management or other anthropogenic activities (Gosz, 1991; Gosz, 1992). However, those seasonal changes which occur in a certain homogenous area without change across space, may not contribute to heterogeneity of the area. The spatial and temporal scale of the imagery used proved sufficient for this diverse and complex landscape. This is evident from results shown in Figure 4.3, in which there is no such anthropogenic factors such roads, gardens etc. can be seen as pointed out by de Bie et al., (2012) in case of MODIS imagery.

4.6 *Conclusion*

In conclusion, this study has served to highlight the utility of applying the LaHMa method to the task of characterizing the heterogeneity of natural and semi-natural landscapes. The method is useful for gradients representation. The validation results showed the method's potential; however a more rigorous evaluation of the methodology with the incorporation of more study sites into ground sampling and over a greater variety of land cover is required. It is recommended that a comparative analysis be conducted of the performance and informative abilities of the LaHMa technique and other

landscape heterogeneity characterization techniques. The method is robust and can help ecologist to further strengthen their analysis with respect to landscape structure in natural and semi natural landscape.

Acknowledgements

The authors gratefully acknowledge the financial support of the Higher Education Commission of Pakistan, the Pakistan Space and Upper Atmosphere Research Commission (SUPARCO) and of the ITC research fund. We would also like to thank ITC MSc students Johanna Ngule Niipele and Shirin Taheri for their help in collecting field data for this study. Special thanks are extended to Janice Collins for help with English editing's. We would like to thank two anonymous reviewers for their constructive comments to improve this manuscript.

5 CoverCAM - a land cover composition change assessment method[4]

[4] Chapter is based on: A. Ali., C. A. J. M. de Bie., W. Nieuwenhuis., A.K. Skidmore., CoverCAM – a Land Cover Composition Change Assessment Method (Under review in JAG).

Abstract

The cover-composition on a specific piece of land can change over time due to natural and anthropogenic factors. Accurate detection of where and when changes occur requires a method that uses remotely sensed imagery that represents a continuous and consistent record on the state of the green land-cover. Such data are offered through hyper-temporal NDVI-imagery. Until recently, NDVI-images were mainly used for anomaly mapping to monitor the influence of weather on vegetation; the monitoring basically assume that, over time, the land cover composition of a studied area remains static. This study presents a novel cover change assessment method, labelled 'CoverCAM' that extracts from hyper-temporal NDVI-imagery the probabilities that the original land cover composition did change. CoverCAM, unlike all existing change-detection methods, makes adjustments based on seasonal NDVI-anomalies experienced at landscape level. We tested the method by processing SPOT-VGT NDVI-imagery (10-day Maximum Value Composites; 1km pixels) for Andalucía, Spain. CoverCAM requires specification that two time periods are specified: a reference period (we used 2000-04), and a change detection period (we used 2005-10). All images of the reference period were classified using the ISODATA algorithm and by evaluating divergence statistics. The generated map depicts strata (group of polygons), characterized by temporal NDVI and standard deviation (SD) profiles. For the change assessment period, first, mean NDVI-values were calculated by decade and polygon ($NDVI_{d,p}$), and then for each pixel of the polygon its pixel change values specified through the remaining difference between the pixel NDVI and [$NDVI_{d,p}$ ± the SD value of the stratum for that decade] (Euclidean Distance). The above process was repeated to produce decadal land cover change probability maps, each with its own undefined scale. The decadal change maps were then aggregated to annual change probability maps. The 2010 map was validated using field data and high-resolution ortho-imagery. This validation was only carried out for natural and semi-natural areas. Results showed that the CoverCAM estimates explained significantly ($p=0.00$) 72% of the variability in observed land-cover composition changes (BC-dissimilarity values). The success of the method to detect land cover composition changes thus delivered an improved quantitative tool to

(i) carry out continuous monitoring to detect land cover-changes, and
(ii) to timely detect hot-spots where the land-cover composition recently changed.

Keywords**:** Land cover, Change, SPOT, Monitoring, Hyper-Temporal

5.1 *Introduction*

Accurate information about changes in green land cover composition is important for management of biodiversity (Jones et al., 2009), hydrology (Eshleman, 2004), geomorphology (Foulds and Macklin, 2006), food production (Foley et al., 2005) and climate studies (Feddema et al., 2005; McAlpine et al., 2009). The issue of climate change enhanced the importance of quantifying changes in land cover composition as it is responsible for approximately 20% of the global carbon dioxide (CO_2) emissions to the atmosphere (Batjes, 2004; Houghton, 2005). Land cover change information is required in a timely manner to detect on-going processes and to support resource management planning (Loveland et al., 2002; Lunetta et al., 2006; Lupo et al., 2007; Bontemps et al., 2008; Nielsen et al., 2008).

The term 'land cover' refers to the biophysical surface of the earth at a specific moment. It includes both natural and man-made features. Water, bare land, rock, sand, ice are included in land cover (de Bie, 2000; Campbell, 2002; Gomarasca, 2009). Land cover composition in this study refers to the relative density and areal extent of different land cover components such as trees, shrubs, grass, bare soil, litter and stones as present in a certain area. Land cover composition continuously changes in space and time due to different natural and anthropogenic factors (Lambin, 1996). To accurately detect and represent land cover composition changes, both seasonality aspects (Loveland et al., 2002; Coppin et al., 2004; Lunetta et al., 2006) as well as longer duration processes (e.g. abrupt and gradual inter-annual changes) must be considered (Southworth et al., 2004; Pontius and Cheuk, 2006).

Seasonality is an important attribute of a land cover type (Sakamoto et al., 2006; Zhang et al., 2009; de Bie et al., 2011; Nguyen et al., 2011; de Bie et al., 2012). To accurately characterize changes in land cover composition, cover variability due to seasonality aspects (as reflected by species phenology and crop calendars) must be removed from the data to detect the required change information (Geoghegan et al., 2001; Coppin et al., 2004; Lunetta et al., 2004; Southworth et al., 2004; Lunetta et al., 2006; Lupo et al., 2007; Turner et al., 2007). Coppin et al. (2004) considered seasonality to be an important aspect in the monitoring of land cover. To accurately track and remove seasonal aspects for change detection requires a high temporal frequency of image capturing (Geoghegan et al., 2001; Southworth et al., 2004; Lunetta et al., 2006; Turner et al., 2007). The use of continuous series of imagery, captured at a high temporal frequency (hyper-temporal) imagery (Piwowar and LeDrew, 1995; Khan et al., 2010) has been found to be effective for the study of seasonality aspects (phenology and crop calendars)

of land cover and land use practiced (Khan et al., 2010; Khan et al., 2011; Nguyen et al., 2011).
The speed of land cover composition change varies depending on the extent and strength of causal factors (Lambin and Geist, 2006) and is represented using continuous values over time (Cihlar, 2000; Southworth et al., 2004). Lambin (1996) considered 'change' a continuous variable that varies in both space and time. Discrete representation (change or no-change) is deemed inappropriate to represent land cover composition changes (Foody and Boyd, 1999; Bontemps et al., 2008). Discrete change-maps are thus less useful for users due to the limited information they contain (Coppin et al., 2004; Ola, 2008). Use of remotely sensed is considered crucial and their data interpretation challenging when one aims to present cover change on a quantitative scale (Lambin and Linderman, 2006; Pontius and Cheuk, 2006).

Traditionally, change detection techniques have used multi-temporal imagery, captured at irregular intervals, through:

- image differencing (Weismiller et al., 1977; Ingram and Dawson, 2005),
- image rationing (Nelson, 1983),
- post-classification comparison (Howarth and Wickware, 1981; Chen and Wang, 2010),
- principal component analysis (Byrne et al., 1980; Young and Wang, 2001),
- selective principal component analysis (Chavez and Kwarting, 1989),
- regression models (Fraser and Latifovic, 2005),
- change vector analysis (Lambin and Strahlers, 1994; Bayarjargal et al., 2006),
- neural networks (Woodcock et al., 2001),
- coupling spectral un-mixing and trend analysis (Hostert et al., 2003),
- correspondence analysis (Cakir et al., 2006),
- object oriented methods (Desclée et al., 2006; Conchedda et al., 2008; Zhou et al., 2008), and
- the RGB composite approach (Schroeder et al., 2011).

Due to the limited number of imagery used in these studies, none were able to remove seasonality aspects from their change detection routines, thus compromising achieved accuracies (Lunetta et al., 2002; Coppin et al., 2004; Lu et al., 2004; de Beurs and Henebry, 2005; Lunetta et al., 2006). Typically, the older methods did not aim specifically at the detection of cover changes, but focused more on the production of discrete maps depicting change versus no-change information.

Some techniques already use time series imagery to a limited extent to detect land cover composition changes quantitatively, e.g.: trajectory based change detection (Kennedy et al., 2007), fuzzy methods (Foody and Boyd,

1999; Graciela, 1999; Foody, 2001; Metternicht, 2001; Fisher et al., 2006), probability methods (Fraser et al., 2005; Nielsen et al., 2008), regression models (Hayes et al., 2008), a temporal segmentation algorithm (Kennedy et al., 2012), and the gradient nearest neighbor (GNN) imputation method (Ohmann et al., 2012). They however all fail to remove seasonality aspects from their change detection logic and are thus still unable to characterize land cover composition changes at a required level of accuracy.

Recently, a few studies have reported the use of hyper-temporal imagery to detect land cover change, for example: time profiles descriptive statistic's method (Borak et al., 2000), change vector analysis (He et al., 2011), change in phenological cycles (Beurs and Henebry, 2005), change metrics (Lupo et al., 2007), object based method (Bontemps et al., 2008). These studies derived seasonal composites, annual composites or phenological matrices to determine inter-annual land cover changes. Their logic failed to consider common seasonality variability as caused by for example weather conditions. Remaining recent techniques resorted to trend analysis or to the detection of anomalies in hyper-temporal imagery without aiming specifically at capturing cover-composition changes, e.g.: BFAST (Breaks For Additive Seasonal and Trend) (Verbesselt et al., 2010a; Verbesselt et al., 2010b), temporal trajectory analysis (Lunetta et al., 2006), wavelet analysis (Martínez and Gilabert, 2009). Basically, these techniques pool detection in changes of cover performance (biomass effects) with changes in cover composition.

At present no specific quantitative land cover composition change assessment method exists that (i) removes seasonality variability like anomalies, (ii) considers phenological cycles and crop calendars, and (iii) pinpoints where and when the cover composition likely underwent or undergoes changes, expressed in quantitative terms. Accordingly, this study introduces a land cover composition change assessment method (CoverCAM) that addresses these issues. It generates land cover composition change assessment maps through the use of hyper-temporal NDVI imagery as captured by the SPOT-VGT or MODIS sensors.

5.2 *Land cover change probability mapping method*

The method processes hyper-temporal imagery in two steps: (a) classifying NDVI imagery of a reference time period (e.g. 2000-04) and (b) estimating change probabilities using NDVI imagery of a change assessment period (following years). Details of all required processing steps are explained below (Figure 5.1); section 3 presents details on imagery used to test CoverCAM. All steps that constitute CoverCAM were implemented in a prototype using Integrated Data Language (IDL).

Processing imagery of the reference time period

1. Geo-referenced hyper-temporal NDVI imagery (*Jan.2000-Dec.'04*) were classified using the Iterative Self-Organizing Data Analysis Technique (ISODATA) (Ball and Hall, 1965; Tou and Gonzalez, 1974). ISODATA was run with 50 iterations and a convergence threshold of 1. In total 64 runs were completed covering all pre-set number of clusters from 10 to 75 (Figure 5.1a-1).

2. Divergence statistics expressed as average and minimum separability values were calculated for each classified map (Figure 5.1a-2). These were subsequently used to select the optimal classified map (Swain and Davis, 1978; de Bie et al., 2012). The selected map was used as base map for land cover change detection during the change assessment period.

3. Standard deviation (SD) values were retrieved for each NDVI class on decadal basis for all the reference period years (180 values). By class, these decadal SD-values were then summarized (Eq.1a) to derive pooled SD-values (Headrick, 2009) representing the annual SD-behaviour of a NDVI-class (36 values). Equation 1a is simplified on the basis that n_i (sample size or number of pixels per class) remains constant (Eq.1b).

$$SD_{d,c} = \left[\frac{\sum_{i=1}^{y}\{(n_i-1)\,SD_{i,d,c}^2\}}{\sum_{i=1}^{y}(n_i-1)}\right]^{1/2} \xrightarrow{n_i = \text{constant}} \left[\frac{\sum_{i=1}^{y} SD_{i,d,c}^2\}}{y}\right]^{1/2} \qquad \text{(Eq. 1a \& 1b)}$$

   where: $SD_{d,c}$ is the pooled SD, *d and c* respectively the decadal number and NDVI-class, *i* the year number (*1* to *y*), and *y* the total number of pooled years (Figure 5.1a-3).

4. Each NDVI class comprises multiple areas (polygons or map units; red enclosed areas in Figure 5.1-3) scattered across the study area. These individual areas were treated as separate units because over time, each one can show different stochastic behaviour, for example due to area specific weather differences. Polygons that comprised less than 3 pixels were not further processed because their SD-values were considered meaningless (Conley et al., 1998) (Figure 5.1a-4). These small polygons were flagged as 'not assessed'.

Estimating change probabilities for a change assessment period

5. For the NDVI imagery of the change assessment period (*Jan.2005 to Dec.'10*), mean NDVI-values were calculated by polygon and decade ($NDVI_{d,p}$). Then, by decadal unit and for all pixels of each polygon, the actual pixel-values ($NDVI_d$) were compared to and established range of pooled SD around NDVI values: $NDVI_{d,p} \pm SD_{d,c}$ (Figure 5.1a-4). The pixel

change ratio for decade *d* was then defined by the remaining difference (Euclidean Distance) from $NDVI_{d,p} \pm SD_{d,c}$ (Figure 5.1b-5). During this study, due to the applied accuracy assessment method, negative and positive 'changes' were not treated differently. The above process was repeated to produce decadal land cover change probability maps (180x; *Jan.2005 to Dec.'10*). The change values are ratio data, but do not adhere to a fixed scale.

6. The change probability decadal data can be summed to produce seasonal-specific or annual maps (Figure 5.1b-6). The example map shows the change probabilities as generated using CoverCAM through the use of SPOT VGT NDVI-imagery.

CoverCAM has a functional prototype (in IDL) that provides the required flexibility to users concerning defining input and output specifications, and the choice to generate change maps for periods within years.

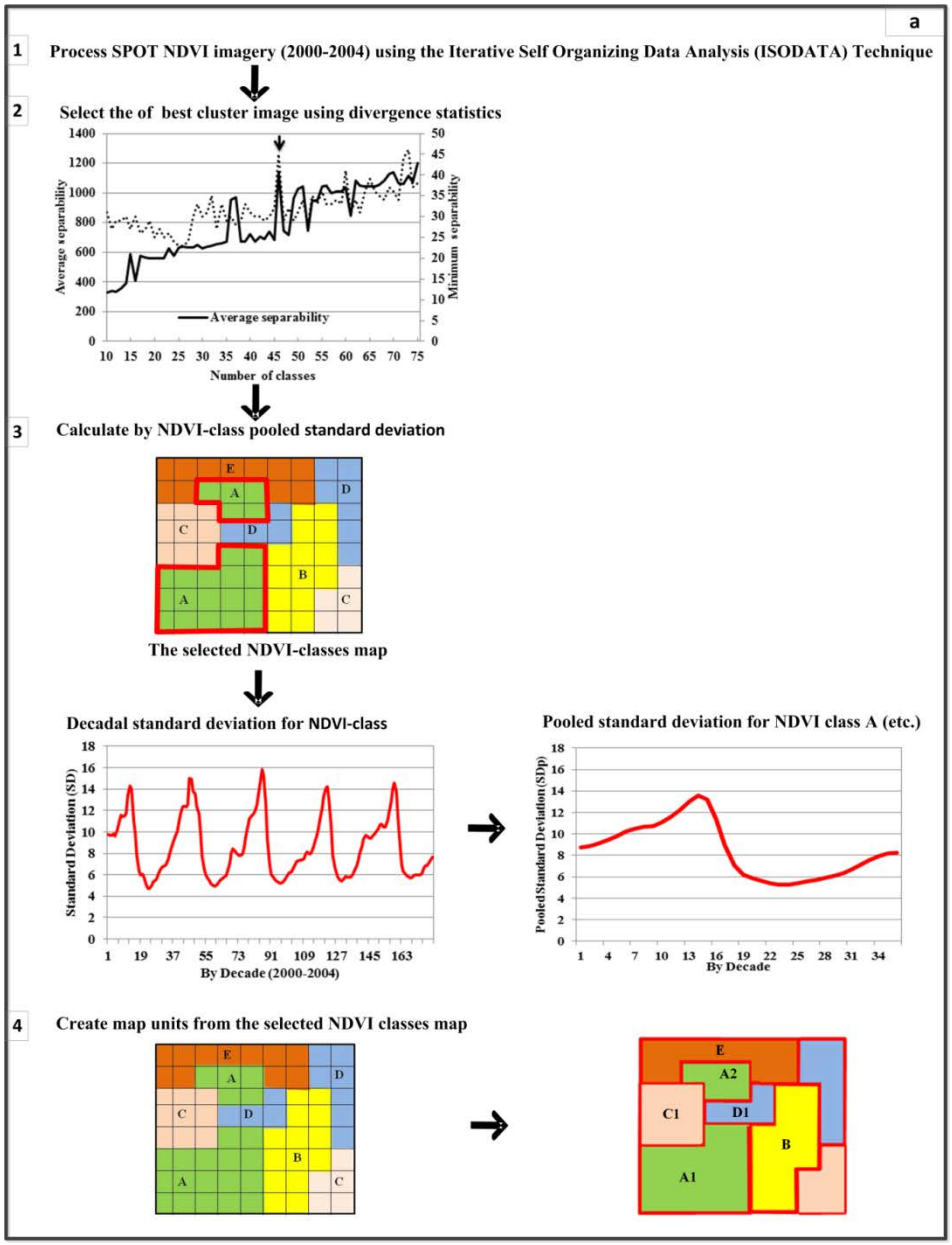
a
1
Process SPOT NDVI imagery (2000-2004) using the Iterative Self Organizing Data Analysis (ISODATA) Technique
2
Select the of best cluster image using divergence statistics
Average separability
Minimum separability
Average separability
Number of classes
3
Calculate by NDVI-class pooled standard deviation
The selected NDVI-classes map
Decadal standard deviation for NDVI-class
Standard Deviation (SD)
By Decade (2000-2004)
Pooled standard deviation for NDVI class A (etc.)
Pooled Standard Deviation (SDp)
By Decade
4
Create map units from the selected NDVI classes map
E
A2
C1
D1
B
A1

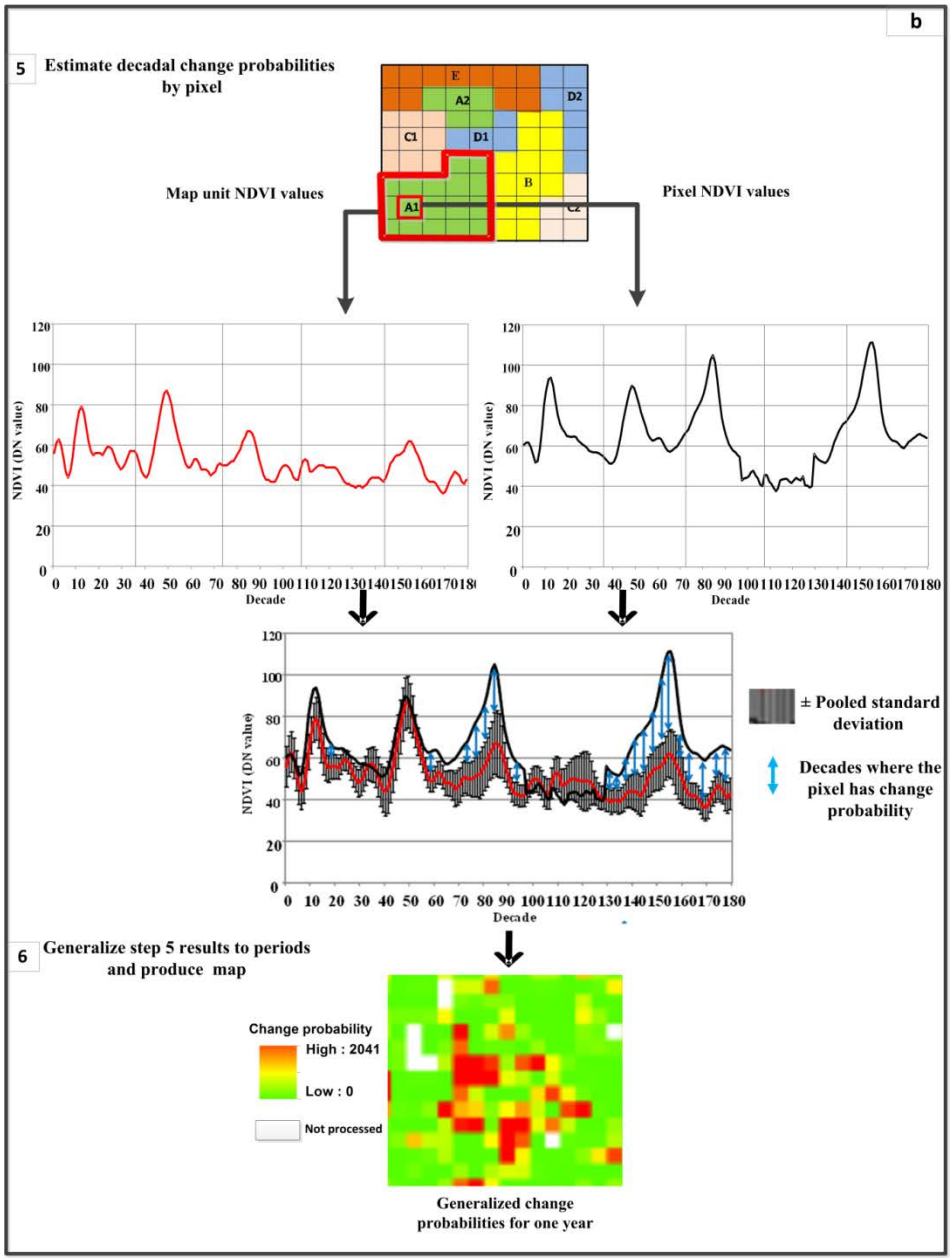

Figure 5.1. Steps of CoverCAM: (a) to process NDVI imagery of a reference time period (2000-04), and (b) to derive change probabilities using NDVI-imagery of a change assessment period (2005-10).

5.3 *CoverCAM Test*

CoverCAM was tested for the Southern part of Andalucía, Spain (Figure 5.2). The area has a Mediterranean climate, characterized by hot dry summers and mild rainy winters (Muñoz-Rojas et al., 2011). The annual precipitation drops from 2000 mm in the west to 170 mm in the east (Font, 2000). Dominant natural vegetation types typically contain oak, pines, fir species and shrubs. In the area, agriculture is the main land use; it occupies 67% of the land. Important land cover changes in Andalucía are: agricultural expansion and intensification in certain areas and abandonment in others, declining grazing intensities in natural areas, expansion of (plastic) greenhouses, urbanization, and forest loss due to fire (González-Pérez et al., 2004).

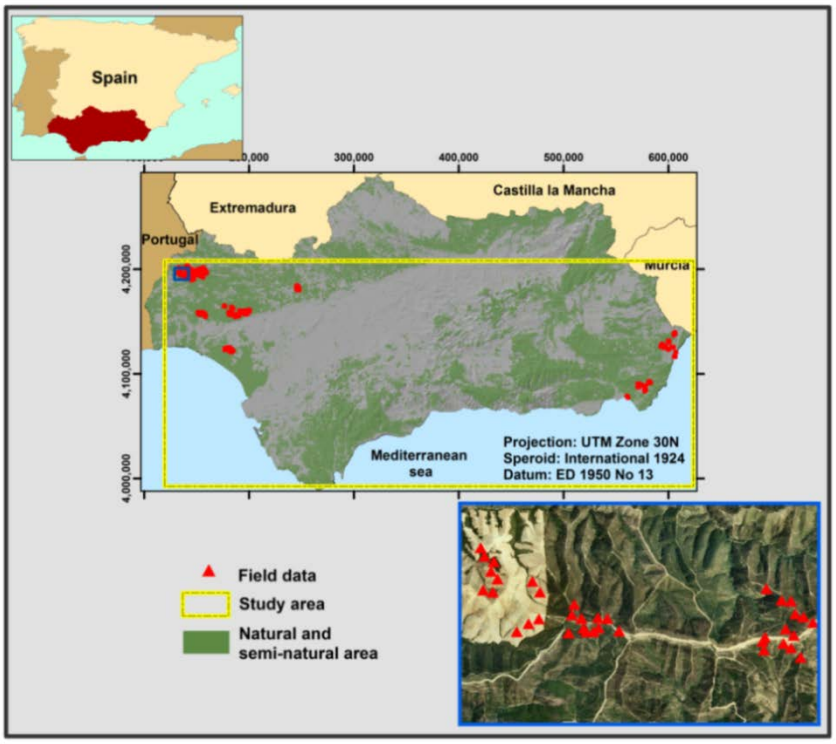

Figure 5.2. Study area (yellow box) as part of Andalucía, Spain, with (semi-) natural areas in green and ground survey points in red. Blue box: ortho-photo 2004 with ground survey points in red.

The hyper-temporal SPOT-VGT NDVI-images were downloaded from www.vgt.vito.be (10-day composites; 1 km^2 resolution; Jan.2000 to Dec.'09). The image-data are provided as DN-values, specified as: *DN-value = (NDVI+0.01)/0.004*. Information on data quality (SM-images) accompanying the NDVI images were used to set NDVI-values contaminated

by clouds or affected by other atmospheric problems, as 'missing'. By pixel, all missing values and remaining cloud and haze effects were adjusted by applying an upper envelope filter (Adaptive Savitzky Golay filter) to the pixel-based time-series of DN-values (Jönsson and Eklundh, 2004; Beltran-Abaunza, 2009). Then, the imagery was divided into two data-sets (Figure 5.1), i.e. *a*: Jan.2000-Dec.'04 (reference time period) and *b*: Jan.2005-Dec.'10 (change assessment period). Finally, the CoverCAM routine was carried out to prepare change maps for complete years.

For the validation, only the 2010 change probability map was tested. Field data were collected on a pixel-by pixel basis (1 km^2 area) within forests and semi-natural areas (Corine 2006; www.eea.europa.eu/data-and-maps/data/clc-2006-vector-data-version-1, Accessed on 2 July'10); fieldwork and data analysis were supported by ortho-photos (1m resolution, dated 2004; http://80.81.99.236/Descargas/Principal.do, Accessed on 10 May'11), and screen-captured imagery of Google Earth® (dated 2010).

Details concerning the steps needed for sampling and the validation protocol are explained below (Figure 5.3). Note that the ortho-photos as used during fieldwork were assumed to represent the reference time period (2000-04), and the Google Earth® images to represent the change assessment and fieldwork periods. Google Earth® has been increasingly used for validating land cover products (Montesano et al., 2009; Clark et al., 2010; Dorais and Cardille, 2011; Thomas et al., 2011).

1. Sampling (Figure 5.3-1): In Andalucía, field data were collected during Sep.-Oct. 2010. A random clustered sampling scheme was used to collect the data. Survey areas chosen to sample (55x35 km areas, being the extent of 1 ortho-photo) covered always (semi-) natural areas, and contained according to the CoverCAM-2010 map, pixels with low, medium, and high land cover change. For each pixel (1km^2; Figure 5.3-1), all relevant image-objects, as pre-identified from the 2004 ortho-photos and 2010 Google Earth® images, were sampled in a random manner. For each sample (20x20m), vertical cover percentages of all cover-components present were estimated, i.e. trees, shrubs, grass/herbs, stone, litter, and bare soil. Visual signs of past impacts, including fire or deforestation, were recorded. In total, all image objects of 242 pixels of 1km^2 were surveyed.
2. Legend construction (Figure 5.3-2): For each pixel surveyed, for the 2004 ortho-photos and the 2010 Google Earth® images jointly, a simple legend was constructed on the basis of pre-identified image-objects (visually unique screen snap-shots representing 20x20m areas). Then the closely resembling image objects were grouped and unique identification codes

were assigned to each group. Then, by legend-class, all allocated records were averaged to derive a final cover description for each image-object.

3. Map unit delineation (Figure 5.3-3): Based on the pre-identified image-objects (legend), visually both ortho-photos and Google Earth® images were interpreted into map units, which were pre-delineated using eCognition.
4. Cover estimates by pixel (Figure 5.3-4): Using the two polygon-based land cover maps (of 2004 and 2010) and area weights by legend-class, generalized 1km resolution (pixel-based) maps were prepared, containing cover-component statistics.
5. Change calculation (Figure 5.3-5): By 1km pixel, the actual (observed) composition change between 2004 and 2010 was calculated using the Bray-Curtis dissimilarity function (Eq. 2) (Bray and Curtis, 1957). The function is a standardized non-metric robust estimate concerning changes in land cover fractions (Eq. 2). Bray-Curtis dissimilarity is one of the most commonly applied metric used in ecology and environmental sciences (Clarke et al., 2006). A Bray-Curtis dissimilarity value of *0* means complete similarity between two data records, a value of *1* signifies complete dissimilarity.

$$BCD_{2004,2010} = \frac{\sum_{k=1}^{6} |x_{2004,k} - x_{2010,k}|}{\sum_{k=1}^{6} (x_{2004,k} + x_{2010,k})} \quad \text{(Eq. 2)}$$

Where: $BCD_{2004,2010}$ is the Bray-Curtis Dissimilarity between the 2004 and 2010 imagery, k is the sequence number of a variable (in this case 1 to 6), and x the actual estimates (cover fractions over the 1km^2 pixel).

Finally, simple linear regression analysis was carried out to test the relationship between the CoverCAM estimates and the observed changes Bray-Curtis dissimilarity values). Results were assessed based on the coefficient of determination (R^2) and 'p' value (< 0.5).

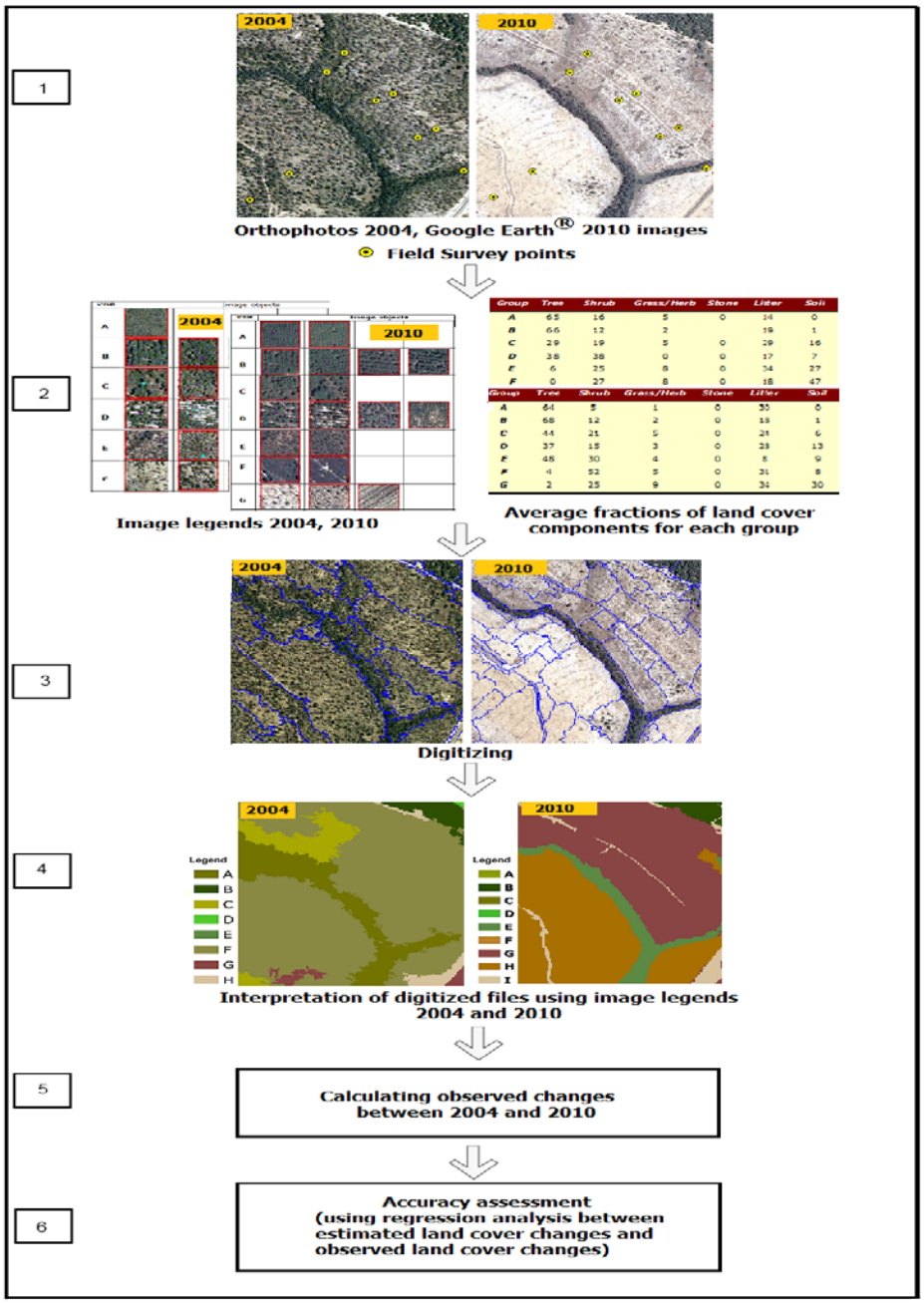

Figure 5.3. Steps needed for the accuracy assessment of CoverCAM estimates.

5.4 *Results*

5.4.1 *Land cover change probability mapping method*

Figure 5.4 shows the divergence statistics result for the maps containing 10 to 75 classes (clusters). It shows locally high separability values for the "46 classes map"; that map was therefore selected as the 'best' clustering option for the imagery of the reference time period. This map of 46 classes formed the 'base map' to detect changes for the change assessment period.

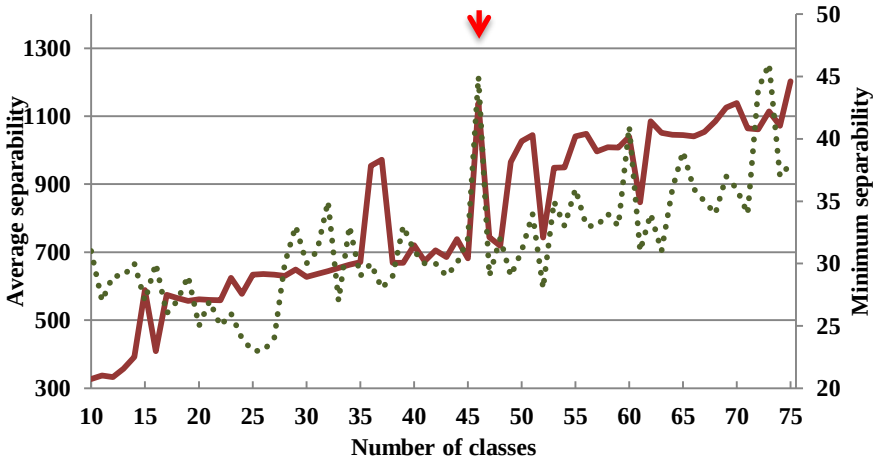

Figure 5.4. Divergence statistics for maps having 10 to 75 classes (clusters). Red arrow: the 46 classes map.

Figure 5.5 depicts the 2010 land cover composition change map as generated by CoverCAM. Green indicates areas with relatively no-change (value ≥ 0) to high change (value ≤ 2041). High change values can be observed in the eastern and western parts of the study areas; these are mainly (semi-) natural areas. Figure 5.6 shows three typical examples of areas where land cover composition changes were identified through CoverCAM. The change values must be read as 'change probabilities'. No absolute scale is used, meaning that rescaling the values between 0 and 1 could not be done, because it is unknown which (high) value represents 100% change. In addition, no information on 'what' changes into 'what' is inferred. CoverCAM thus basically identified hot-spots at which to focus attention.

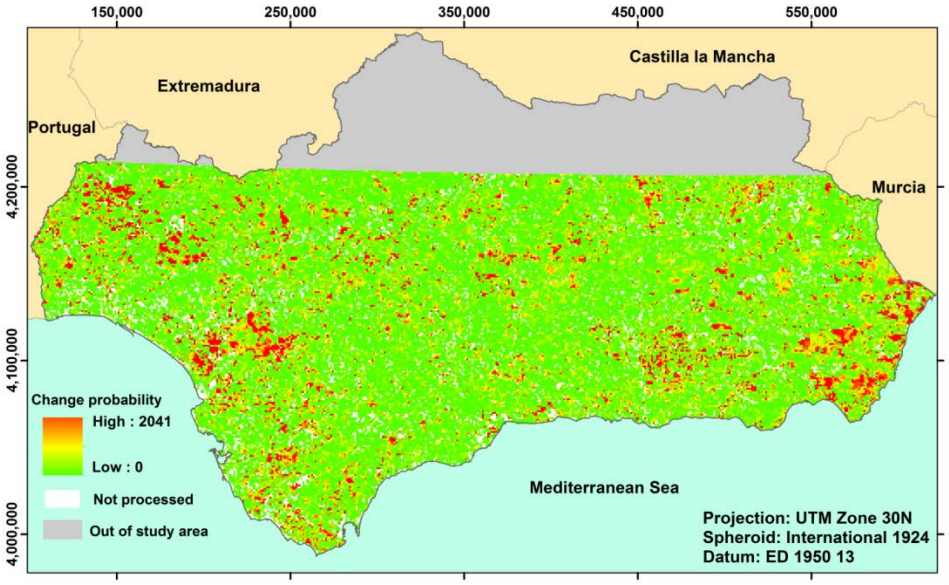

Figure 5.5. Land cover composition change map of 2010 (Andalucía, Spain).

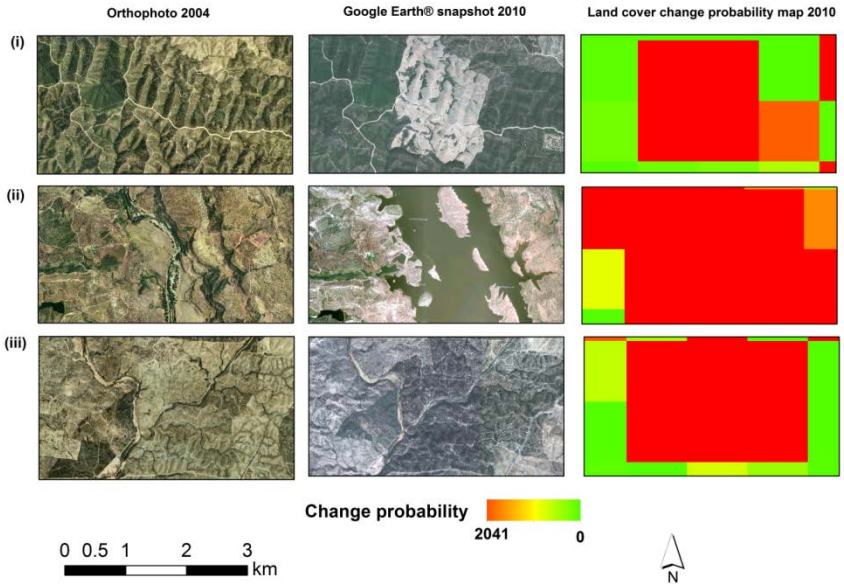

Figure 5.6. Three typical examples of areas where CoverCAM successfully detected land cover changes.

5.5 *Accuracy assessment*

The method successfully generated the required data for 242 1km^2 pixels. Regression analysis results between CoverCAM estimates and observed land

cover change probability values proved significant (p=0.00). The explained variability was high (R^2=0.72) and most of the observations fall within the relatively small range of the 95% confidence interval (dashed lines; Figure 5.7).

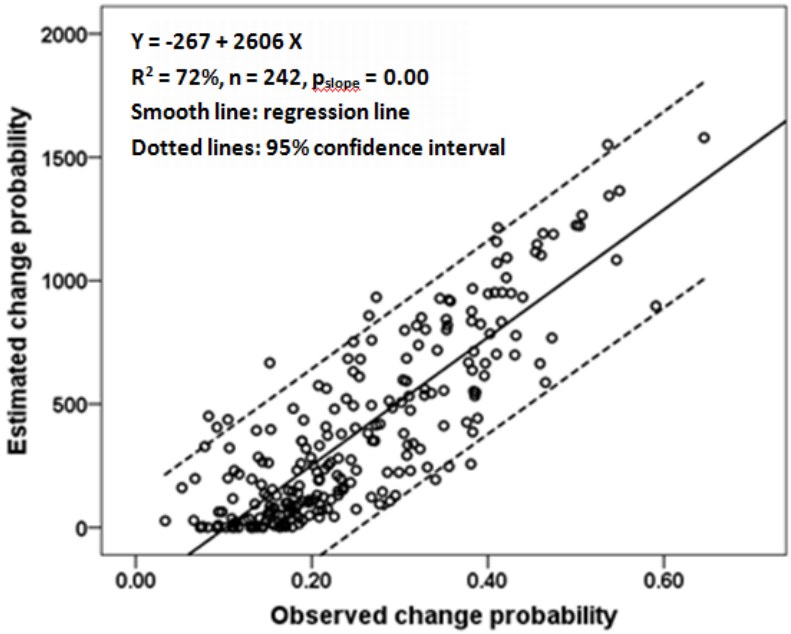

Figure 5.7. Scatter plot between observed change (BC-dissimilarity values) and CoverCAM estimates.

5.6 *Discussion*

CoverCAM produces robust results because it removes seasonal stochastic effects such as local rain showers. The calculation of pooled standard deviation using a five-year window (2000-2004) makes interpretation more reliable, because pooled SD-values are less affected by outliers (Rumsey, 2011). Methods that use original SD-values to detect changes suffer from inaccuracies of the original NDVI values (Cakir et al., 2006). CoverCAM compares image by image NDVI-values at pixel level with the average pixel-readings of individual polygons. Other change detection methods lack that adjustment routine; they process images on a pixel-by-pixel strategy, resulting in noisy and unreliable outputs (Radke et al., 2005). The use of single-time imagery as reference or of multi-temporal imagery to capture and compare seasonal or annual variations also makes change detection unreliable (Ingram and Dawson, 2005; Bayarjargal et al., 2006; Chen and Wang, 2010). The use of the hyper-temporal imagery as the case of CoverCAM clearly eliminates such problems. CoverCAM aggregates the detailed estimates over time to derive season- or year-specific change ratio

estimates, thus emphasizing pixels that show a consistent continuous deviation from the set norm. Aggregating results to monthly or seasonal data reduces the influence of temporal data inaccuracies, such as the effect of minor time-shifts in the phenological cycle causing short duration differences (de Jong et al., 2011). Using a reference and monitor period aims to bridge the intervals that inventory surveys take place (e.g. 10-yearly Corine in the EU).

The method is only validated for (semi-) natural areas because cover present there within a year does not show sudden changes due to ploughing, planting and harvesting as is characteristic of arable systems. To validate CoverCAM for arable crops requires within-year multi-temporal ortho-photos for the years selected to compare. Crop calendar information collected through farmer's interviews can support the interpretation of high-resolution imagery (Nguyen et al., 2011).

The estimated change probabilities provide relative indication about land cover changes. The range in generated land cover change values is specific to the NDVI imagery used. The relative index indicates when and where a change is detected. This information is important in order to monitor and understand land cover changes (Loveland et al., 2002; Coppin et al., 2004).

Introducing the use of polygons as reference units instead of the full extent of an NDVI-class to detect changes was essential to achieve the set objectives. It aims to eliminate local short-term and seasonal anomalies and other stochastic events such as early/late greening or early/late maturing. This makes CoverCAM especially suitable to detect cover changes within large and diverse landscapes under varying climatic conditions.

5.7 *Conclusion*

This study introduced a new land cover change assessment method (CoverCAM) based on long term hyper-temporal NDVI imagery. The method was successfully applied and verified in a case study area of Andalucía, Spain, having R2 of 0.72. CoverCAM has proved simple to implement, is fully repeatable, and requires no prior knowledge of the area. Future work concerns repeats of the accuracy assessment for different land cover types, for example agricultural areas. Reporting on differences between gradual and abrupt change plus their respective periods and dates needs further attention, so that additional useful information is generated. The success of the method to detect land cover composition changes thus delivered an improved quantitative tool to (i) carry out continuous monitoring to detect land cover-changes, and (ii) to timely detect hot-spots where the land-cover composition recently changed.

Acknowledgements
The authors like to thank the constructive collaboration they received from Amit Kumar Srivastava, Lina Estupiansuarez, Jose Maria Beltran-Abaunza and Mina Naeimi. All are ITC alumni.

6 Synthesis

6.1 *Introduction*

In recent years, impacts on natural resources increased due to the increasing global population and through climatic changes (Cihlar, 2000; Kok, 2004). Formulation and implementation of required mitigation strategies do require, amongst others, accurate and informative land cover maps and monitoring products. The current omission in land cover maps to clearly represent gradients that exist and the practice to prepare them through using limited imagery over time, underexploits the present-day options to generate more informative maps that carry improved legends that do describe gradients and to exploit modern representation techniques of the gradients-extent. Maps that present land cover classes using over-generalized descriptions and/or that insufficient depict the spatial/temporal extent of spatial relationships between classes that matter, as that depict the changes in their mixed composition occurrences, do impose limitations on their utility for natural resources management purposes. The use of a limited time-coverage of imagery for interpretation causes loss in the ability to capture seasonality aspects of the green land cover present (natural vegetation and crops), and hence poses limitations on meaningful characterization. Capturing aspects of phenology and followed crop calendars does matter. These shortcomings are carry-over into subsequent monitoring products.

Research to address the stated issues of present-day land cover maps through the use of hyper-temporal remote sensing data, as available in different spatial and temporal resolutions, was the aim of this thesis. The highly repetitive coverage of hyper-temporal image dataset does capture seasonality aspects of vegetation over time (vegetative growth patterns) (Reed, 2006; Xiao et al., 2006a; Wardlow et al., 2007; de Bie et al., 2008; Zhang et al., 2008) that helps to improve characterization and visualization of land cover present. To achieve that, new methods and tools were developed and tested. They supplement existing methods.

Accordingly, this research started by testing and exploring methods that aim at spatial-temporal pattern recognition, using information on spatial-temporal seasonal variability of vegetation as contained within hyper-temporal NDVI-datasets. Following the exploration, the following specific research objectives were defined: (i) to devise a simple technique to detect long-duration cloud contamination in hyper-temporal NDVI imagery (chapter 2), (ii) to identify and map land cover gradients through the analysis of hyper-temporal NDVI imagery (chapter 3), (iii) to test an explicit spatial-temporal gradient and heterogeneity detection method at landscape level (chapter 4), and (iv) to develop and test a land cover composition change assessment method (CoverCAM) that is insensitive to short duration spatial-temporal variability (chapter 5).

This chapter first highlight by chapter progress achieved, then their practical implications, and finally it discusses various future research possibilities.

6.2 *Achieved results*

6.2.1 *Detecting long duration cloud contamination affects in hyper-temporal NDVI imagery*

Hyper-temporal NDVI time series imagery have increasingly been used for land use/land cover mapping and monitoring due to its spatiotemporal explicitness and its ability to characterize land cover accurately (Xiao et al., 2006a; Wardlow et al., 2007; Bontemps et al., 2008; Zhang et al., 2008; Julien and Sobrino, 2010; de Bie et al., 2011; Nguyen et al., 2011). However, cloud contamination impacts on the quality of hyper-temporal NDVI imagery and their subsequent interpretation (Jonsson and Eklundh, 2002; Fensholt *et al.*, 2006; Ma and Veroustraete, 2006; Hird and McDermid, 2009; Clark *et al.*, 2010). Currently, the pre-processing routines of satellite data such as the use of quality flags, maximum value composite imagery (Holben, 1986; Stowe et al., 1991) and cloud corrections and adjustments algorithms are not able to overcome the effects. (Jonsson and Eklundh, 2002; Chen et al., 2004; Jönsson and Eklundh, 2004; Lu et al., 2007; Atzberger and Eilers, 2011a) This is particularly important in cloud prone areas such as tropics. In chapter 2 of this thesis, a simple method is developed which detects the data values affected by long duration cloud. After detection, a user can avoid their use during subsequent analysis. The tested method is built on statistically derived unsupervised classification of the hyper-temporal time series imagery. A synchronous decline in seasonal NDVI values below a lower limit 95% confidence interval and an increase in the standard deviation above an upper limit 95% confidence interval are used as indicator of possible long-term cloud contamination. The results were thoroughly validated using additional remote sensing data as reference (Terra and Aqua combine). However, it needs to be validated with real cloud cover data.

6.2.2 *Land cover gradients representation*

The green cover of the earth shows various spatial gradients that represent gradual changes in space of vegetation density and/or in species composition. However, Most of the available land cover mapping methods differentiates, mapping units with different cover densities and/or species compositions, but fail to express such differences as gradients**.** Similarly they used limited imagery of irregular time period which limits its capacity to characterize and visualize gradients in land cover. In chapter 3, hyper-temporal NDVI imagery was successfully used to detect and delineate land cover gradients. The resultant land cover gradient map (Figure 3.5) shows groups of land cover based the intensity of NDVI and similarities in their

temporal characteristics**.** Each group reflects a separate dominant gradient in vegetation density and species composition**.** Using field data, correlations of cover densities with NDVI-values and of species composition (phenology differences) with the temporal behavior of NDVI values were also established. The results (Figure 3.6) indicates that within each NDVI group, the collected cover fraction data are significantly linearly related with the given NDVI data and these linear relationships between NDVI-groups are significantly different with respect to tree cover, shrub cover, grass cover, bare soil, stone cover and litter cover fractions. This has proved that hyper-temporal imagery properly captures temporal aspects of land cover (seasonality) and delineates vegetation density. This is due to the sensitivity of NDVI to vegetation green biomass (Purevdorj et al., 1998; Shunlin, 2004) and repetitive coverage of the imagery used which help in accurately characterizing of land cover(Sakamoto et al., 2006; Zhang et al., 2009; de Bie et al., 2011; Nguyen et al., 2011; de Bie et al., 2012).

6.2.3 *Landscape heterogeneity mapping*

In chapter 4, a spatial-temporal gradient and heterogeneity detection method called LaHMa was applied and tested for mapping landscape heterogeneity of natural and semi natural landscapes. Based on results, the LaHMa approach was found suitable for mapping heterogeneity of natural and semi natural landscapes. The validation results show that the heterogeneity output map is relatable to spatial variation on ground (Figure 4.3). The LaHMa method represents gradients in heterogeneity values of pixels and it takes into account long term spatiotemporal behaviour of landscape. The continuous spatial representation of landscape heterogeneity is more realistic and is consistent with ground conditions (Whittaker, 1967; Whittaker, 1978b; Cushman et al., 2010). The spatial patterns arranged in the form of gradients are due to the continuous changes in the physical environment (Legendre et al., 2002) (Gosz, 1992). The repetitive nature of hyper-temporal imagery used in this method helps to track closely the vegetative growth patterns. The spatiotemporally explicit and gradient based representation of landscape heterogeneity is more important for ecological studies.

6.2.4 *Improved land cover monitoring*

The available land cover change methods do not remove seasonal aspects from change detection process hence limits their ability to track and identify land cover changes accurately. Most of the methods used limited imagery of irregular time period which cannot track seasonal changes hence it is difficult to remove from the change detection process. A new land cover composition change assessment method (CoverCAM) introduced in chapter 5 of this thesis (Figure 5.5) successfully produced over time land cover composition change map. The estimated change ratio gives relative indication about land cover

changes. The method removed seasonal differences from the mapping process which ensure accurate characterization of land cover composition changes. Seasonal sequences (green cover phenology and followed crop calendars) is important attribute of a specific cover composition or type (Sakamoto et al., 2006; Zhang et al., 2009; de Bie et al., 2011; Nguyen et al., 2011; de Bie et al., 2012) therefore to accurately track seasonal aspects and to remove it from change detection, hyper-temporal imagery is important. The continuous representation of change composition is more accurate way of representing maps (Cihlar, 2000; Southworth et al., 2004). The method also remove local variability due to weather which is not related to actual changes such as early greening, late greening, early or late drying and greening effects. The method is simple and easily repeatable. It is self-regulated with no trial and error involved. It does not require any prior knowledge of the area.

Validation performed for specifically for natural and semi natural areas showed close agreement (72%) between land cover composition change map and observed land cover composition changes (Figure 5.6). This was done due to the unavailability of frequent imagery of the area for validation.

6.3 *Practical implication of the achieved results*

The methods tested and developed in this study helps in accurate mapping and monitoring of land cover and its changes over time. They utilized free imagery available from different sources in different spatial and temporal resolution such as SPOT, MODIS etc. The techniques are adaptable to wide range of datasets available. They can be useful to monitor effects of global warming, droughts, deforestation, desertification, flooding, food security, biodiversity etc. It can be easily utilized by decision-makers for sustainable development and management of land cover.

6.3.1 *Improved quality of interpretation of land cover in cloud prone areas*

The method introduced in chapter 2, successfully detects the data affected by long duration cloud contamination. After detection, a user can recode such values as missing and avoid their use during subsequent analysis. It offers scientists interested in time series analysis a method of masking by area (class) the periods when pre-cleaned NDVI values remain affected by long duration clouds. It can be specifically useful for mapping and monitoring in areas where cloud cover is prevalent such as tropics. This is very important contribution because the pre-processing routines of satellite data are still not fully able to adjust the data affected by long duration cloud contamination (Jonsson and Eklundh, 2002; Chen et al., 2004; Jönsson and Eklundh, 2004; Lu et al., 2007; Atzberger and Eilers, 2011a). This method improved the

quality of maps and its interpretation. This can be specifically useful in studies based on identification of simple anomalies such as used by Lunetta et al., 2006.

6.3.2 *Improvement in land cover maps visualization*

Land cover gradient representation is accurate and realistic way of mapping and visualizing land cover (Whittaker, 1973; Whittaker, 1978b; Gosz, 1992). It is important for ecological studies (Gosz, 1992) because this gives more information about land cover behaviour over time and landscape structural. In chapter 3 successfully identification of land cover gradients through spatio-temporal analysis of hyper-temporal NDVI imagery is shown. The gradients map clearly shows the intensity of NDVI and similarities in their temporal characteristics (Figure 3.7). The inter-relationships between land cover groups gives more insight about structure of landscape. The detailed information from a single set of data over a large area makes it feasible and suitable for extracting land cover information

Similarly landscape heterogeneity of natural and semi-natural a landscape is successfully depicted the form of gradients. The tested method shows the relative heterogeneity of each pixel area in natural and semi-natural landscape. The continuous form of information presented which is based on spatiotemporally explicit data analysis can help to study effects of fire disturbances, moisture availability, species compositions, local patterns in soils, micro-topography, effects of grazing management or other anthropogenic activities. The heterogeneity is calculated based on long-term spatiotemporal variability in land cover which is important to monitor land cover changes and incorporate in the mapping process. It can be specifically helpful to identify and study boundary structures such as ecotones and ecoclines, which is functional and structural units of any landscape (de Bie et al., 2013).

6.3.3 *Can contribute to improve available data collection mechanisms of area frame sampling*

Agricultural statistics and land surveys are traditional methods of estimating land use/ land cover. Area frame sampling is one of the widely used data collection technique used for generating agricultural statistics. Area frame sampling involved stratifications of land cover using fraction land cover or density of vegetation. The stratification performed is usually based on one or two time imagery. They do not consider spatiotemporal characteristics of land cover which may introduce errors in stratification of land cover (FAO 1995; USDA 2004). Therefore, the gradients based output maps produced as a result of spatiotemporal analysis of land cover could aid researchers in stratifying sampling regimes based on natural land cover groupings and

direction of gradients in land cover. The inter-related and the directionally ordered map units from low to high can be useful for finalizing sampling scheme. Due to the proper knowledge of the direction and status of areas over time, one can optimize sampling to save time and money.

6.3.4 *Monitor land cover composition changes*

The CoverCAM method (chapter 5) can help to estimate land cover composition change ratios over time. The method is capable to produce change maps for each decade and user can also cumulate it to specific period of interest or any season or years. This can help to accurately monitor both gradual and abrupt land cover composition changes (Figure 5.6 and 5.7).

The method is insensitive to any noise due to clouds, haze and other atmospheric effects because the spectro-temporal behaviors of individual map units are compared to each pixel values in similar land use / land cover segments at different locations.
The method employed hyper-temporal imagery for both reference and change assessment period which make the comparison of two time periods reliable (Ingram and Dawson, 2005; Bayarjargal et al., 2006; Chen and Wang, 2010).

The input imagery is free and easily available in different spatial and temporal resolutions. In contrast most of the available techniques are not spatiotemporally explicit and the changes are depicted in discrete form. The discrete change-maps are less useful for users due to the limited information they contain (Coppin et al., 2004; Ola, 2008).

6.4 *Relevance, utility and possible impact on large programmes and organizations*

To get accurate estimation of current status of vegetation and its changes for implementing any vegetation conservation program (He et al., 2005), the new land cover mapping (chapter 2, 3 and 4) and monitoring methods (chapter 5) can help to assess land use and land cover situation and monitor it with time more accurately and efficiently. The spatiotemporally explicit mapping and monitoring methods produce timely, accurate and sharable spatial information. The techniques are easily adaptable and can be useful for regular monitoring of the most important indicator of the any development or conservation program in placed by world organization such as NASA, UN organizations, USDA (United States Department of Agriculture) etc. The results can be useful to monitor effects of global warming, droughts, deforestation, desertification, flooding, food security, biodiversity etc. The information produced can expedite and ease decision making process and promote inter-organizational cooperation to support e.g. alleviating

poverty/hunger (MDG 1) and promote sustainable developments (MDG 7). The methods are easy to execute and the imagery used is free and easily available from different sources in different spatial and temporal resolution. The procedures worked out are applicable at country and regional levels. The techniques developed can contribute to the cause for global research programs such as the International Geosphere-Biosphere Program (IGBP), the Framework Convention for Climate Change, the Kyoto Protocol, the Biodiversity Convention, NASA's Land Cover-Land Use Change (LCLUC) program, FAO land use and land cover information program and Intergovernmental Panel on Climate Change (IPCC) (IPCC, 2001).

6.5 *Recommendations for future research*

- The long duration cloud contamination (chapter 2) was validated with additional satellite data Aqua (Terra-Aqua combine) however it needs to be validated with a real cloud cover data provided necessary arrangements are made to collect real cloud cover data over large area and long time period.

- In case of land cover gradient mapping (chapter 3), work in the near-future should focus on quantitative analysis of phenological indicators extracted from NDVI profiles. Study of the underlying factors responsible for land cover gradient could be also investigated to further explore the landscape characteristics associated with land cover distributions and influences spatiotemporal aspects of land cover.

- Further evaluation of the LaHMa method with the incorporation of more study sites into ground sampling and over a greater variety of land cover is required (chapter 4). It is recommended that a comparative analysis be conducted of the performance and informative abilities of the LaHMa technique and other landscape heterogeneity characterization techniques.

- Future work regarding CoverCAM method (chapter 5) concerns repeats of the accuracy assessment for different land cover types, e.g. for agricultural areas. Direction of change and its rate would be interesting to use for planning and management purpose. Differences between gradual and abrupt change with respect to time needs further attention to make it more useful method.

Bibliography

Ackerman, S. A., Strabala, K. I., Menzel, W. P., Frey, R. A., Moeller, C. C., Gumley, L. E., 1998. Discriminating clear sky from clouds with MODIS. Journal of Geophysical Research 103, 32141-32157.

Addink, E. A., Stein, A., 1999. A comparison of conventional and geostatistical methods to replace clouded pixels in NOAA-AVHRR images. International Journal of Remote Sensing 20, 961-977.

Alexandridis, T. K., Gitas, I. Z., Silleos, N. G., 2008. An estimation of the optimum temporal resolution for monitoring vegetation condition on a nationwide scale using MODIS/Terra data. International Journal of Remote Sensing 29, 3589-3607.

Ali, A., de Bie, C. A. J. M., Skidmore, A. K., Scarrott, R. G., Hamad, A., Venus, V., Lymberakis, P., 2013. Mapping land cover gradients through analysis of hyper-temporal NDVI imagery. International Journal of Applied Earth Observation and Geoinformation 23, 301–312.

Anand, M., Li, B. L., 2001. Spatiotemporal dynamics in a transition zone: patchiness, scale, and an emergent property. Community Ecology 2, 161-169.

Arnot, C., Fisher, P., 2007a. Mapping the ecotone with fuzzy sets. in: Morris, A., Kokhan, S., (eds), Geographic Uncertainty in Environmental Security. Springer, Netherlands, pp. 19-32.

Arnot, C., Fisher, P., 2007b. Mapping Type 2 Change in Fuzzy Land Cover. in: Morris, A., Kokhan, S., (eds), Geographic Uncertainty in Environmental Security. Springer, Netherlands, pp. 167-186.

Atzberger, C., Eilers, P. H. C., 2011a. Evaluating the effectiveness of smoothing algorithms in the absence of ground reference measurements. International Journal of Remote Sensing 32, 3689-3709.

Atzberger, C., Eilers, P. H. C., 2011b. A time series for monitoring vegetation activity and phenology at 10-daily time steps covering large parts of South America. International Journal of Digital Earth 4, 365-386.

Austin, M. P., 1990. Community theory and competition in vegetation. in: Grace, J. B., Tilman, D., (eds), Perspectives in Plant Competition. Academic Press, New York, pp. 215-233.

Baker, W. L., Cai, Y., 1992. The r.le programs for multiscale analysis of landscape structure using the GRASS geographical information system. Landscape Ecology 7, 291-302.

Ball, G. H., Hall, D. J., 1965. Isodata: A Method of Data Analysis and Pattern Classification, Stanford Research Institute, Menelo Park, California, United States.

Bastin, L., 1997. Comparison of fuzzy c-means classification, linear mixture modelling and MLC probabilities as tools for unmixing coarse pixels. International Journal of Remote Sensing 18, 3629-3648.

Batjes, N. H., 2004. Soil carbon stocks and projected changes according to land use and management: A case study for Kenya. Soil Use and Management 20, 350-356.

Bayarjargal, Y., Karnieli, A., Bayasgalan, M., Khudulmur, S., Gandush, C., Tucker, C. J., 2006. A comparative study of NOAA-AVHRR derived drought indices using change vector analysis. Remote Sensing of Environment 105, 9-22.

Beck, P. S. A., Wang, T. J., Skidmore , A. K., Liu., X., 2008. Displaying remotely sensed vegetation dynamics along natural gradients for ecological studies. International Journal of Remote Sensing 29, 4277-4283.

Begon, M., Harper, J. L., Townsend, C. R., 1990. Ecology: Individuals, populations and communities, Second.ed. Blackwell Scientific Publications, Oxford.

Beltran-Abaunza, J. M., 2009. Method Development to Process Hyper-temporal Remote Sensing (RS) Images for Change Mapping. Enschede, The Netherlands, University of Twente.

Bénié, G. B., Kaboré, S. S., Goïta, K., Courel, M. F., 2005. Remote sensing-based spatio-temporal modeling to predict biomass in Sahelian grazing ecosystem. Ecological Modelling 184, 341-354.

Berberoglu, S., Curran, P. J., Lloyd, C. D., Atkinson, P. M., 2007. Texture classification of Mediterranean land cover. International Journal of Applied Earth Observation and Geoinformation 9, 322-334.

Beurs, K. M. d., Henebry, G. M., 2005. A statistical framework for the analysis of long image time series. International Journal of Remote Sensing 26, 1551-1573.

Bezdek, J. C., Pal, N. R., 1998. Some new indexes of cluster validity. Systems, Man, and Cybernetics, Part B: Cybernetics, IEEE Transactions on 28, 301-315.

Bontemps, S., Bogaert, P., Titeux, N., Defourny, P., 2008. An object-based change detection method accounting for temporal dependences in time series with medium to coarse spatial resolution. Remote Sensing of Environment 112, 3181-3191.

Borak, J. S., Lambin, E. F., Strahler, A. H., 2000. The use of temporal metrics for land cover change detection at coarse spatial scales. International Journal of Remote Sensing 21, 1415-1432.

Boschetti, M., Stroppiana, D., Brivio, P. A., Bocchi, S., 2009. Multi-year monitoring of rice crop phenology through time series analysis of MODIS images. International Journal of Remote Sensing 30, 4643-4662.

Boyd, D. S., Foody, G. M., 2011. An overview of recent remote sensing and GIS based research in ecological informatics. Ecological Informatics 6, 25-36.

Bradshaw, G. A., Spies, T. A., 1992. Characterizing canopy gap structure in forests using wavelet analysis. Journal of Ecology 80, 205-215.

Bray, J. R., Curtis, J. T., 1957. An ordination of the upland forest communities of southern wisconsin. Ecological Monographs 27, 326-349.

Burns, R., Burns, R. P., 2008. Business Research Methods and Statistics Using SPSS. SAGE Publications, London.

Byrne, G. F., Crapper, P. F., Mayo, K. K., 1980. Monitoring land-cover change by principal component analysis of multitemporal landsat data. Remote Sensing of Environment 10, 175-184.

Cakir, H. I., Khorram, S., Nelson, S. A. C., 2006. Correspondence analysis for detecting land cover change. Remote Sensing of Environment 102, 306-317.

Camarero, J. J., Gutiérrez, E., Fortin, M.-J., 2006. Spatial patterns of plant richness across treeline ecotones in the Pyrenees reveal different locations for richness and tree cover boundaries. Global Ecology and Biogeography 15, 182-191.

Campbell, J. B., 2002. Introduction to Remote Sensing, 2nd.ed. Taylor and Francis, London.

Černá, L., Chytrý, M., 2005. Supervised classification of plant communities with artificial neural networks. Journal of Vegetation Science 16, 407-414.

Chartzoulakis, K., Psarras, G., 2005. Global change effects on crop photosynthesis and production in Mediterranean: the case of Crete, Greece. Agriculture, Ecosystems and Environment 106, 147-157.

Chartzoulakis, K. S., Paranychianakis, N. V., Angelakis, A. N., 2001. Water resources management in the Island of Crete, Greece, with emphasis on the agricultural use. Water Policy 3, 193-205.

Chavez, P. S., Jr , Kwarting, A., 1989. Extracting spectral contrast in Landsat Thematic Mapper image data using selective principal component analysis. Photogrammetric Engineering and Remote Sensing 55, 339-348.

Chen , J., Jönsson , P., Tamura , M., Gu , Z., Matsushita , B., Eklundh , L., 2004. A simple method for reconstructing a high-quality NDVI time-series data set based on the Savitzky-Golay filter. Remote Sensing of Environment 91, 332-344.

Chen, Z., Wang, J., 2010. Land use and land cover change detection using satellite remote sensing techniques in the mountainous Three Gorges Area, China. International Journal of Remote Sensing 31, 1519 - 1542.

Cihlar, J., 2000. Land cover mapping of large areas from satellites: Status and research priorities. International Journal of Remote Sensing 21, 1093-1114.

Cihlar, J., Ly, H., Li, Z., Chen, J., Pokrant, H., Huang, F., 1997. Multitemporal, multichannel AVHRR data sets for land biosphere studies-artifacts and corrections. Remote Sensing of Environment 60, 35-57.

Clark, M. L., Aide, T. M., Grau, H. R., Riner, G., 2010. A scalable approach to mapping annual land cover at 250 m using MODIS time series data: a case study in the Dry Chaco ecoregion of South America. Remote Sensing of Environment 114, 2816-2832.

Clarke, K. R., Somerfield, P. J., Chapman, M. G., 2006. On resemblance measures for ecological studies, including taxonomic dissimilarities and a zero-adjusted Bray–Curtis coefficient for denuded assemblages. Journal of Experimental Marine Biology and Ecology 330, 55-80.

Conchedda, G., Durieux, L., Mayaux, P., 2008. An object-based method for mapping and change analysis in mangrove ecosystems. ISPRS Journal of Photogrammetry and Remote Sensing 63, 578-589.

Conley, P., Packard, D., Purdy, W., 1998. Space Vehicle Mechanisms: Elements of Successful Design. Wiley.

Coppin, P., Jonckheere, I., Nackaerts, K., Muys, B., Lambin, E., 2004. Review ArticleDigital change detection methods in ecosystem monitoring: a review. International Journal of Remote Sensing 25, 1565 - 1596.

Couteron, P., Barbier, N., Gautier, D., 2006. Textural ordination based on fourier spectral decomposition: a method to analyze and compare landscape patterns. Landscape Ecology 21, 555-567.

Csillag, F., Kabos, S., 2002. Wavelets, boundaries, and the spatial analysis of landscape pattern. Ecoscience 9, 177-190.

Cushman, S. A., Gutzweiler, K., Evans, J. S., McGarigal, K., 2010. The gradient paradigm: a conceptual and analytical framework for landscape ecology. in: Cushman, S. A., Huettmann, F., (eds), Spatial Complexity, Informatics, and Wildlife Conservation. Springer, Japan, pp. 83-108.

Dai, X., Khorram, S., 1998. A hierarchical methodology framework for multisource data fusion in vegetation classification. International Journal of Remote Sensing 19, 3697-3701.

Davies, D. L., Bouldin, D. W., 1979. A Cluster Separation Measure. Pattern Analysis and Machine Intelligence, IEEE Transactions on PAMI-1, 224-227.

de Beurs, K. M., Henebry, G. M., 2005. A statistical framework for the analysis of long image time series. International Journal of Remote Sensing 26, 1551-1573.

de Bie, C. A. C. M., 2000. Comparative performance analysis of agro-ecosystems. ITC.

de Bie, C. A. J. M., Khan, M. R., Smakhtin, V. U., Venus, V., Weir, M. J. C., Smaling, E. M. A., 2011. Analysis of multi-temporal SPOT NDVI images for small-scale land-use mapping. International Journal of Remote Sensing 32, 6673-6693.

de Bie, C. A. J. M., Khan, M. R., Toxopeus, A. G., Venus, V., Skidmore, A. K., 2008. Hyper temporal image analysis for crop mapping and change detection. ISPRS : Proceedings of the XXI congress: Comm. VII, WG VII/5, Beijing.

de Bie, C. A. J. M., Nguyen, T. T. H., Ali, A., Scarrott, R., Skidmore, A. K., 2012. LaHMa: a landscape heterogeneity mapping method using hyper-temporal datasets. International Journal of Geographical Information Science 26, 1-16.

Deer, P. J., Eklund, P., 2003. A study of parameter values for a Mahalanobis Distance fuzzy classifier. Fuzzy Sets and Systems 137, 191-213.

Defries, R. S., Belward, A. S., 2000. Global and regional land cover characterization from satellite data: an introduction to the Special Issue. International Journal of Remote Sensing 21, 1083-1092.

Delcourt, H. R., Delcourt, P. A., 1991. Quaternary ecology: a paleoecological perspective. Chapman & Hall.

Desclée, B., Bogaert, P., Defourny, P., 2006. Forest change detection by statistical object-based method. Remote Sensing of Environment 102, 1-11.

Dixon, B., Candade, N., 2008. Multispectral landuse classification using neural networks and support vector machines: one or the other, or both? International Journal of Remote Sensing 29, 1185-1206.

Dorais, A., Cardille, J., 2011. Strategies for Incorporating High-Resolution Google Earth Databases to Guide and Validate Classifications: Understanding Deforestation in Borneo. Remote Sensing 3, 1157-1176.

Dunn, C. P., Sharpe, D. M., Guntenspergen, G. R., Yang, Z., 1991. Methods for analyzing temporal changes in landscape pattern. in: Turner, M. G., Gardner, R. H., (eds), Quantitative Methods in Landscape Ecology. Springer-Verlag, New York, pp. 173-198.

Dutoit, T., Buisson, E., Gerbaud, E., Roche, P., Tatoni, T., 2007. The status of transitions between cultivated fields and their boundaries: ecotones, ecoclines or edge effects? Acta Oecologica 31, 127-136.

Efron, B., Tibshirani, R., 1986. Bootstrap Methods for Standard Errors, Confidence Intervals, and Other Measures of Statistical Accuracy. Statistical Science 1, 54-75.

Elvidge, C. D., Miura, T., Jansen, W. T., Groeneveld, D. P., Ray, J., 1998. Monitoring trends in wetland vegetation using a Landsat MSS time series. in: Elvidge, R. S. L. a. C. D., (eds), Remote Sensing Change

Detection: Environmental Monitoring Methods and Applications. Chelsea, MI: Ann Arbor Press, pp. pp. 191-210.

Eshleman, K. N., 2004. Hydrological consequences of land use change: A review of the state-of-science in: R.S. DeFries, G. P. A., & R. A. Houghton. (eds), Ecosystems and land use change American Geophysical Union, Washington, DC, pp. 13–29.

Fagan, W. F., Fortin, M. J., Soykan, C., 2003. Integrating edge detection and dynamic modeling in quantitative analyses of ecological boundaries. BioScience 53, 730-738.

Fahrig, L., 1992. Relative importance of spatial and temporal scales in a patchy environment. Theoretical Population Biology 41, 300-314.

Feddema, J. J., Oleson, K. W., Bonan, G. B., Mearns, L. O., Buja, L. E., Meehl, G. A., Washington, W. M., 2005. The Importance of Land-Cover Change in Simulating Future Climates. Science 310, 1674-1678.

Feng, G., Morisette, J. T., Wolfe, R. E., Ederer, G., Pedelty, J., Masuoka, E., Myneni, R., Bin, T., Nightingale, J., 2008. An algorithm to produce temporally and spatially continuous MODIS-LAI time series. IEEE Geoscience and Remote Sensing Letters 5, 60-64.

Fensholt, R., Anyamba, A., Stisen, S., Sandholt, I., Park, E., Small, J., 2007. Comparisons of compositing period length for vegetation index data from polar-orbiting and geostationary satellites for the cloud-prone region of West Africa. Photogrammetric Engineering and Remote Sensing 73, 297-309.

Fensholt, R., Sandholt, I., Proud, S. R., Stisen, S., Rasmussen, M. O., 2010. Assessment of MODIS sun-sensor geometry variations effect on observed NDVI using MSG SEVIRI geostationary data. International Journal of Remote Sensing 31, 6163-6187.

Fensholt, R., Sandholt, I., Stisen, S., Tucker, C., 2006. Analysing NDVI for the African continent using the geostationary meteosat second generation SEVIRI sensor. Remote Sensing of Environment 101, 212-229.

Feranec, J., 1999. Interpretation element “association”: analysis and definition. International journal of applied Earth observation and geoinformation 1, 64-67.

Fisher, P., Arnot, C., Wadsworth, R., Wellens, J., 2006. Detecting change in vague interpretations of landscapes. Ecological Informatics 1, 163-178.

Fisher, P., Cheng, T., Wood, J., 2007. Higher Order Vagueness in Geographical Information: Empirical Geographical Population of Type n Fuzzy Sets. GeoInformatica 11, 311-330.

Fisher, P. F., 2010. Remote sensing of land cover classes as type 2 fuzzy sets. Remote Sensing of Environment 114, 309-321.

Foley, J. A., DeFries, R., Asner, G. P., Barford, C., Bonan, G., Carpenter, S. R., Chapin, F. S., Coe, M. T., Daily, G. C., Gibbs, H. K., Helkowski, J. H., Holloway, T., Howard, E. A., Kucharik, C. J., Monfreda, C., Patz, J. A., Prentice, I. C., Ramankutty, N., Snyder, P. K., 2005. Global Consequences of Land Use. Science 309, 570-574.

Fonte, C. C., Lodwick, W. A., 2004. Areas of fuzzy geographical entities. International Journal of Geographical Information Science 18, 127-150.

Foody, G. M., 1992. On the compensation for chance agreement in image classification accuracy assessment. Photogrammetric Engineering Remote Sensing 58, 1459-1460.

Foody, G. M., 1995. Land cover classification by an artificial neural network with ancillary information. International Journal of Geographical Information Science 9, 527 - 542.

Foody, G. M., 1996a. Approaches for the production and evaluation of fuzzy land cover classifications from remotely-sensed data. International Journal of Remote Sensing 17, 1317-1340.

Foody, G. M., 1996b. Fuzzy modelling of vegetation from remotely sensed imagery. Ecological Modelling 85, 3-12.

Foody, G. M., 2001. Monitoring the magnitude of land-cover change around the southern limits of the Sahara. Photogrammetric Engineering and Remote Sensing 67, 841–847.

Foody, G. M., 2002. Status of land cover classification accuracy assessment. Remote Sensing of Environment 80, 185-201.

Foody, G. M., Boyd, D. S., 1999. Fuzzy mapping of tropical land cover along an environmental gradient from remotely sensed data with an artificial neural network. Journal of Geographical Systems 1, 23-35.

Foody, G. M., Trodd, N. M., 1993. Non-classificatory analysis and representation of heathland vegetation from remotely sensed imagery. GeoJournal 29, 343-350.

Fortin, M. J., Olson, R. J., Ferson, S., Iverson, L., Hunsaker, C., Edwards, G., Levine, D., Butera, K., Klemas, V., 2000. Issues related to the detection of boundaries. Landscape Ecology 15, 453-466.

Foulds, S. A., Macklin, M. G., 2006. Holocene land-use change and its impact on river basin dynamics in Great Britain and Ireland. Progress in Physical Geography 30, 589-604.

Franklin, S. E., 2001. Remote Sensing for Sustainable Forest Management. Taylor & Francis.

Fraser, R. H., Abuelgasim, A., Latifovic, R., 2005. A method for detecting large-scale forest cover change using coarse spatial resolution imagery. Remote Sensing of Environment 95, 414-427.

Fraser, R. H., Latifovic, R., 2005. Mapping insect-induced tree defoliation and mortality using coarse spatial resolution satellite imagery. International Journal of Remote Sensing 26, 193-200.

Gallo, K., Ji, L., Reed, B., Eidenshink, J., Dwyer, J., 2005. Multi-platform comparisons of MODIS and AVHRR normalized difference vegetation index data. Remote Sensing of Environment 99, 221-231.

Gauch, H. G., Jr., Whittaker, R. H., 1981. Hierarchical Classification of Community Data. Journal of Ecology 69, 537-557.

Geerken, R., Zaitchik, B., Evans, J. P., 2005. Classifying rangeland vegetation type and coverage from NDVI time series using Fourier Filtered Cycle Similarity. International Journal of Remote Sensing 26, 5535-5554.

Geoghegan, J., Villar, S. C., Klepeis, P., Mendoza, P. M., Ogneva-Himmelberger, Y., Chowdhury, R. R., Turner, B. L., Vance, C., 2001. Modeling tropical deforestation in the southern Yucatán peninsular region: comparing survey and satellite data. Agriculture, Ecosystems & Environment 85, 25-46.

Ghana Environmental Protection Agency. 2001. Ghana's Initial National Communications Report under the United Nations Framework Convention on Climate Change. Accra, Ghana.

Gomarasca, M. A., 2009. Land Use/Land Cover Classification Systems. (eds), Basics of Geomatics. Springer Netherlands, pp. 561-598.

Gonza´ Lez Loyarte, M. M., Menenti, M., 2000. Usefulness of Fourier parameters to detect regional and local droughts within a time series of NOAA/AVHRR-NDVI data (GAC). in: Roerink, G. J., Menenti, M., (eds), Time Series of Satellite Data: Development of New Products. Netherlands Remote Sensing Board, Wageningen, pp. 63–70.

González-Pérez, J. A., González-Vila, F. J., Almendros, G., Knicker, H., 2004. The effect of fire on soil organic matter--a review. Environment International 30, 855-870.

Goodchild, M. F., Quattrochi, D. A., 1997. Scale, Multiscaling, Remote Sensing, and GIS. in: Goodchild, M., Quattrochi, D., (eds), Scale in remote sensing and GIS. CRC Press, Florida, pp. 406.

Gopal, S., Woodcock, C. E., Strahler, A. H., 1999. Fuzzy Neural Network Classification of Global Land Cover from a 1° AVHRR Data Set. Remote Sensing of Environment 67, 230-243.

Gosz, J. R., 1991. Fundamental ecological characteristics of landscape boundaries. in: Holland, M. M., Risser, P. G., Naiman, R. J., (eds), Ecotones: The role of landscape boundaries in the management and restoration of changing environment. Chapman and Hall Inc, New York, pp. 8–30.

Gosz, J. R., 1992. Gradient analysis of ecological change in time and space: Implications for forest management. Ecological Applications 2, 248-261.

Goward, S. N., Markham, B., Dye, D. G., Dulaney, W., Yang, J., 1991. Normalized difference vegetation index measurements from the advanced very high resolution radiometer. Remote Sensing of Environment 35, 257-277.

Graciela, M., 1999. Change detection assessment using fuzzy sets and remotely sensed data: an application of topographic map revision. ISPRS Journal of Photogrammetry and Remote Sensing 54, 221-233.

Greene, W. H., 1997. Econometric Analysis, Third.ed. Prentice Hall, Upper Saddle River, NJ.

Gu, J., Li, X., Huang, C., Okin, G. S., 2009. A simplified data assimilation method for reconstructing time-series MODIS NDVI data. Advances in Space Research 44, 501-509.

Gulinck, H., Dufourmont, H., Brunovsky, M., Andries, A., Wouters, P., 1993. Satellite images for the detection of changes in rural landscapes: a landscape–ecological perspective. EARSeL advances in Remote Sensing 2, 84-90.

Gustafson, E. J., 1998. Quantifying landscape spatial pattern: what is the state of the art? Ecosystems 1, 143-156.

Halkidi, M., Batistakis, Y., Vazirgiannis, M., 2001. On Clustering Validation Techniques. Journal of Intelligent Information Systems 17, 107-145.

Hansen, M. C., Defries, R. S., Townshend, J. R. G., Sohlberg, R., 2000. Global land cover classification at 1 km spatial resolution using a classification tree approach. International Journal of Remote Sensing 21, 1331-1364.

Haralick, R. M., Shanmugam, K., Dinstein, I. H., 1973. Textural features for image classification. IEEE Transactions on Systems, Man and Cybernetics 3, 610-621.

Hayes, D. J., Cohen, W. B., 2007. Spatial, spectral and temporal patterns of tropical forest cover change as observed with multiple scales of optical satellite data. Remote Sensing of Environment 106, 1-16.

Hayes, D. J., Cohen, W. B., Sader, S. A., Irwin, D. E., 2008. Estimating proportional change in forest cover as a continuous variable from multi-year MODIS data. Remote Sensing of Environment 112, 735-749.

He, C., Wei, A., Shi, P., Zhang, Q., Zhao, Y., 2011. Detecting land-use/land-cover change in rural-urban fringe areas using extended change-vector analysis. International Journal of Applied Earth Observation and Geoinformation 13, 572-585.

He, C., Zhang, Q., Li, Y., Li, X., Shi, P., 2005. Zoning grassland protection area using remote sensing and cellular automata modeling—A case study in Xilingol steppe grassland in northern China. Journal of Arid Environments 63, 814-826.

He, K. S., Zhang, J. T., Zhang, Q. F., 2009. Linking variability in species composition and MODIS NDVI based on beta diversity measurements. Acta Oecologica-International Journal of Ecology 35, 14-21.

Headrick, T. C., 2009. Statistical simulation: power method polynomials and other transformations. Chapman & Hall/CRC.

Helmer, E. H., Brown, S., Cohen, W. B., 2000. Mapping montane tropical forest successional stage and land use with multi-date Landsat imagery. International Journal of Remote Sensing 21, 2163-2183.

Henebry, G. M., 1993. Detecting change in grasslands using measures of spatial dependence with landsat TM data. Remote Sensing of Environment 46, 223-234.

Hennenberg, K. J., Goetze, D., Kouamé, L., Orthmann, B., Porembski, S., Austin, M. P., 2005. Border and ecotone detection by vegetation composition along forest-savanna transects in Ivory Coast. Journal of Vegetation Science 16, 301-310.

Hird, J. N., McDermid, G. J., 2009. Noise reduction of NDVI time series: An empirical comparison of selected techniques. Remote Sensing of Environment 113, 248-258.

Holben, B. N., 1986. Characteristics of maximum-value composite images from temporal AVHRR data. International Journal of Remote Sensing 7, 1417 - 1434.

Homer, C., Huang, C., Yang, L., Wylie, B., Coan, M., 2004. Development of a 2001 National Land-Cover Database for the United States. Photogrammetric Engineering and Remote Sensing 70, 829-840.

Hostert, P., Röder, A., Hill, J., 2003. Coupling spectral unmixing and trend analysis for monitoring of long-term vegetation dynamics in Mediterranean rangelands. Remote Sensing of Environment 87, 183-197.

Houghton, R. A., 2005. Aboveground forest biomass and the global carbon balance. Global Change Biology 11, 945-958.

Howarth, P. J., Wickware, G. M., 1981. Procedures for change detection using Landsat digital data. International Journal of Remote Sensing 2, 277-291.

Ingram, J. C., Dawson, T. P., 2005. Technical Note: Inter-annual analysis of deforestation hotspots in Madagascar from high temporal resolution satellite observations. International Journal of Remote Sensing 26, 1447 - 1461.

Ingram, J. C., Dawson, T. P., Whittaker, R. J., 2005. Mapping tropical forest structure in southeastern Madagascar using remote sensing and artificial neural networks. Remote Sensing of Environment 94, 491-507.

IPCC. 2001. Third Assessment Report-climate change.

Islam, A. S., Bala, S. K., 2008. Assessment of Potato Phenological Characteristics Using MODIS-Derived NDVI and LAI Information. Giscience & Remote Sensing 45, 454-470.

Jain, A. K., Murty, M. N., Flynn, P. J., 1999. Data clustering: a review. ACM computing surveys (CSUR) 31, 264-323.

Jensen, J. R., 1996. Introductory Digital Image Processing: a Remote Sensing Perspective. Prentice-Hall, Englewood Cliffs, NJ.

Jensen, J. R., 2000. Remote sensing of the environment: an earth resource perspective. Pearson Prentice Hall, Saddle River, NJ.

Jones, D. A., Hansen, A. J., Bly, K., Doherty, K., Verschuyl, J. P., Paugh, J. I., Carle, R., Story, S. J., 2009. Monitoring land use and cover around parks: A conceptual approach. Remote Sensing of Environment 113, 1346-1356.

Jongman, R. H. G., Terbraak, C. J. F., Van Tongeren, O. F. R., 1995. Data Analysis in Community and Landscape Ecology. Cambridge University Press, Cambridge.

Jonsson, P., Eklundh, L., 2002. Seasonality extraction by function fitting to time-series of satellite sensor data. IEEE Transactions on Geoscience and Remote Sensing 40, 1824-1832.

Jönsson, P., Eklundh, L., 2004. TIMESAT - a program for analyzing time-series of satellite sensor data. Computers and Geosciences 30, 833-845.

Julien, Y., Sobrino, J. A., 2010. Comparison of cloud-reconstruction methods for time series of composite NDVI data. Remote Sensing of Environment 114, 618-625.

Justice, C. O., Townshend, J. R. G., Holben, B. N., Tucker, C. J., 1985. Analysis of the phenology of global vegetation using meteorological satellite data. International Journal of Remote Sensing 6, 1271 - 1318.

Kakane, V. C. K., Sogaard, H., 1997. Estimation of surface temperature and rainfall in Ghana Geografisk Tidsskrift, Danish Journal of Geography 97, 76-85.

Kavzoglu, T., Mather, P. M., 2003. The use of backpropagating artificial neural networks in land cover classification. International Journal of Remote Sensing 24, 4907-4938.

Kennedy, R. E., Cohen, W. B., Schroeder, T. A., 2007. Trajectory-based change detection for automated characterization of forest disturbance dynamics. Remote Sensing of Environment 110, 370-386.

Kennedy, R. E., Yang, Z., Cohen, W. B., Pfaff, E., Braaten, J., Nelson, P., 2012. Spatial and temporal patterns of forest disturbance and regrowth within the area of the Northwest Forest Plan. Remote Sensing of Environment 122, 117-133.

Kent, M., Gill, W. J., Weaver, R. E., Armitage, R. P., 1997. Landscape and plant community boundaries in biogeography. Progress in Physical Geography 21, 315-353.

Khan, M. R., de Bie, C. A. J. M., van Keulen, H., Smaling, E. M. A., Real, R., 2010. Disaggregating and mapping crop statistics using hypertemporal remote sensing. International Journal of Applied Earth Observation and Geoinformation 12, 36-46.

Khan, M. R., Smaling, E. M. A., van Keulen, H., de Bie, C. A. J. M., 2011. Crops from space : improved earth observation capacity to map crop areas and to quantify production. Enschede, University of Twente Faculty of Geo-Information and Earth Observation (ITC) Enschede.

Knight, J., Lunetta, R., Ediriwickrema, J., Khorram, S., 2006. Regional scale land cover characterization using MODIS-NDVI 250 m multi-temporal imagery: A phenology-based approach. GIScience and Remote Sensing 43, 1-23.

Kok, K., 2004. The role of population in understanding Honduran land use patterns. Journal of Environmental Management 72, 73-89.

Körner, C., 2000. Why are there global gradients in species richness? mountains might hold the answer. Trends in ecology and evolution 15, 513-514.

Krishnaswamy, J., Bawa, K. S., Ganeshaiah, K. N., Kiran, M. C., 2009. Quantifying and mapping biodiversity and ecosystem services: Utility of a multi-season NDVI based Mahalanobis distance surrogate. Remote Sensing of Environment 113, 857-867.

Lambin, E. F., 1996. Change detection at multiple temporal scales: seasonal and annual variations in landscape variables. Photogrammetric engineering and remote sensing. 62, 931-938.

Lambin, E. F., Geist, H., 2006. Land-use and land-cover change: local processes and global impacts. Springer.

Lambin, E. F., Linderman, M., 2006. Time series of remote sensing data for land change science. Geoscience and Remote Sensing, IEEE Transactions on 44, 1926-1928.

Lambin, E. F., Strahlers, A. H., 1994. Change-vector analysis in multitemporal space: A tool to detect and categorize land-cover change processes using high temporal-resolution satellite data. Remote Sensing of Environment 48, 231-244.

Lasaponara, R., 2006. Estimating spectral separability of satellite derived parameters for burned areas mapping in the Calabria region by using SPOT-Vegetation data. Ecological Modelling 196, 265-270.

Legendre, P., Dale, M. R. T., Fortin, M.-J., Gurevitch, J., Hohn, M., Myers, D., 2002. The consequences of spatial structure for the design and analysis of ecological field surveys. Ecography 25, 601-615.

Legendre, P., Legendre, L., 1998. Numerical Ecology. Elsevier, Amsterdam, The Netherlands.

Li, H., Reynolds, J. F., 1995. On definition and quantification of heterogeneity. Oikos 73, 280-284.

Lillesand, T. M., Kiefer, R. W., Chipman, J. W., 2004. Remote Sensing and Image Interpretation, Fifth.ed. John Wiley and Sons.

Lo, C. P., Choi, J., 2004. A hybrid approach to urban land use/cover mapping using Landsat 7 Enhanced Thematic Mapper Plus (ETM+) images. International Journal of Remote Sensing 25, 2687-2700.

Löffler, J., Finch, O., 2005. Spatio-temporal gradients between high mountain ecosystems of Central Norway. Arctic, Antarctic, and Alpine Research 37, 499-513.

Looijen, R. C., van Andel, J., 1999. Ecological communities: conceptual problems and definitions. Perspectives in Plant Ecology, Evolution and Systematics 2, 210-222.

Loveland, T., Sohl, T., Stehman, S., Gallant, A., Sayler, K., Napton, D., 2002. A strategy for estimating the rates of recent United States land-cover changes. Photogrammetric Engineering and Remote Sensing 68, 1091-1099.

Lovell, J. L., Graetz, R. D., 2001. Filtering Pathfinder AVHRR Land NDVI data for Australia. International Journal of Remote Sensing 22, 2649-2654.

Loyarte, M. M. G., Menenti, M., 2008. Impact of rainfall anomalies on Fourier parameters of NDVI time series of northwestern Argentina. International Journal of Remote Sensing 29, 1125-1152.

Lu, D., Mausel, P., BrondÃ-zio, E., Moran, E., 2004. Change detection techniques. International Journal of Remote Sensing 25, 2365 - 2401.

Lu, D., Weng, Q., 2007. A survey of image classification methods and techniques for improving classification performance. International Journal of Remote Sensing 28, 823-870.

Lu, X., Liu, R., Liu, J., Liang, S., 2007. Removal of noise by wavelet method to generate high quality temporal data of terrestrial MODIS products. Photogrammetric Engineering and Remote Sensing 73, 1129-1139.

Lunetta, R. S., Alvarez, R., Edmonds, C. M., Lyon, J. G., Elvidge, C. D., Bonifaz, R., Garcia, C., 2002. NALC/Mexico land-cover mapping results: Implications for assessing landscape condition. International Journal of Remote Sensing 23, 3129-3148.

Lunetta, R. S., Balogh, M. E., 1999. Application of multi-temporal Landsat 5 TM imagery for wetland identification. Photogrammetric Engineering and Remote Sensing 65, 1303-1310.

Lunetta, R. S., Johnson, D. M., Lyon, J. G., Crotwell, J., 2004. Impacts of imagery temporal frequency on land-cover change detection monitoring. Remote Sensing of Environment 89, 444-454.

Lunetta, R. S., Knight, J. F., Ediriwickrema, J., Lyon, J. G., Worthy, L. D., 2006. Land-cover change detection using multi-temporal MODIS NDVI data. Remote Sensing of Environment 105, 142-154.

Lupo, F., Linderman, M., Vanacker, V., Bartholomé, E., Lambin, E. F., 2007. Categorization of land-cover change processes based on phenological indicators extracted from time series of vegetation index data. International Journal of Remote Sensing 28, 2469-2483.

Ma, M., Veroustraete, F., 2006. Reconstructing pathfinder AVHRR land NDVI time-series data for the Northwest of China. Advances in Space Research 37, 835-840.

Martín, M., De Pablo, C., De Agar, P., 2006. Landscape changes over time: comparison of land uses, boundaries and mosaics. Landscape Ecology 21, 1075-1088.

Martínez, B., Gilabert, M. A., 2009. Vegetation dynamics from NDVI time series analysis using the wavelet transform. Remote Sensing of Environment 113, 1823-1842.

McAlpine, C. A., Syktus, J., Ryan, J. G., Deo, R. C., McKeon, G. M., McGowan, H. A., Phinn, S. R., 2009. A continent under stress: interactions, feedbacks and risks associated with impact of modified land cover on Australia's climate. Global Change Biology 15, 2206-2223.

McCloy, K. R., 2006. Resource Management Information Systems: Remote Sensing, GIS and Modeling, Second.ed. CRC Press, Boca Raton, Florida.

Mendel, J. M., John, R. I. B., 2002. Type-2 fuzzy sets made simple. IEEE Transactions on Fuzzy Systems 10, 117-127.

Metternicht, G., 2001. Assessing temporal and spatial changes of salinity using fuzzy logic, remote sensing and GIS. Foundations of an expert system. Ecological Modelling 144, 163-179.

Mitrakis, N. E., Mallinis, G., Koutsias, N., Theocharis, J. B., 2011. Burned area mapping in Mediterranean environment using medium-resolution multi-spectral data and a neuro-fuzzy classifier. International Journal of Image and Data Fusion, 1-20.

Montesano, P. M., Nelson, R., Sun, G., Margolis, H., Kerber, A., Ranson, K. J., 2009. MODIS tree cover validation for the circumpolar taiga–tundra transition zone. Remote Sensing of Environment 113, 2130-2141.

Montmollin, d., B, Iatrou, G. A., 1995. Connaissance et conservation de la flore de l' île de Crète. Ecologia Mediterranea 21, 173-184.

Moody, A., Johnson, D. M., 2001. Land-surface phenologies using the discrete Fourier transform. Remote Sensing of Environment 75, 305-323.

Moulin, S., Bondeau, A., Delecolle, R., 1998. Combining agricultural crop models and satellite observations: From field to regional scales. International Journal of Remote Sensing 19, 1021-1036.

Müller, F., 1998. Gradients in ecological systems. Ecological Modelling 108, 3-21.

Muñoz-Rojas, M., De la Rosa, D., Zavala, L. M., Jordán, A., Anaya-Romero, M., 2011. Changes in land cover and vegetation carbon stocks in Andalusia, Southern Spain (1956–2007). Science of The Total Environment 409, 2796-2806.

Myers, J. C., 1997. Geostatistical Error Management : Quantifying Uncertainty for Environmental Mapping. Van Nostrand Reinhold, New York.

Neeti, N., Rogan, J., Christman, Z., Eastman, J. R., Millones, M., Schneider, L., Nickl, E., Schmook, B., Turner, B. L., Ghimire, B., 2011. Mapping seasonal trends in vegetation using AVHRR-NDVI time series in the Yucatán Peninsula, Mexico. Remote Sensing Letters 3, 433-442.

Nelson, R. F., 1983. Detecting forest canopy change due to insect activity using Landsat MSS Photogrammetric Engineering and Remote Sensing 49, 1303-1314.

Nguyen, T. T. H., de Bie, C. A. J. M., Ali, A., Smaling, E. M. A., Chu, T. H., 2011. Mapping the irrigated rice cropping patterns of the Mekong delta, Vietnam, through hyper-temporal SPOT NDVI image analysis. International Journal of Remote Sensing 33, 415-434.

Nielsen, E. M., Prince, S. D., Koeln, G. T., 2008. Wetland change mapping for the U.S. mid-Atlantic region using an outlier detection technique. Remote Sensing of Environment 112, 4061-4074.

Ohmann, J. L., Gregory, M. J., Roberts, H. M., Cohen, W. B., Kennedy, R. E., Yang, Z., 2012. Mapping change of older forest with nearest-neighbor imputation and Landsat time-series. Forest Ecology and Management 272, 13-25.

Ola, A., 2008. Extending post-classification change detection using semantic similarity metrics to overcome class heterogeneity: A study of 1992 and 2001 U.S. National Land Cover Database changes. Remote Sensing of Environment 112, 1226-1241.

Owusu, K., Waylen, P., Qiu, Y., 2008. Changing rainfall inputs in the Volta basin: implications for water sharing in Ghana. GeoJournal 71, 201-210.

Peel, M. C., Finlayson, B. L., McMahon, T. A., 2007. Updated world map of the Koppen-Geiger climate classification. Hydrology and Earth System Sciences 11, 1633-1644.

Pellemans, A. H. J. M., Jordans, R. W. L., Allewijn, R., 1993. Merging multispectral and panchromatic SPOT images with respect to the

radiometric properties of the sensor. Photogrammetric Engineering & Remote Sensing 59, 81-87.

Peres, C. A., Terborgh, J. W., 1995. Amazonian Nature Reserves: An Analysis of the Defensibility Status of Existing Conservation Units and Design Criteria for the Future

Las Reservas Naturales Amazónicas: un análisis del estado relativo de protección de las unidades de conservación existentes y del criterio de diseño para el futuro. Conservation Biology 9, 34-46.

Perry, J. N., Liebhold, A. M., Rosenberg, M. S., Dungan, J., Miriti, M., Jakomulska, A., Citron-Pousty, S., 2002. Illustrations and guidelines for selecting statistical methods for quantifying spatial pattern in ecological data. Ecography 25, 578-600.

Peters, D., Gosz, J., Pockman, W., Small, E., Parmenter, R., Collins, S., Muldavin, E., 2006. Integrating Patch and Boundary Dynamics to Understand and Predict Biotic Transitions at Multiple Scales. Landscape Ecology 21, 19-33.

Piwowar, J. M., LeDrew, E. F., 1995. Hypertemporal analysis of remotely sensed sea-ice data for climate change studies. Progress in Physical Geography 19, 216-242.

Piwowar, J. M., Peddle, D. R., Ledrew, E. F., 1998. Temporal mixture analysis of arctic sea ice imagery: A new approach for monitoring environmental change. Remote Sensing of Environment 63, 195-207.

Pontius, R. G., Cheuk, M. L., 2006. A generalized cross-tabulation matrix to compare soft-classified maps at multiple resolutions. International Journal of Geographical Information Science 20, 1-30.

Puech, C., 1994. Thresholds of homogeneity in targets in the landscape. Relationship with remote sensing. International Journal of Remote Sensing 15, 2421-2435.

Purevdorj, T., Tateishi, R., Ishiyama, T., Honda, Y., 1998. Relationships between percent vegetation cover and vegetation indices. International Journal of Remote Sensing 19, 3519-3535.

Radke, R. J., Andra, S., Al-Kofahi, O., Roysam, B., 2005. Image change detection algorithms: a systematic survey. IEEE Transactions on Image Processing 14, 294-307.

Ray, D. K., Pielke, R. A., Sr., Nair, U. S., Welch, R. M., Lawton, R. O., 2009. Importance of land use versus atmospheric information verified from cloud simulations from a frontier region in Costa Rica. J. Geophys. Res. 114, D08113.

Reed, B. C., 2006. Trend analysis of time-series phenology of North America derived from satellite data. GIScience and Remote Sensing 43, 24-38.

Richards, J. A., Jia, X., 2006. Remote sensing digital image analysis : an introduction, Fourth edition.ed. Springer-Verlag, Berlin etc.

Roderick, M., Smith, R., Cridland, S., 1996. The precision of the NDVI derived from AVHRR observations. Remote Sensing of Environment 56, 57-65.

Rodriguez-Yi, J. L., Shimabukuro, Y. E., Rudorff, B. F. T., 2000. Image segmentation for classification of vegetation using NOAA-AVHRR data. International Journal of Remote Sensing 21, 167-172.

Roerink, G. J., Menenti, M., Verhoef, W., 2000. Reconstructing cloudfree NDVI composites using Fourier analysis of time series. International Journal of Remote Sensing 21, 1911-1917.

Rogan, J., Chen, D., 2004. Remote sensing technology for mapping and monitoring land-cover and land-use change. Progress in Planning 61, 301-325.

Romme, W. H., 1982. Fire and landscape diversity in subalpine forests of Yellowstone National Park. Ecological Monographs 52, 199-221.

Rumsey, D., 2011. Statistics For Dummies. John Wiley & Sons.

Sakamoto, T., Van Nguyen, N., Kotera, A., Ohno, H., Ishitsuka, N., Yokozawa, M., 2007. Detecting temporal changes in the extent of annual flooding within the Cambodia and the Vietnamese Mekong Delta from MODIS time-series imagery. Remote Sensing of Environment 109, 295-313.

Sakamoto, T., Van Nguyen, N., Ohno, H., Ishitsuka, N., Yokozawa, M., 2006. Spatio-temporal distribution of rice phenology and cropping systems in the Mekong Delta with special reference to the seasonal water flow of the Mekong and Bassac rivers. Remote Sensing of Environment 100, 1-16.

Sakamoto, T., Yokozawa, M., Toritani, H., Shibayama, M., Ishitsuka, N., Ohno, H., 2005. A crop phenology detection method using time-series MODIS data. Remote Sensing of Environment 96, 366-374.

Sarkar, S., Kafatos, M., 2004. Interannual variability of vegetation over the Indian sub-continent and its relation to the different meteorological parameters. Remote Sensing of Environment 90, 268-280.

Sarris, A., Karakoudis, S., Vidaki, C., Soupios, P., 2005a. Study of the morphological attributes of crete through the use of remote sensing techniques. IASME / WSEAS International Conference on energy, environment, ecosystems and sustainable development. Athens, Greece. 2**:** 1043-1051.

Sarris, A., Maniadakis, M., Lazaridou, O., Kalogrias, V., Bariotakis, M., Pirintsos, S. A., 2005b. Studying land use patterns in Crete Island, Greece, through a time sequence of Landsat images and mapping vegetation patterns. WSEAS Transactions on Environment and Development 1, 272–279.

Schroeder, T. A., Wulder, M. A., Healey, S. P., Moisen, G. G., 2011. Mapping wildfire and clearcut harvest disturbances in boreal forests

with Landsat time series data. Remote Sensing of Environment 115, 1421-1433.

Shahin, M., 2002. Hydrology and Water Resources of Africa. Kluwer Academic, Dordrecht, Netherlands.

Shunlin, L., 2004. Quantitative remote sensing of land surfaces Wiley-Interscience, Hoboken, N.J

Singh, A., 1984. Some clarifications about the pairwise divergence measure in remote sensing. International Journal of Remote Sensing 5, 623-627.

Skidmore, A. K., Turner, B. J., 1992. Map accuracy assessment using line intersect sampling. Photogrammetric Engineering and Remote Sensing 58, 1453-1457.

Sklenár, P., Bendix, J., Balslev, H., 2008. Cloud frequency correlates to plant species composition in the high Andes of Ecuador. Basic and Applied Ecology 9, 504-513.

Sluiter, R., 1998. Desertification and Grazing on south Crete, A model approach, Universty of Utrecht.

Sohn, Y., Rebello, N. S., 2002. Supervised and unsupervised spectral angle classifiers. Photogrammetric Engineering and Remote Sensing 68, 1271-1282.

Sørensen, T., 1948. A method of establishing groups of equal amplitude in plant sociology based on similarity of species content, and its application to analyses of the vegetation on Danish Commons. Kongelige Danske Videnskabernes Selskabs Biologiske Skrifter 5, 1-34.

Southworth, J., Munroe, D., Nagendra, H., 2004. Land cover change and landscape fragmentation - comparing the utility of continuous and discrete analyses for a western Honduras region. Agriculture, Ecosystems and Environment 101, 185-205.

Stowe, L. L., Davis, P. A., McClain, E. P., 1999. Scientific basis and initial evaluation of the CLAVR-1 Global Clear/Cloud Classification Algorithm for the Advanced Very High Resolution Radiometer. Journal of Atmospheric and Oceanic Technology 16, 656-681.

Stowe, L. L., McClain, E. P., Carey, R., Pellegrino, P., Gutman, G. G., Davis, P., Long, C., Hart, S., 1991. Global distribution of cloud cover derived from NOAA/AVHRR operational satellite data. Advances in Space Research 11, 51-54.

Stroppiana, D., Pinnock, S., Pereira, J. M. C., Grégoire, J. M., 2002. Radiometric analysis of SPOT-VEGETATION images for burnt area detection in Northern Australia. Remote Sensing of Environment 82, 21-37.

Stuart, N., Barratt, T., Place, C., 2006. Classifying the Neotropical savannas of Belize using remote sensing and ground survey. Journal of Biogeography 33, 476-490.

Swain, P. H., Davis, S. M., 1978. Remote Sensing : the quantitative approach. McGraw-Hill, New York.

Swets, D. L., Reed, B. C., Rowland, J. D., Marko, S. E., 1999. A weighted least-squares approach to temporal NDVI smoothing. In: Proceedings of the 1999 ASPRS Annual Conference, Portland, Oregon.

Tang, X., Kainz, W., Wang, H., 2010. Topological relations between fuzzy regions in a fuzzy topological space. International Journal of Applied Earth Observation and Geoinformation 12, S151-S165.

Tapia, R., Stein, A., Bijker, W., 2005. Optimization of sampling schemes for vegetation mapping using fuzzy classification. Remote Sensing of Environment 99, 425-433.

Thomas, N. E., Huang, C., Goward, S. N., Powell, S., Rishmawi, K., Schleeweis, K., Hinds, A., 2011. Validation of North American Forest Disturbance dynamics derived from Landsat time series stacks. Remote Sensing of Environment 115, 19-32.

Tou, J. T., Gonzalez, R. C., 1974. Pattern Recognition Principles. Addison-Wesley, Reading, MA.

Townsend, P. A., 2000. A quantitative fuzzy approach to assess mapped vegetation classifications for ecological applications. Remote Sensing of Environment 72, 253-267.

Trodd, N. M., 1992. Gradient analysis of heath land vegetation from near ground level remotely sensed data Remote Sensing and Spatial Information, Proceedings of the Sixth Australasian Remote Sensing Conference, New Zealand.

Trodd, N. M., 1993. Characterizing semi-natural vegetation: continua and ecotones. Towards Operational Applications, Proceedings of the 19th Annual Conference of the Remote Sensing Society, Nottingham, Remote Sensing Society.

Tucker, C. J., Sellers, P. J., 1986. Satellite remote sensing of primary production. International Journal of Remote Sensing 7, 1395–1416.

Tucker, C. J., Slayback, D. A., Pinzon, J. E., Los, S. O., Myneni, R. B., Taylor, M. G., 2001. Higher northern latitude normalized difference vegetation index and growing season trends from 1982 to 1999. International Journal of Biometeorology 45, 184-190.

Turland, N. J., Chilton, L., Press, J. R., 1993. Flora of the Cretan Area. Annotated checklist and atlas, London.

Turner, B. L., Lambin, E. F., Reenberg, A., 2007. The emergence of land change science for global environmental change and sustainability. Proceedings of the National Academy of Sciences 104, 20666-20671.

Turner, M. G., Gardner, R. H., 1991. Quantitative Methods in Landscape Ecology. Springer-Verlag, New York.

Turner, M. G., Pearson, S. M., Bolstad, P., Wear, D. N., 2003. Effects of land-cover change on spatial pattern of forest communities in the

Southern Appalachian Mountains (USA). Landscape Ecology 18, 449-464.

Van der Meer, F., 2012. Remote-sensing image analysis and geostatistics. International Journal of Remote Sensing 33, 5644-5676.

Verbesselt, J., Hyndman, R., Newnham, G., Culvenor, D., 2010a. Detecting trend and seasonal changes in satellite image time series. Remote Sensing of Environment 114, 106-115.

Verbesselt, J., Hyndman, R., Zeileis, A., Culvenor, D., 2010b. Phenological change detection while accounting for abrupt and gradual trends in satellite image time series. Remote Sensing of Environment 114, 2970-2980.

Verhoef, W., Menenti, M., Azzali, S., 1996. A colour composite of NOAA-AVHRR-NDVI based on time series analysis (1981-1992). International Journal of Remote Sensing 17, 231-235.

Verstraete, J., Hallez, A., Tré, G., 2007. Fuzzy Regions: Theory and Applications. in: Morris, A., Kokhan, S., (eds), Geographic Uncertainty in Environmental Security. Springer, Netherlands, pp. 1-17.

Viovy, N., Arino, O., Belward, A. S., 1992. The Best Index Slope Extraction (BISE): A method for reducing noise in NDVI time-series. International Journal of Remote Sensing 13, 1585-1590.

Vogelmann, J. E., Sohl, T. L., Campbell, P. V., Shaw, D. M., 1998. Regional Land Cover Characterization Using Landsat Thematic Mapper Data and Ancillary Data Sources. Environmental Monitoring and Assessment 51, 415-428.

Vogiatzakis, L. N., Griffiths, G. H., 2001. Vegetation-environment relationships in Lefka Ori (Crete, Greece):ordination results from montane-mediterranean and oromediterranean communities. Ecologia Mediterranea 27, 15-32.

Wagenseil, H., Samimi, C., 2006. Assessing spatio-temporal variations in plant phenology using Fourier analysis on NDVI time series: results from a dry savannah environment in Namibia. International Journal of Remote Sensing 27, 3455-3471.

Wardlow, B. D., Egbert, S. L., Kastens, J. H., 2007. Analysis of time-series MODIS 250 m vegetation index data for crop classification in the U.S. Central Great Plains. Remote Sensing of Environment 108, 290-310.

Weismiller, R. A., Kristof, S. j., Scholz, D. K., Anuta, P. E., Momin, S. A., 1977. Change detection in coastal zone environments. Photogrammetric Engineering and Remote Sensing 43, 1533–1539.

Whittaker, R. H., 1967. Gradient analysis of vegatation. Biological Reviews 42, 207-264.

Whittaker, R. H., 1973. Gradient analysis of vegetation. Biological Review 49, 207-264.

Whittaker, R. H., 1978a. Classification of Plant Communities. W. Junk, The Hague, pp. 408.

Whittaker, R. H., 1978b. Ordination of Plant Communities. W. Junk, The Hague.

Whittaker, R. H., Levin, S. A., 1977. The role of mosaic phenomena in natural communities. Theoretical Population Biology 12, 117-139.

Williams, D. L., Goward, S., Arvidson, T., 2006. Landsat: Yesterday, today, and tomorrow. Photogrammetric Engineering and Remote Sensing 72, 1171-1178.

Wood, T. F., Foody, G. M., 1989. Analysis and representation of vegetation continua from Landsat Thematic Mapper data for lowland heaths. International Journal of Remote Sensing 10, 181-191.

Woodcock, C. E., Macomber, S. A., Pax-Lenney, M., Cohen, W. B., 2001. Monitoring large areas for forest change using Landsat: Generalization across space, time and Landsat sensors. Remote Sensing of Environment 78, 194-203.

Wooldridge, J., 2009. Introductory Econometrics: A Modern Approach, Fourth.ed. South-Western College Pub, USA.

Wu, X., Archer, S., 2005. Scale - Dependent Influence of Topography - Based Hydrologic Features on Patterns of Woody Plant Encroachment in Savanna landscapes. Landscape Ecology 20, 733-742.

Xiao, X., Boles, S., Frolking, S., Li, C., Babu, J. Y., Salas, W., Moore III, B., 2006a. Mapping paddy rice agriculture in South and Southeast Asia using multi-temporal MODIS images. Remote Sensing of Environment 100, 95-113.

Xiao, X., Hagen, S., Zhang, Q., Keller, M., Moore III, B., 2006b. Detecting leaf phenology of seasonally moist tropical forests in South America with multi-temporal MODIS images. Remote Sensing of Environment 103, 465-473.

Xie, Y., Sha, Z., Yu, M., 2008. Remote sensing imagery in vegetation mapping: a review. Journal of Plant Ecology 1, 9-23.

Young, S. S., Wang, C. Y., 2001. Land-cover change analysis of China using global-scale Pathfinder AVHRR Landcover (PAL) data, 1982-92. International Journal of Remote Sensing 22, 1457-1477.

Zhan, X., Sohlberg, R. A., Townshend, J. R. G., DiMiceli, C., Carroll, M. L., Eastman, J. C., Hansen, M. C., DeFries, R. S., 2002. Detection of land cover changes using MODIS 250 m data. Remote Sensing of Environment 83, 336-350.

Zhang, J., Foody, G. M., 1998. A fuzzy classification of sub-urban land cover from remotely sensed imagery. International Journal of Remote Sensing 19, 2721-2738.

Zhang, X., Friedl, M. A., Schaaf, C. B., 2009. Sensitivity of vegetation phenology detection to the temporal resolution of satellite data. International Journal of Remote Sensing 30, 2061-2074.

Zhang, X., Friedl, M. A., Schaaf, C. B., Strahler, A. H., Hodges, J. C. F., Gao, F., Reed, B. C., Huete, A., 2003. Monitoring vegetation phenology using MODIS. Remote Sensing of Environment 84, 471-475.

Zhang, X., Sun, R., Zhang, B., Tong, Q., 2008. Land cover classification of the North China plain using MODIS_EVI time series. ISPRS Journal of Photogrammetry and Remote Sensing 63, 476-484.

Zhao, B., Yan, Y., Guo, H., He, M., Gu, Y., Li, B., 2009. Monitoring rapid vegetation succession in estuarine wetland using time series MODIS-based indicators: An application in the Yangtze River Delta area. Ecological Indicators 9, 346-356.

Zhou, W., Troy, A., Grove, M., 2008. Object-based land cover classification and change analysis in the baltimore metropolitan area using multitemporal high resolution remote sensing data. Sensors 8, 1613-1636.

Summary

The research objective was to develop and test mapping and monitoring methods for accurate representation and characterization of land cover and its changes by considering land cover gradients and use of hyper-temporal remote sensing. It includes (i) a technique for characterizing long-duration cloud contamination in hyper-temporal NDVI imagery, (ii) identifying and mapping land cover gradients, (iii) testing a landscape heterogeneity mapping approach in natural and semi-natural landscapes, and (iv) developing a land cover composition change assessment method.

An exploratory method was developed to detect for hyper-temporal NDVI time series imagery, data that are affected by long duration cloud contamination. Using this, such values can be flagged as missing and their use avoided during subsequent analysis. The method is built on statistically derived unsupervised classification of the hyper-temporal time series imagery. Then by class, plots were prepared to depict changes over time of the means and the standard deviations in NDVI-values. By comparing plots of similar classes, long-duration cloud contamination appeared to display a decline in mean NDVI below the lower limit 95% confidence interval with a coinciding increase in standard deviation above the upper limit 95% confidence interval. This approach is tested to detect when and where long-duration clouds are responsible for unreliable NDVI readings. The approach is simple, robust and easily reproducible.

A map depicting gradients in land cover was successfully extracted using spatio-temporal analysis of hyper-temporal NDVI imagery. The land cover gradient map is composed of NDVI classes, grouped on the basis of their NDVI-values and similarities in temporal characteristics. Validation of the results indicates that within groups, the collected cover fraction data are significantly linearly related with the given NDVI data. These linear relationships are significantly different between groups with respect to tree cover (adj. R^2=0.96), shrub cover (adj. R^2=0.83), grass cover (adj. R^2=0.71), bare soil (adj. R^2=0.88), stone cover (adj. R^2=0.81) and litter cover (adj. R^2=0.69) fractions. Hyper-temporal imagery properly captures temporal and spatial differences in land cover greenness caused by differences (gradients) in species composition and/or in their densities.

The LaHMa method captures spatio-temporal variability in greenness through depicting gradients, hard boundaries, and internal unit heterogeneity. The methods were tested and found suitable to support mapping natural and semi-natural landscapes. The method derives heterogeneity statistics at both pixel and area levels, using the long-term spatiotemporal variability in land cover. The gradient based representation of landscape heterogeneity is

consistent with landscape theories that support the existence of land cover gradients. The heterogeneity output maps were validated using spatial ground data capturing variation in land cover. The evaluation revealed that differences in land cover could be related (R^2 for two transects were 0.60 and 0.63) to the variation in heterogeneity values expressed in the LaHMA map.

A new land cover composition change assessment and mapping method (CoverCAM) was developed; it uses long term hyper-temporal NDVI imagery. The method removes the seasonal variability component from the change detection process. The method was tested for Andalucía, Spain, and validated for the year 2010 (only natural and semi natural areas). The validation showed that the predicted land cover composition change map correlated for 72% with the observed land cover composition changes. The method successfully produced over time by location (as a map) land cover composition change probabilities. What actually changed is not detected. The method is simple and repeatable. It requires no prior knowledge of the study area. CoverCAM presents land cover change probabilities as a continuous scale, as is the proper way to depict land cover change assessments of coarse pixels over time.

Summarizing, this study succeeded to develop and test methods that support, complement and improve accuracies of land cover mapping and monitoring techniques, through the use of hyper-temporal remotely sensed imagery.

Samenvatting

De studie had als doelstelling kartering en observatie methoden te ontwikkelen en te testen, die leiden tot verbeterde en meer accurate beschrijvingen van groene landbedekking; dit met behulp van hyper-temporele aardobservatie data en rekening houdende met voorkomende ruimtelijke gradiënten en landbedekking veranderingen. De studie betreft (i) het ontwikkelen van technieken ter herkenning van langdurige contaminatie door (sluier-) bewolking van gebruikte satelliet beelden, (ii) identificatie en kartering van ruimtelijke gradiënten betreffende de groene landbedekking, (iii) testen van een heterogeniteit kartering methode voor een (semi-) natuurlijk landschap, en (iv) het ontwikkelen van een groene landbedekking verandering detectie methode.

Een prototype methode was ontwikkeld voor detectie van contaminatie door langdurige (sluier-) bewolking in tijdseries van hyper-temporale satellietbeelden met NDVI (groenheid) waarden. Na detectie, kunnen beïnvloedde waarden buiten verdere beeld analyse gehouden worden. De methode bouwt voort op een automatische statistische classificatie algoritme van gebruikte beelden. Per klasse worden grafisch veranderingen over tijd in gemiddelde NDVI waarden en de bijbehorende standaard deviaties getoond. Door vergelijk van de grafieken van vergelijkbare klassen, wordt langdurige contaminatie herkend door zowel een tijdelijke afname van de gemiddelde waarden als een toename van de standaard deviaties. Gebruik van 95% confidentie intervallen bepaald dan de gebieden waar wanneer contaminatie verantwoordelijk is voor onbetrouwbare NDVI waarden. Het is een simpele, robuuste, en makkelijk herhaalbare methode.

Een landkaart die gradiënten toont in landbedekking was succesvol geproduceerd door analyse van hyper-temporale satellietbeelden. De gradiënt geeft graduele verschillen aan in NDVI waarden tussen diverse gegenereerde klassen. Deze zijn gegroepeerd op basis van NDVI waarden en het temporele verloop daarvan. Validatie van de gemaakte kaart toonde aan dat verzamelde veldgegevens tussen groepen behorende tot een gradiënt, significant gecorreleerd zijn met de specifieke NDVI waarden. Tussen groepen die verschillende gradiënten vertegenwoordigen, zijn deze waarden juist significant verschillend. Dit betreft verschillen in de bedekking fracties door bomen (R2 van 0.96), struik bedekking (R2 van 0.83), gras bedekking (R2 van 0.71), kale grond (R2 van 0.88), bedekking door stenen (R2 van 0.81), en bedekking door blad en dood organisch materiaal (R2 van 0.69). Het gebruik van hyper-temporele satelliet beelden is dus zeer geschikt om graduele ruimtelijke verschillen in de groene landbedekking veroorzaakt voor verloop in species composities en hun densiteit in kaart te brengen.

De LaHMa methode analyseert ruimtelijke-temporele variabiliteit in de groene landbedekking door gradiënt herkenning, het vaststellen van grenzen tussen duidelijk verschillende landbedekking klassen en diverse gradiënten, en het ruimtelijk detecteren van interne heterogeniteit binnen iedere unieke landbedekking klassen. LaHMa werd getest en geschikt bevonden voor het karteren van (semi-) natuurlijke landschappen. De methode herkent heterogeniteit in groene landbedekking op grid niveau van gebruikte beelden, als tussen gebieden die verschillende bedekking klassen vertegenwoordigen. Dit door analyse van de langdurige ruimtelijk-temporele variabiliteit in groene landbedekking. Gevonden verschillen bevestigen bekende landschap theorieën. LaHMa kaarten zijn gevalideerd door verschillen in landbedekking te relateren aan gekarteerde verschillen. Data verzameld in het veld voor twee transect lijnen correleerde voor 60 en 63% met de gemaakte vergelijking.

Een nieuwe methode ter identificatie van landbedekking veranderingen werd ontwikkeld, genaamd: CoverCAM. Gedetecteerde veranderingen betreft de compositie van de groene landbedekking. De methode maakt gebruik van hyper-temporele NDVI beelden, en verwijdert seizoen specifieke variabiliteit in groene landbedekking voordat tot identificatie van bedekking verandering wordt overgegaan. De methode werd toegepast voor Andalusië, Spanje, en de gedetecteerde veranderingen voor 2010 werden onderzocht in het veld. In (semi-) natuurlijke gebieden werd een overeenkomst van 72% vastgesteld tussen veld data en gekarteerde data. De methode identificeert probleemloos over tijd de locaties (als kaarten) waar met een bepaalde kans bedekking veranderingen plaats vonden. Welke veranderingen dat betreft blijft onderhevig aan inspecties in het veld. CoverCAM is eenvoudig en volledig herhaalbaar. Het vereist geen specifieke kennis betreffende het gebied waarvan veranderingen worden gedetecteerd. CoverCAM bepaald enkel de numerieke kans per grid van de gebruikte beelden, dat er verandering optrad.

In enkele woorden bevat deze studie validatie van methoden die waarde toevoegen aan studies betreffende de groene landbedekking; dit betreft zowel ruimtelijke als temporele aspecten, met gebruik van hyper-temporele NDVI beelden.

Journal Articles

- **A. Ali,** C. A. J. M. de Bie, A. K. Skidmore, R. G. Scarrott, A. Hamad, V. Venus and P. Lymberakis., 2013, Mapping land cover gradients through analysis of hyper-temporal NDVI imagery, International Journal of Applied Earth Observation and Geoinformation 23, 301–312.

- C.A.J.M. de Bie, T.T.H. Nguyen, **A. Ali,** R. Scarrott and A.K. Skidmore., 2012, LaHMa: a landscape heterogeneity mapping method using hyper-temporal datasets, International Journal of Geographical Information Science. 26, 1-16.

- **A. Ali.,** C.A.J.M. de Bie., R.G. Scarrott., T.T.H. Nguyen., and A.K. Skidmore., 2012. Comparative performance analysis of a hyper-temporal NDVI analysis approach and a landscape-ecological mapping approach, ISPRS Ann. Photogramm. Remote Sens. Spatial Inf. Sci., I-7, 105-110.

- **Ali, A.**, C. A. J. M. de Bie., A. K. Skidmore., 2013. Detecting long-duration cloud contamination in hyper-temporal NDVI imagery. International Journal of Applied Earth Observation and Geoinformation 24, 22-31.

- T. T. H. Nguyen, C. A. J. M. de Bie, **A. Ali,** E. M. A. Smaling, and T. H. Chu., 2011, Mapping the irrigated rice cropping patterns of the Mekong delta, Vietnam, through hyper-temporal SPOT NDVI image analysis. International Journal of Remote Sensing 33, 415-434.

- **A. Ali.,** C. A. J. M. de Bie., A. K. Skidmore., R. G. Scarrott., and P. Lymberakis., 2013, Mapping the heterogeneity of natural and semi-natural landscapes, International Journal of Applied Earth Observation and Geoinformation 26, 176-183.

Conferences presentations

- **A. Ali,** C.A.J.M. de Bie, A.K. Skidmore, R.G. Scarrott, 2012, Detection of long duration cloud contamination in hyper-temporal NDVI imagery, European Geosciences Union General Assembly 2012, Vienna, Austria, 22–27 April 2012 Geophysical Research Abstracts Vol. 14, EGU 2012-348-1.

- **A. Ali.,** C.A.J.M. de Bie., A.K Srivastava., A.K Skidmore., M.R Khan., 2012. CoverCAM – a Land Cover Composition Change Assessment Method: PowerPoint. Presented at: GIN Symposium PhD presentations, Apeldoorn, 15 November 15 slides.

- **A. Ali.,** C.A.J.M. de Bie., A. K. Skidmore., R. G. Scarrott., 2012. A new landscape heterogeneity method for accurately mapping natural and semi natural landscape. 2nd TERRABITES Symposium, ESRIN, Frascati, Italy, 06FEB-08FEB-2012.

- **A. Ali.,** C.A.J.M. de Bie., R.G. Scarrott., T.T.H. Nguyen., and A. K. Skidmore., 2012. Comparative performance analysis of a hyper-temporal NDVI analysis approach and a landscape-ecological mapping approach, ISPRS congress/conference, Australia, Melbourne, 25 May-31 June 2012.

- **A. Ali.,** C.A.J.M. de Bie., A.K. Skidmore., 2013. Assessment of long-term land use/land cover change through hyper-temporal remote sensing, United Nations / Pakistan International workshop on Integrated use of Space technologies for food and water security, 11-15 March 2013, Islamabad, Pakistan.

- **A. Ali.,** 2013, Hyper-temporal remote sensing based land use/land cover mapping and monitoring, AgMIP-Pakistan Kickoff Workshop & International Seminar on Climate Change, June 4-6, 2013, Faisalabad-Pakistan.

Conference papers

- Nguyen Thi Thu Ha., C.A.J.M. de Bie., **Amjad, Ali** and E.M.A. Smaling., 2012. Remote Sensing-based Method to Map Irrigated Rice Cropping Patterns of the Mekong Delta, Viet Nam, in: GMS 2020 International Conference: Balancing Economic Growth and Environmental Sustainability 20 Feb Bangkok.

- A. K. Mohmand., M. Aljoufi., J. Flacke, M. Brussels., M. Karimi., **Amjad. Ali.,** 2012. Developing a Cellular Automata Land Use Model for Jeddah City, Kingdom of Saudi Arabia; Geomatics conference, Jeddah KSA

Biography

Amjad Ali was born on 15th March 1978 in Parachinar, Kurram Agency, Pakistan. He completed secondary and higher secondary schooling in Parachinar. He received BSc (Hons) and MSc (Hons) degrees in Agriculture from Agricultural University Peshawar, Pakistan. He then joined the national space agency Pakistan Space and Upper Atmosphere Research Commission Pakistan (SUPARCO) in 2003. He was awarded scholarship for MSc leading to PhD in 2007. He joined Faculty of Geo-Information Science and Earth Observation of the University of Twente in October 2007. MSc in Geo-Information Science and Earth Observation was done in 2009 and then continued with PhD (March 2009) in the theme of Forest Agriculture and Environment in the Spatial Sciences. He worked under the kind supervision of Prof. Dr Andrew Skidmore and Dr. Ir. C.A.J.M de Bie which resulted in this dissertation.

ITC Dissertation List

http://www.itc.nl/research/phd/phd_graduates.aspx